THE UNIVERSITY OF QUEENSLAND

SCHOOL OF CIVIL ENGINEERING

REPORT CH83/11

TURBULENT VELOCITY AND SUSPENDED SEDIMENT CONCENTRATION MEASUREMENTS IN AN URBAN ENVIRONMENT OF THE BRISBANE RIVER FLOOD PLAIN AT GARDENS POINT ON 12-13 JANUARY 2011

AUTHOR: Richard BROWN, Hubert CHANSON,
Dave McINTOSH and Jai MADHANI

HYDRAULIC MODEL REPORTS

This report is published by the School of Civil Engineering at the University of Queensland. Lists of recently-published titles of this series and of other publications are provided at the end of this report. Requests for copies of any of these documents should be addressed to the Civil Engineering Secretary.

School of Civil Engineering
The University of Queensland
Brisbane QLD 4072
AUSTRALIA

Telephone: (61 7) 3365 4163
Fax: (61 7) 3365 4599

URL: http://www.eng.uq.edu.au/civil/

First published in 2011 by
School of Civil Engineering
The University of Queensland, Brisbane QLD 4072, Australia

ISBN No. 9781742720272

The University of Queensland, St Lucia QLD

Turbulent Velocity and Suspended Sediment Concentration Measurements in an Urban Environment of the Brisbane River Flood Plain at Gardens Point on 12-13 January 2011

by

Richard BROWN

Associate Professor, Queensland University of Technology, Faculty of Built Environment and Engineering, Brisbane QLD 4000, Australia, Email: richard.brown@qut.edu.au

Hubert CHANSON

Professor, The University of Queensland, School of Civil Engineering, Brisbane QLD 4072, Australia, Email: h.chanson@uq.edu.au

Dave McINTOSH

Queensland University of Technology, Faculty of Built Environment and Engineering, Brisbane QLD 4000, Australia

and **Jai MADHANI**

Queensland University of Technology, Faculty of Built Environment and Engineering, Brisbane QLD 4000, Australia

REPORT No. CH83/11

ISBN 9781742720272

School of Civil Engineering, The University of Queensland, June 2011

Gardens Point Road on Thursday 13 January 2011 at 11:39 - Note the ADV system on the far right

ABSTRACT

The flood flow in urbanised areas constitutes a major hazard to the population and infrastructure as seen during the summer 2010-2011 floods in Queensland (Australia). Flood flows in urban environments have been studied relatively recently, although no study considered the impact of turbulence in the flow. During the 12-13 January 2011 flood of the Brisbane River, some turbulence measurements were conducted in an inundated urban environment in Gardens Point Road next to Brisbane's central business district (CBD) at relatively high frequency (50 Hz). The properties of the sediment flood deposits were characterised and the acoustic Doppler velocimeter unit was calibrated to obtain both instantaneous velocity components and suspended sediment concentration in the same sampling volume with the same temporal resolution. While the flow motion in Gardens Point Road was subcritical, the water elevations and velocities fluctuated with a distinctive period between 50 and 80 s. The low frequency fluctuations were linked with some local topographic effects: i.e, some local choke induced by an upstream constriction between stairwells caused some slow oscillations with a period close to the natural sloshing period of the car park. The instantaneous velocity data were analysed using a triple decomposition, and the same triple decomposition was applied to the water depth, velocity flux, suspended sediment concentration and suspended sediment flux data. The velocity fluctuation data showed a large energy component in the slow fluctuation range. For the first two tests at z = 0.35 m, the turbulence data suggested some isotropy. At z = 0.083 m, on the other hand, the findings indicated some flow anisotropy. The suspended sediment concentration (SSC) data presented a general trend with increasing SSC for decreasing water depth. During a test (T4), some long-period oscillations were observed with a period about 18 minutes. The cause of these oscillations remains unknown to the authors. The last test (T5) took place in very shallow waters and high suspended sediment concentrations. It is suggested that the flow in the car park was disconnected from the main channel. Overall the flow conditions at the sampling sites corresponded to a specific momentum between 0.2 to 0.4 m^2 which would be near the upper end of the scale for safe evacuation of individuals in flooded areas. But the authors do not believe the evacuation of individuals in Gardens Point Road would have been safe because of the intense water surges and flow turbulence. More generally any criterion for safe evacuation solely based upon the flow velocity, water depth or specific momentum cannot account for the hazards caused by the flow turbulence, water depth fluctuations and water surges.

Keywords: Flood plain measurements, 2010, 2011 Queensland, Australia, urban environment, turbulent velocity measurements, triple decomposition, Brisbane River, suspended sediment concentration SSC, suspended sediment flux, resonance, inundated street.

TABLE OF CONTENTS

LIST OF SYMBOLS

The following symbols are used in this report:

Ampl ADV signal amplitude (counts);

B building car park width (m);

B_1 constriction width (m) between the stairwells;

BSI acoustic backscatter intensity;

d water depth (m) measured above the invert;

d_{10} sediment grain size (m) defined as the size for which 10% by weight of the material is finer;

d_{50} median grain size (m) defined as the size for which 50% by weight of the material is finer;

d_{90} sediment grain size (m) defined as the size for which 90% by weight of the material is finer;

E specific energy (m) defined as:

$$E = d + \frac{V_x^2}{2 \times g};$$

Fr Froude number locally defined as:

$$Fr = \frac{< V_x >}{\sqrt{g \times d}};$$

f Darcy-Weisbach friction factor;

g gravity constant: g = 9.80 m/s^2 in Brisbane QLD, Australia;

H total head (m);

h instantaneous pressure head (m) or water level measured above the ADV pressure sensor;

<h> mean water level (m) calculated as low-pass filtered data with a cut-off frequency of 0.002 Hz (1/500 s^{-1});

[h] slow fluctuating water level (m) calculated as the band-passed signal with the upper and lower cut-off frequencies set at 0.33 Hz and 0.002 Hz (1/3 s^{-1} and 1/500 s^{-1} respectively);

h' standard deviation of the water level fluctuation (m) calculated over 500 s;

k energy loss coefficient;

L building car park length (m);

l characteristic length scale (m);

M specific momentum (m^2) defined as:

$$M = \frac{d^2}{2} + d \times \frac{V_x^2}{g};$$

m exponent;

q instantaneous longitudinal velocity flux (m^2/s): $q = h \times V_x$;

q_s instantaneous longitudinal suspended sediment flux (kg/s/m^2): $q_s = SSC \times V_x$;

$<q>$ mean velocity flux (m^2/s) calculated as low-pass filtered data with a cut-off frequency of 0.002 Hz (1/500 s^{-1});

$<q_s>$ mean suspended sediment flux ($kg/s/m^2$) calculated as low-pass filtered data with a cut-off frequency of 0.002 Hz (1/500 s^{-1});

$[q]$ slow fluctuating velocity flux (m^2/s) calculated as the band-passed signal with the upper and lower cut-off frequencies set at 0.33 Hz and 0.002 Hz (1/3 s^{-1} and 1/500 s^{-1} respectively);

$[q_s]$ slow fluctuating suspended sediment flux ($kg/s/m^2$) calculated as the band-passed signal with the upper and lower cut-off frequencies set at 0.33 Hz and 0.002 Hz (1/3 s^{-1} and 1/500 s^{-1} respectively);

q' standard deviation of the velocity flux (m^2/s) calculated over 500 s;

q_s' standard deviation of the suspended sediment flux ($kg/s/m^2$) calculated over 500 s;

Re Reynolds number defined in terms of the mean longitudinal velocity $<V_x>$ and hydraulic diameter;

S_f friction slope:

$$S_f = -\frac{\partial H}{\partial X};$$

SSC instantaneous suspended sediment concentration (kg/m^3);

<SSC> mean suspended sediment concentration (kg/m^3) calculated as low-pass filtered data with a cut-off frequency of 0.002 Hz (1/500 s^{-1});

[SSC] slow fluctuating suspended sediment concentration (kg/m^3) calculated as the band-passed signal with the upper and lower cut-off frequencies set at 0.33 Hz and 0.002 Hz (1/3 s^{-1} and 1/500 s^{-1} respectively);

ssc' standard deviation of the suspended sediment concentration (kg/m^3) calculated over 500 s;

s wet sediment relative density;

T period (s);

T_{res} resonance period (s) or sloshing period;

t time (s);

V instantaneous velocity (m/s):

$$V = < V > + [V] + v;$$

V_x instantaneous longitudinal velocity component (m/s);

V_y instantaneous transverse velocity component (m/s);

V_z instantaneous vertical velocity component (m/s);

V_1 velocity (m/s) in the stairwell constriction;

<V> mean velocity (m/s) calculated as low-pass filtered data with a cut-off frequency of 0.002 Hz (1/500 s^{-1});

$<V_x>$ mean longitudinal velocity (m/s) calculated as low-pass filtered data with a cut-off frequency of 0.002 Hz (1/500 s^{-1});

$\langle V_y \rangle$ mean transverse velocity (m/s) calculated as low-pass filtered data with a cut-off frequency of 0.002 Hz (1/500 s^{-1});

$\langle V_z \rangle$ mean vertical velocity (m/s) calculated as low-pass filtered data with a cut-off frequency of 0.002 Hz (1/500 s^{-1});

$[V]$ slow fluctuating velocity (m/s) calculated as the band-passed signal with the upper and lower cut-off frequencies set at 0.33 Hz and 0.002 Hz (1/3 s^{-1} and 1/500 s^{-1} respectively);

$[V_x]$ slow fluctuating longitudinal velocity (m/s) calculated as the band-passed signal with the upper and lower cut-off frequencies set at 0.33 Hz and 0.002 Hz (1/3 s^{-1} and 1/500 s^{-1} respectively);

$[V_y]$ slow fluctuating transverse velocity (m/s) calculated as the band-passed signal with the upper and lower cut-off frequencies set at 0.33 Hz and 0.002 Hz (1/3 s^{-1} and 1/500 s^{-1} respectively);

$[V_z]$ slow fluctuating vertical velocity (m/s) calculated as the band-passed signal with the upper and lower cut-off frequencies set at 0.33 Hz and 0.002 Hz (1/3 s^{-1} and 1/500 s^{-1} respectively);

v turbulent velocity fluctuation (m/s): $v = V - \langle V \rangle - [V]$; v is the high-pass filtered data with a cut-off frequency of 0.33 Hz (1/3 s^{-1});

v_x longitudinal turbulent velocity fluctuation (m/s);

v_y transverse turbulent velocity fluctuation (m/s);

v_z vertical turbulent velocity fluctuation (m/s);

v' standard deviation of the turbulent velocity fluctuation (m/s) calculated over 500 s;

v_x' standard deviation of the longitudinal turbulent velocity fluctuation (m/s) calculated over 500 s;

v_y' standard deviation of the transverse turbulent velocity fluctuation (m/s) calculated over 500 s;

v_z' standard deviation of the vertical turbulent velocity fluctuation (m/s) calculated over 500 s;

X longitudinal distance (m) along the river channel centreline (middle thread) and positive downstream;

x longitudinal distance (m) positive downstream;

z vertical distance (m) positive upwards, with z = 0 at the bed;

ΔE energy loss (m);

μ effective viscosity (Pa.s) of mud sludge;

ρ water density (kg/m^3);

τ shear stress (Pa);

τ_c yield stress (Pa) of mud sluge;

Subscript

x	longitudinal direction positive downstream;
y	transverse direction positive towards the left;
z	vertical direction positive upwards;
1	flow property in the stairwell constriction;

Abbreviations

ADV	acoustic Doppler velocimeter;
AHD	Australian Height Datum (or Mean Sea Level);
AMTD	adopted middle thread distance, measured upstream from the river mouth;
BOM	Bureau of Meteorology (Australia);
BSI	acoustic backscatter intensity;
CBD	central business district;
FFT	fast Fourier transform;
Kurto	Fisher kurtosis or excess kurtosis;
PDF	probability density function;
PSD	power spectrum density;
QLD	Queensland, Australia;
QUT	Queensland University of Technology;
Skew	Fisher skewness;
SNR	signal to noise ratio;
SSC	suspended sediment concentration;
Std	standard deviation;
s	second;

Note

All times are expressed in local Queensland time (GMT + 10).

DEDICATION

This report is dedicated to the victims

of the 2010-2011 Queensland floods.

1. INTRODUCTION

1.1 PRESENTATION

Some intense rainfalls were experienced across Australia between November 2010 and January 2011 causing some major flooding (BOM 2011). In Queensland, the floods were unprecedented in the extent of the affected areas. The floods in eastern Australia are sometimes linked with the La Ninã during the El Niño Southern Oscillation (ENSO) cycle: for example, in 1916, 1917, 1950, 1954-1956, 1973-1975 and 2010-2011 (DIAZ and MARKGRAF 1992, BOM 2010). In tropical and sub-tropical Queensland, major floods are a relatively common occurrence. For example, the city of Brisbane experienced four major floods for the 1893 year alone; the Mary River in Gympie had three major floods during the 1970s; the Bohle River in Townsville reached some major flood levels five times between 1991 and 2007. The location of the townships is shown in Figure 1-1. The 2010-2011 flood events illustrated to a certain extent the extreme hydrological and hydraulic conditions in Australia and in Queensland in particular. A few years ago, the state of Queensland was experiencing a long drought period. For example, the combined water supply of the city of Brisbane fell below 17% in 2007.

(A) Map of the Australian continent

Fig. 1-1 - Maps of Australia and Queensland

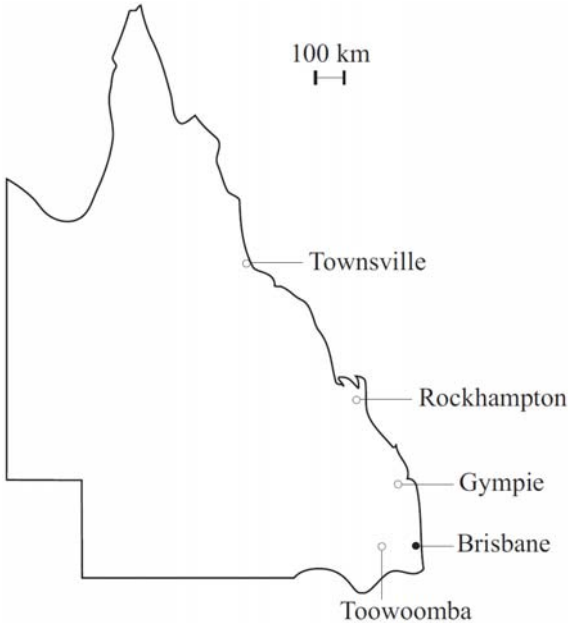

(B) Map of Queensland, Australia

Fig. 1-1 - Maps of Australia and Queensland

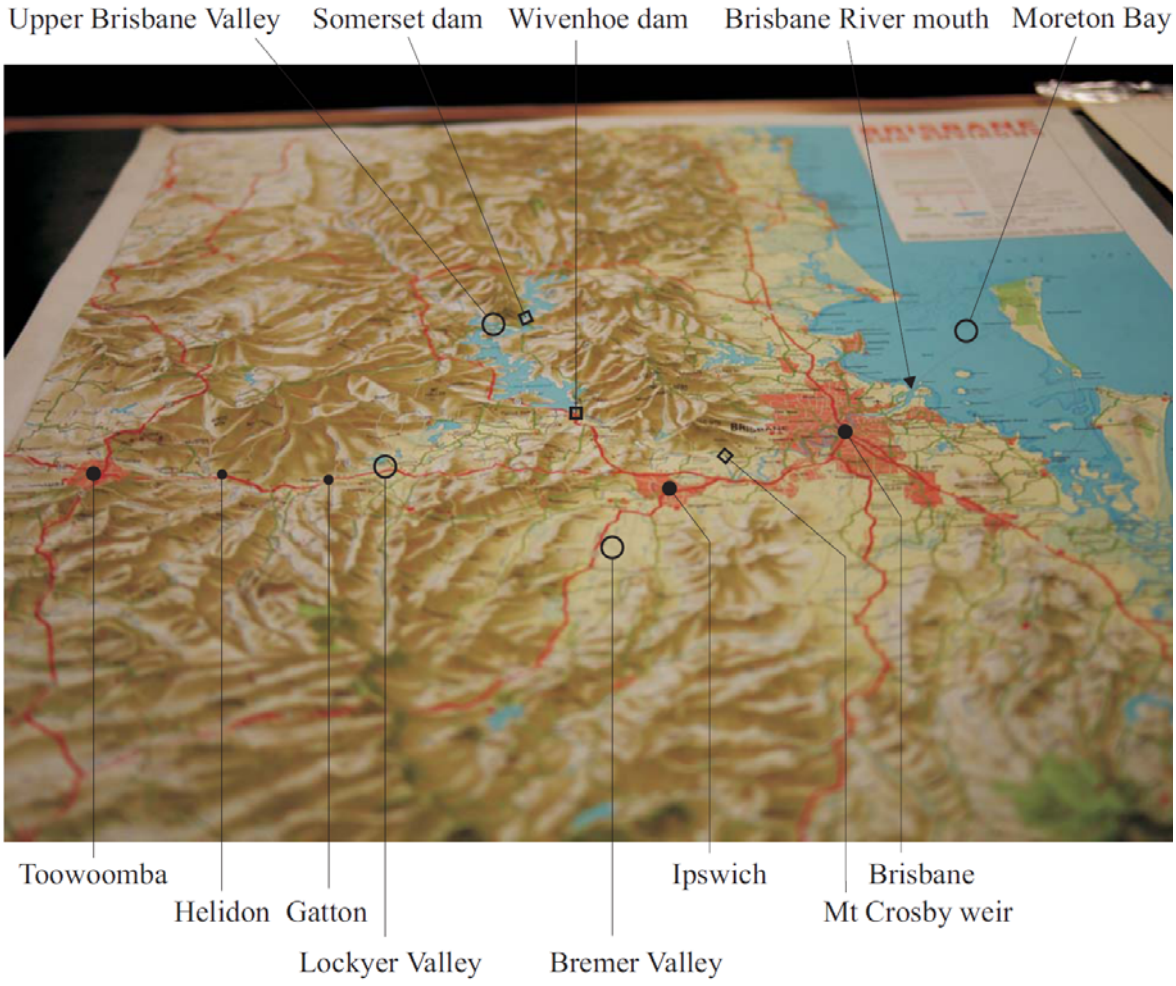

(A) Three-dimensional map of the Brisbane River catchment (after CHANSON 2011)

Fig. 1-2 - Maps of South-East Queensland

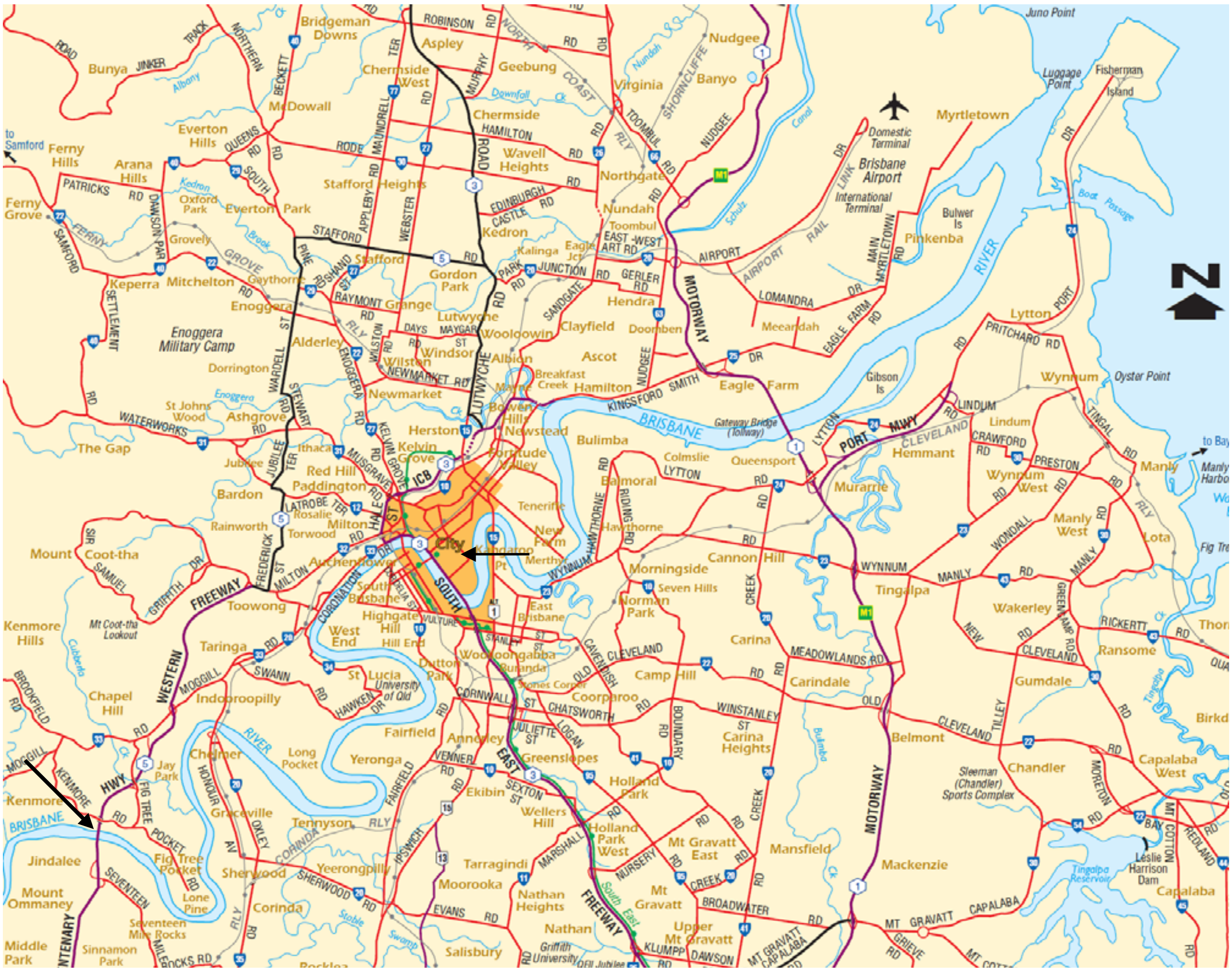

(B) Map of Brisbane suburbs (Courtesy of Queensland Dept of Natural Resources and Water 2007) - The black arrows point to the City and Jindalee gauge locations

Fig. 1-2 - Maps of South-East Queensland

In January 2011 the flood of the Brisbane River was the result of a combination of very soaked catchments after several weeks of continuous rain, some heavy continuous rainfalls during the first two weeks of January 2011 in the Brisbane River catchment, including the Bremer and Upper Brisbane River catchments, and Lockyer Valley, and an intense rainstorm event over the upper catchment on Monday 10 January 2011 and Tuesday 11 January 2011 (BOM 2011, CHANSON 2011). The Bremer and Upper Brisbane River catchments, and Lockyer Valley are shown in Figure 1-2A. These combined to create a major flood in the lower Brisbane River Valley on 11, 12, 13 and 14 January 2011. The flood waters peaked in Brisbane on 12 January afternoon and 13 January morning (Fig. 1-3). The location of the Jindalee and City gauges is highlighted in Figure 1-2B. While the flood was spectacular and affected many people in Brisbane, the city had experienced at least six major floods higher than the January 2011 flood. For example, the maximum water level in January 1974 and February 1893 was about 1.0 m and 3.9 m respectively higher than in 2011 in the

city as illustrated in Figure 1-4.

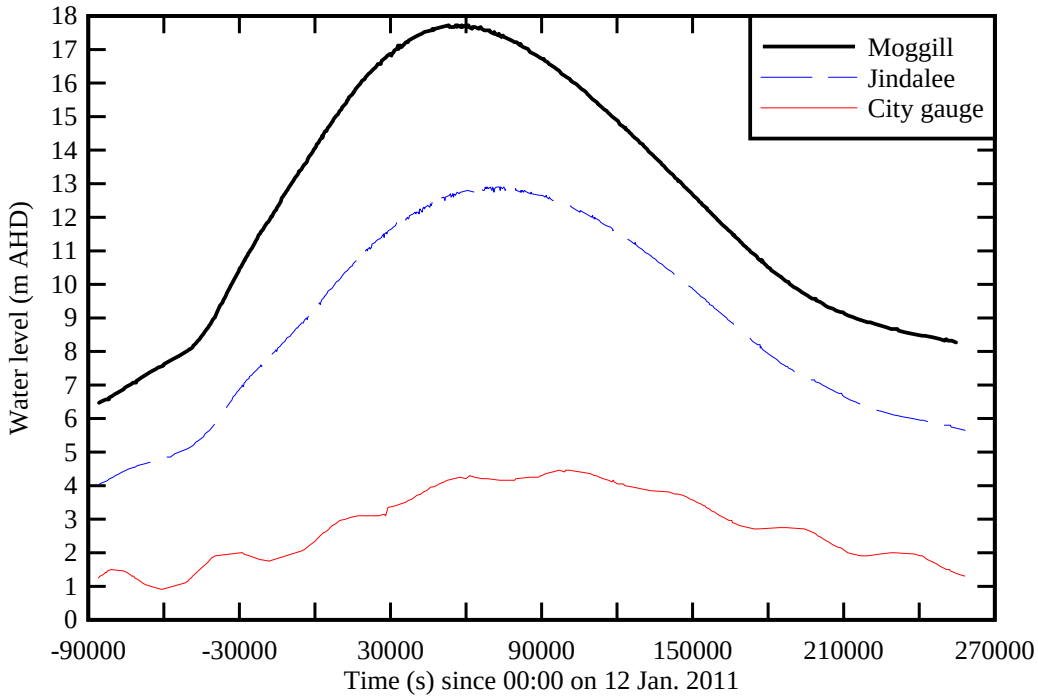

Fig. 1-3 - Flood hydrograph of the 2011 flood of the Brisbane River at the Brisbane City Gauge (Station Number: 540198), Jindalee (Station Number: 540192) and Moggill (Station Number: 540200) - Data: BOM - The City Gauge, Jindalee and Moggill stations are located respectively about 24, 49 and 55 km upstream of the river mouth (Fig. 1-2B)

1.2 FLOOD FLOW IN URBAN ENVIRONMENT

The flood flow in urbanised areas constitutes a hazard to the population and infrastructure. Some recent catastrophes included the inundations of Nîmes (France) in 1998 and Vaison-la-Romaine (France) in 1992, the flooding of New Orleans (USA) in 2005, the flooding in Rockhampton, Bundaberg, Brisbane during the 2010-2011 summer in Queensland (Australia).

Flood flows in urban environments have been studied relatively recently despite many centuries of flood events. Some researchers mentioned the storage effect in urban areas (SOLO-GABRIELE and PERKINS 1997, VELICKOVIC et al. 2011). Several studies looked into the flow patterns and redistribution in streets during storm events and the implication in terms of flood modelling (BATES et al. 2004, NANIA et al. 2004, WERNER et al. 2005, VELICKOVIC et al. 2011). Some studies investigated the impact of dam break surges in an urban setting (SOARES-FRAZAO and ZECH 2008).

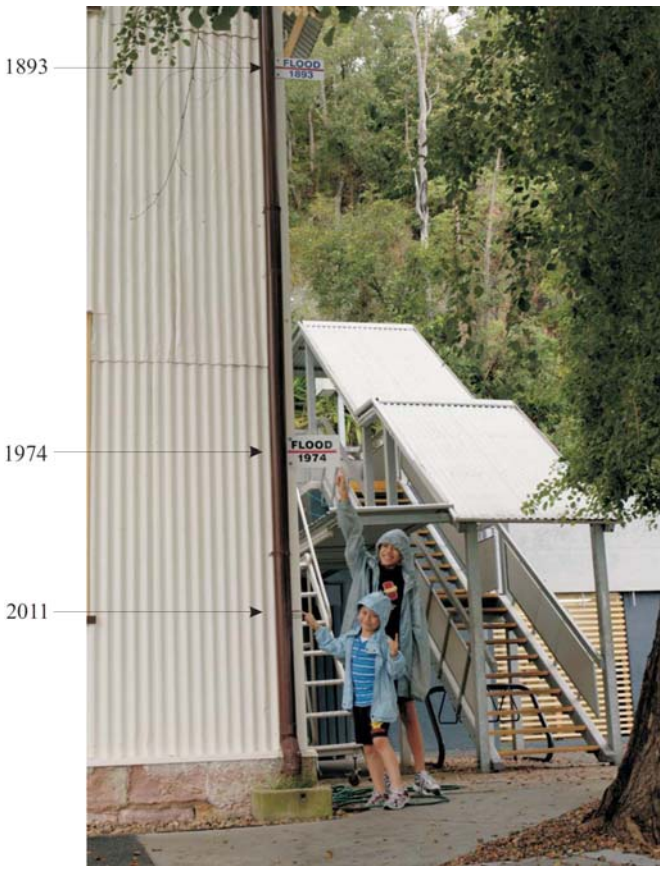

Fig. 1-4 - Peak water levels of the Brisbane River in Kangaroo Point during the 1893, 1974 and 2011 floods - The children point to the 2011 and 1974 flood levels

A number of studies looked at the impact of floods on structures and buildings (THIEKEN et al. 2005). A few considered the potential impact of flowing waters on pedestrians (ASAI et al. 2010). Some used the flow velocity as a design parameter to assess the hazards (ISHIGAKI et al. 2003). ASIA et al. (2010) argued that the specific force per unit width ([1]) is a more suitable parameter to plan the safe evacuation of individuals. Their near-full-scale physical tests implied that the specific force had to be less than 0.80 to 0.20 m^2 depending upon the age and sex of the evacuees, and escape route configuration. Surprisingly no study to date considered the level of turbulence in the flow.

1.3 STRUCTURE OF THE REPORT

In the present study, some detailed turbulent velocity and suspended sediment concentration measurements were conducted at relatively high-frequency (50 Hz) in Gardens Point Road during the 12-13 January 2011 flood of the Brisbane River. An acoustic Doppler velocimeter (ADV) was

[1] Also called momentum function or specific momentum in open channel hydraulics (HENDERSON 1966, MONTES 1998).

fixed to a boom gate pylon and later to a handrail, and the instrument sampled the turbulent velocity components about 0.1 to 0.35 m above the bed. The ADV backscatter amplitude was calibrated in terms of the suspended sediment concentration in a laboratory using some soft mud bed material deposited by the flood flow. The results provided an unique characterisation of the turbulence and sediment flux in the inundated Gardens Point Road. The field investigation and instrumentation are described in section 2. The main results are presented in sections 3 to 5, and summarised in section 6. Appendix A presents some photographs of the investigation site during and after the flood, and Appendix B shows some photographs of Gardens Point, Brisbane. Appendix C develops the ADV calibration for suspended sediment concentration measurement. Appendix D presents the time-variations of the fluctuations of water level, velocity components, suspended sediment concentration and suspended sediment flux, and Appendix E includes the time-variations of the turbulent Reynolds stresses. Some surveyed water levels of the Brisbane River in Brisbane during the January 2011 flood are regrouped in Appendix F. Some survey conducted in eastern Gardens Point is presented in Appendix G.

The study was led by Dr Richard BROWN, and the report's authors are listed in alphabetical order.

2. PHYSICAL INVESTIGATION

2.1 PHYSICAL ENVIRONMENT

The city of Brisbane was established on the Brisbane River in 1834. Gardens Point is located on the left bank, with the Brisbane central business district (CBD) extending northwards of the point (Fig. 2-1). Figure 2-1 presents some recent views of Gardens Point and the CBD. Figure 2-2 shows some historical photographs of Gardens Point taken in 1893. Further photographs are presented in Appendix B. Gardens Point includes Queensland's Parliament House, the Gardens Point campus of the Queensland University of Technology (QUT), and the Brisbane City Botanic Gardens. The point is connected to the right bank by two bridges: the Captain Cook Bridge carrying the South-East Freeway and the Goodwill Bridge for pedestrians and cyclists (Fig. 2-1A, bottom left).

(A) Gardens Point and Brisbane's Central Business District (CBD) behind in 2007 looking North (Courtesy of the University of Queensland, Office of Marketing and Communication) - The Brisbane River flows from left to right - On the left bank, the QUT Gardens Point campus and the City Botanical Gardens are clearly seen

Fig 2-1 - Views of Gardens Point, Brisbane QLD (Australia)

(B) Brisbane River meanders between the city and river mouth in 2007 looking North-East (Courtesy of the University of Queensland, Office of Marketing and Communication) - South Bank is in the foreground, the Captain Cook Bridge on the bottom right, and the river mouth in the far background

Fig 2-1 - Views of Gardens Point, Brisbane QLD (Australia)

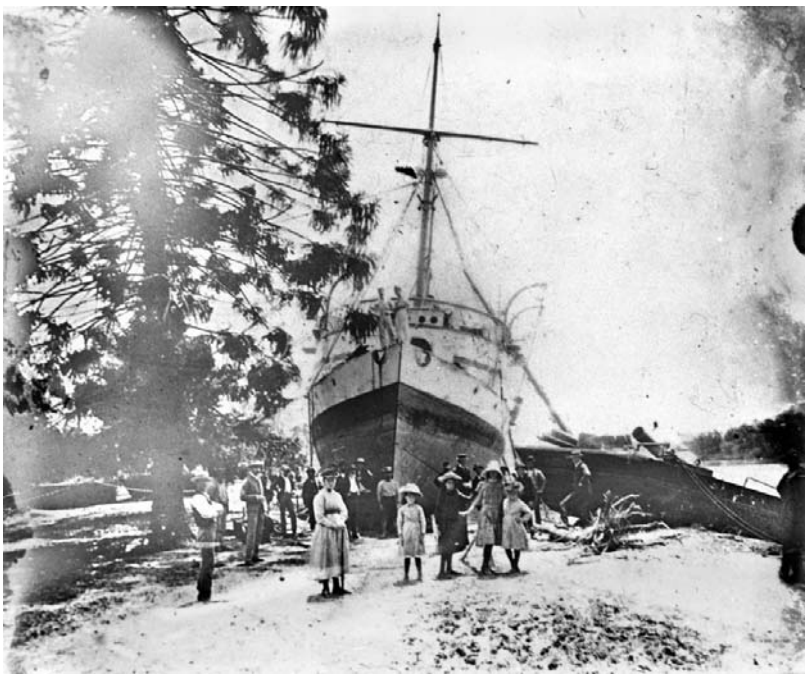

(A) Group of people in front of the gunboat Paluma, aground at the Botanic Gardens, after the 1893 Brisbane flood (Courtesy of John Oxley Library, State Library of Queensland)

Fig. 2-2 - Historical photographs of Gardens Point in February 1893

(B) Looking towards the left bank between 5 and 19 February 1893 (O'CONNOR 1996) - Steamships left high and dry in the Botanic gardens after the 1893 Brisbane flood receded - The ships (from left) were the Elamang, Mary Evans and Paluma - They were carried over the river bank by the flood on 5 February; the flood on 19 February refloated the gunboat Paluma

Fig. 2-2 - Historical photographs of Gardens Point in February 1893

Following some heavy rainfall in the catchment during the beginning of January 2011 including on 10 and 11 January, the Brisbane River water level rose rapidly on Tuesday 11 January and Wednesday 12 January 2011 (BOM 2011). Figure 2-3 shows the flood hydrograph of the Brisbane River at the City Gauge and the data are compared with the predicted tidal level at the same location. In Brisbane, the flood waters peaked on Thursday 14 January 2011 early morning. At Gardens Point, the QUT campus was partially inundated including Gardens Point Road linking Parliament House to the Goodwill Bridge.

Some turbulent velocity measurements were performed in the submerged Gardens Point campus of Queensland University of Technology (QUT) along Gardens Point Road below C Block and beside the Riverside Expressway ([1]) between Wednesday 12 January 2011 evening and Friday 14 January 2011 early morning. The sampling sites were located on the ground floor between the submerged car park and submerged Gardens Point Road (Fig. 2-4). Figure 2-4A shows an aerial view of the site and the red arrow points to the sampling site. Figure 2-4B illustrates a ground view with the two ADV locations. Further photographs are presented in Appendix A. On 12 January 2011, the ADV was attached to a boom gate pylon, placed horizontally (Location A). The mean flow direction was 160.8º relative to the geographic north. On 13 January 2011 mid-day, the ADV was relocated

[1] The Riverside Expressway is located on the western side of the Brisbane CBD and it is connected to the South-East Freeway and Captain Cook Bridge (Fig. 2-1).

vertically (Location B) and the mean flow direction was 172.2º relative to the geographic north. The instrument electronics, data acquisition computer and generator were installed in level 2 of C Block overlooking the ADV system.

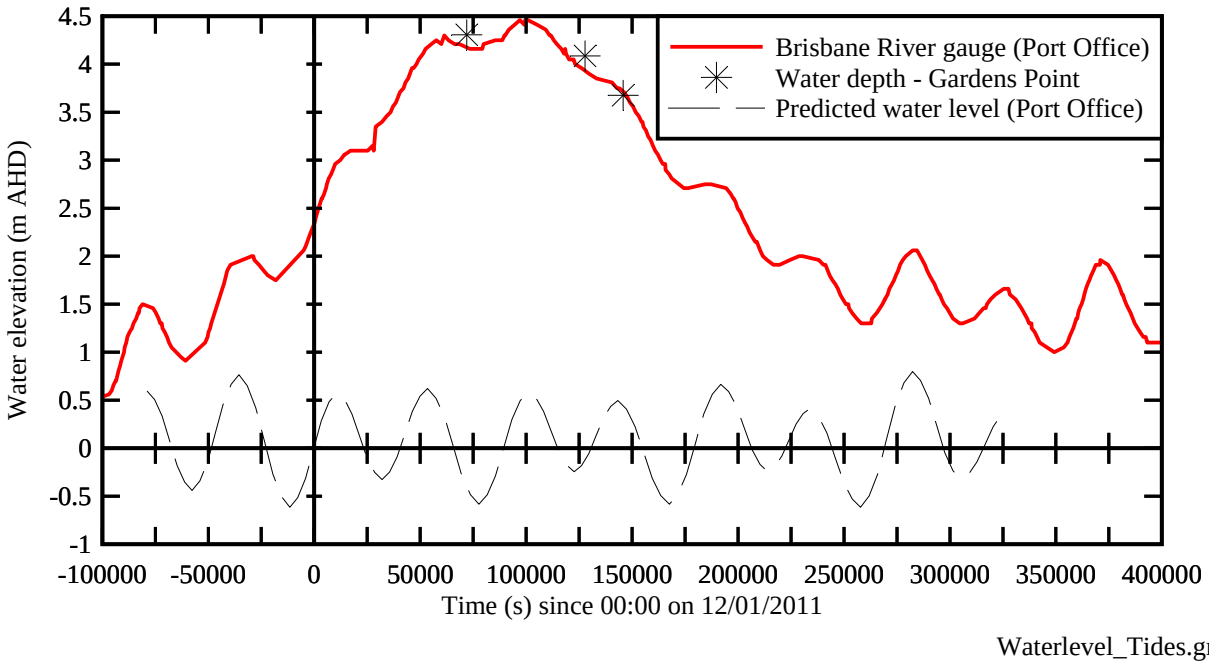

Fig. 2-3 - Water level observations at the City Gauge (Port Office) (Data: BOM) and in Gardens Point Road - Comparison with the predicted tidal levels at the Port Office

(A) Aerial view of Gardens Point in 2007 (Copyright QUT) - The Brisbane River flows from left to right - Note the Captain Cook Bridge in the foreground while the sampling site is marked with a red

arrow

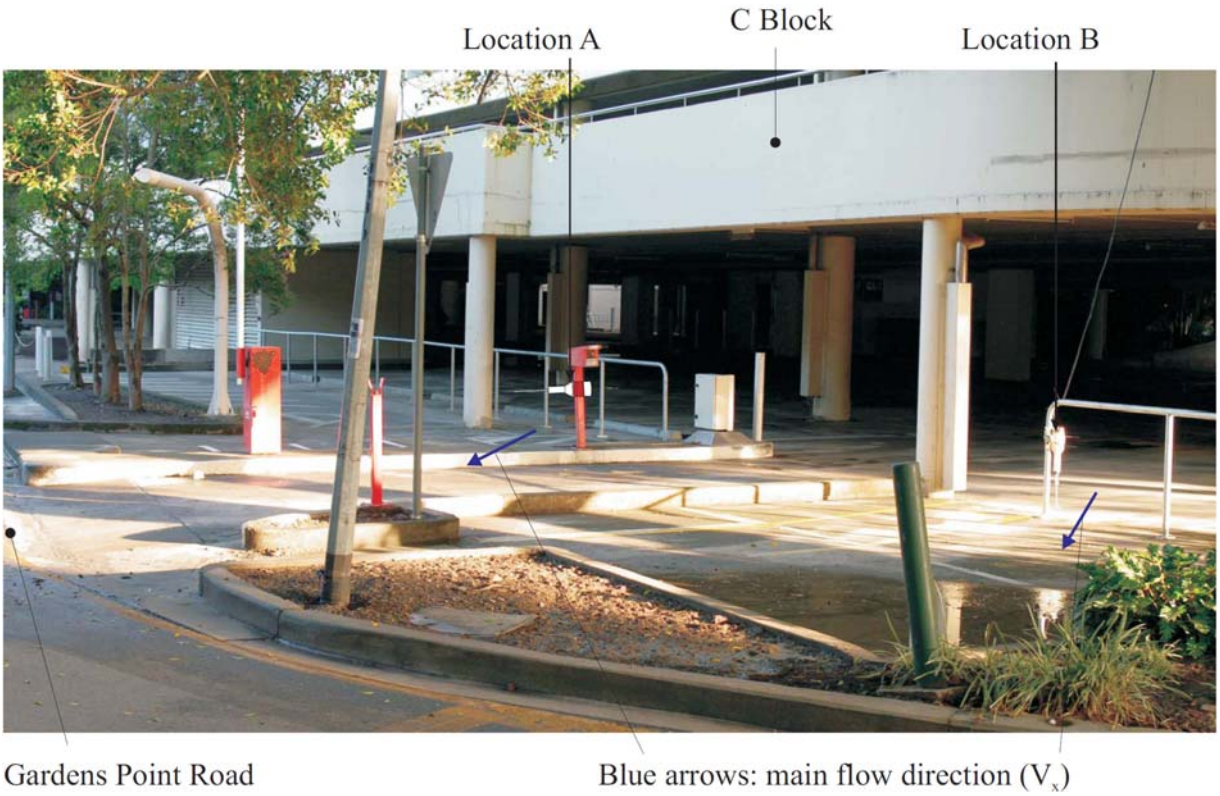

(B) Photograph of Gardens Point Road C Block car park on Friday 14 January 2011 at 06:00 - The two ADV locations A and B are shown with the main flow directions (blue arrows) when the ADV was located there - The ADV unit was at the time mounted in location B

Fig. 2-4 - Photographs of the sampling location

The ADV unit was sampled for five tests (Table 2-1). Tests T1 and T2 were conducted at the location A, and tests T3, T4 and T5 were performed at the location B. Note that the tests T1 and T3 were relatively short and designed to check the ADV unit operation.

2.2 INSTRUMENTATION

The free surface elevations were recorded manually using a measuring tape with reference to landmarks which were surveyed after the flood.

During the investigations, the turbulent velocities were measured with a Sontek^{TM} microADV (16 MHz, serial A843F). The ADV system was equipped with a 3D side-looking head. For one series of data (Table 2-1, Files T1 & T2), the unit was placed horizontally (Fig. 2-4B). The stem was aligned SW perpendicular to Gardens Point Road with the head pointing downwards. For another series (Table 2-1, Files T3, T4 & T5), the unit was placed vertically and attached to a hand rail. The head was looking horizontally, transversely pointing about East (Fig. 2-4B). The ADV unit was equipped with a pressure sensor which was underwater and gave some instantaneous water elevation data

during the first series of data (Files T1 & T2). During the second series, the pressure sensor was out of the water.

Table 2-1 - Turbulent velocity measurements in the flood plain (QUT car park) of the Brisbane River in flood on 12-13 January 2011

Data file (1)	ADV location (2)	Sampling rate Hz (3)	Velocity range m/s (4)	Start time (5)	Duration (6)	z m (7)	V_x direction (8)	Comments (9)
T1	A	50	2.5	12/01/2011 at 20:10:31	23 min 24 s (70,162 samples)	0.350	160.8º	Short ADV test.
T2	A	50	2.5	12/01/2011 at 20:40:08	4 h 26 min 40 s (800,000 samples)	0.350	160.8º	Test stopped when ADV dislodged by timber log and cable became entangled in rubbish bin wheel.
T3	B	50	2.5	13/01/2011 at 11:34:28	10 min 23 s (31,171 samples)	0.083	172.2º	Short ADV test.
T4	B	50	1.0	13/01/2011 at 12:08:55	3 h 48 min 38 s (685,884 samples)	0.083	172.2º	Test stopped to swap generator.
T5	B	50	1.0	13/01/2011 at 17:34:40	1 h 5 min 35 s (196,762 samples)	0.083	172.2º	Test stopped when water level dropped below the upper ADV receiver.

Notes: Location A: ADV unit mounted horizontally on boom gate support; Location B: ADV unit mounted vertically on a hand rail; V_x direction: mean longitudinal flow direction at the sampling location relative to the geographic north; z: vertical elevation above the invert.

All the ADV data underwent a thorough post-processing procedure to eliminate any erroneous or corrupted data from the data sets to be analysed. The post processing was conducted with the software WinADV^{TM} version 2.026, and it included the removal of communication errors, the removal of average signal to noise ratio (SNR) data less than 5 dB ([2]) and the removal of average correlation values less than 60% (McLELLAND and NICHOLAS 2000). In addition, the phase-space thresholding technique developed by GORING and NIKORA (2002) and extended by WAHL

[2] In the present study, a 5 dB SNR threshold was selected because the SNR decreased sharply for suspended sediment concentration (SSC) greater than 40 kg/m^3 (App. C).

(2003) was applied to remove spurious points. The removed data were replaced by linear interpolation.

Further observations were recorded with a digital camera Pentax™ K-7 equipped with SMC Pentax-DA 18-250mm F3.5-6.3 ED AL [IF] and SMC Pentax-FA 31mm F1.8 AL Limited lenses, and a digital camera Canon™ 5D Mk II with a Canon™ EF24-105mm F4L IS USM lens (App. A).

2.3 CHARACTERISATION OF THE BED MATERIAL

Some sediment material was collected next to the high water line on Thursday 13 January 2011 mid-morning and in a nearby flooded car park on Friday 14 January 2011 early morning. The soil samples consisted of fine mud and silt materials collected on the bed within 100 m from the ADV sampling location ([3]). A series of laboratory tests were conducted to characterise the bed material: i.e., the particle size distribution, rheometry and acoustic backscatter properties.

The soil sample granulometry was measured with a Malvern™ laser sizer with duplicate measurements (SHI 2011). The fraction of organic content was determined by loss on ignition tests. The rheological properties of mud samples were tested with a Mettler™ 180 viscometer with a clearance of 0.59 mm between the two cylinders. The tests were repeated for a range of sample dilutions and analysed following SHI and NAPIER-MUNN (1996).

The calibration of the ADV was accomplished by measuring the signal amplitude of known, artificially produced concentrations of material obtained from the bed material sample, diluted in tap water and thoroughly mixed. All the experiments were conducted on Tuesday 18 January 2011. The laboratory experiments were conducted with the same Sontek™ 3D-microADV (16 MHz, serial A843F) system using the same settings as for the field observations on 12 and 13 January 2011.

For each test, a known mass of sediment was introduced in a water tank which was continuously stirred with a paint mixer (Fig. 2-5). The mixer speed was adjusted during the most turbid water tests to prevent any obvious sediment deposition on the tank bottom. The mass of wet sediment was measured with a Kern™ PCB2000-1 (Serial WD080016381) balance, and the error was less than 0.1 g. The mass concentration was deduced from the measured mass of wet sediment and the measured water tank volume. During the tests, the suspended sediment concentrations ranged from less than 0.03 kg/m^3 to 98 kg/m^3.

[3] The parking lot of C Block adjacent to the ADV sampling locations was cleaned during the night of 13-14 January 2011 and mud samples could not be collected there after the flood receded. The mud samples taken on 14 January 2011 were collected in the parking lot of B Block.

(A) Test for SSC = 70.5 kg/m^3 - The ADV system is in the background with the water mixers slightly to the right

(B, Left) Details of the mixer blade (right) with ADV head on the left (no water)

(C, Right) Test for SSC = 12.73 kg/m^3

Fig. 2-5 - Photographs of the laboratory experiments

The acoustic backscatter amplitude measurements were conducted with the same ADV configuration employed in the field (pulse length, scan rate, velocity range). The tank was strongly agitated by the mixer. The ADV signal outputs were scanned at 50 Hz for 60 s for each test. The average amplitude measurements represented the average signal strength of the three ADV receivers. They were measured in counts ([4]). For low SSCs, the ADV data were post-processed with

[4] One count equals 0.43 dB (Sontek 2006, Person. Comm.).

the removal of average signal to noise ratio data less than 15 dB, average correlation values less than 40%, and communication errors. For SSC > 8 kg/m^3, the signal processing included the removal of communication errors and average signal to noise ratio data less than 15 dB (McLELLAND and NICHOLAS 2000). For SSC > 48 kg/m^3, unfiltered data were used since both the SNRs and correlations dropped drastically because of signal attenuation.

2.4 REMARKS

2.4.1 ADV synchronisation and data accuracy

The water elevation measurements and ADV data were synchronised within a second. The digital camera Pentax^{TM} K-7 was also synchronised together with the same reference time within a second.

The accuracy on the ADV velocity measurements was 1% of the velocity range (± 2.5 and 1 m/s) (Sontek 2008). The accuracy of the pressure sensor was 0.5 cm.

The mass of wet sediment was measured with an accuracy of less than 0.1 g, and the SSC was estimated with an accuracy of less than 0.01 g/l.

2.4.2 ADV settings and problems

Two ADV settings were used. The main difference between the two configurations was the velocity range: 2.5 m/s on 12 and 13 January 2011 and 1 m/s on 13 January 2011 (Table 2-1). The lower velocity range was selected for the last two sampling files after the flood started to recede, and the local flow velocity was slower.

During the field deployment, the authors experienced a number of major problems and practical issues and problems. At the end of the second deployment (Data file T2, Table 2-1), the authors found the ADV unit held solely by its cable on 13 January 2011 morning (Fig. 2-6). Based upon the ADV record, it is believed that the ADV was dislodged by the impact of a timber log and that a rubbish bin wheel had become entangled in the ADV cable later.

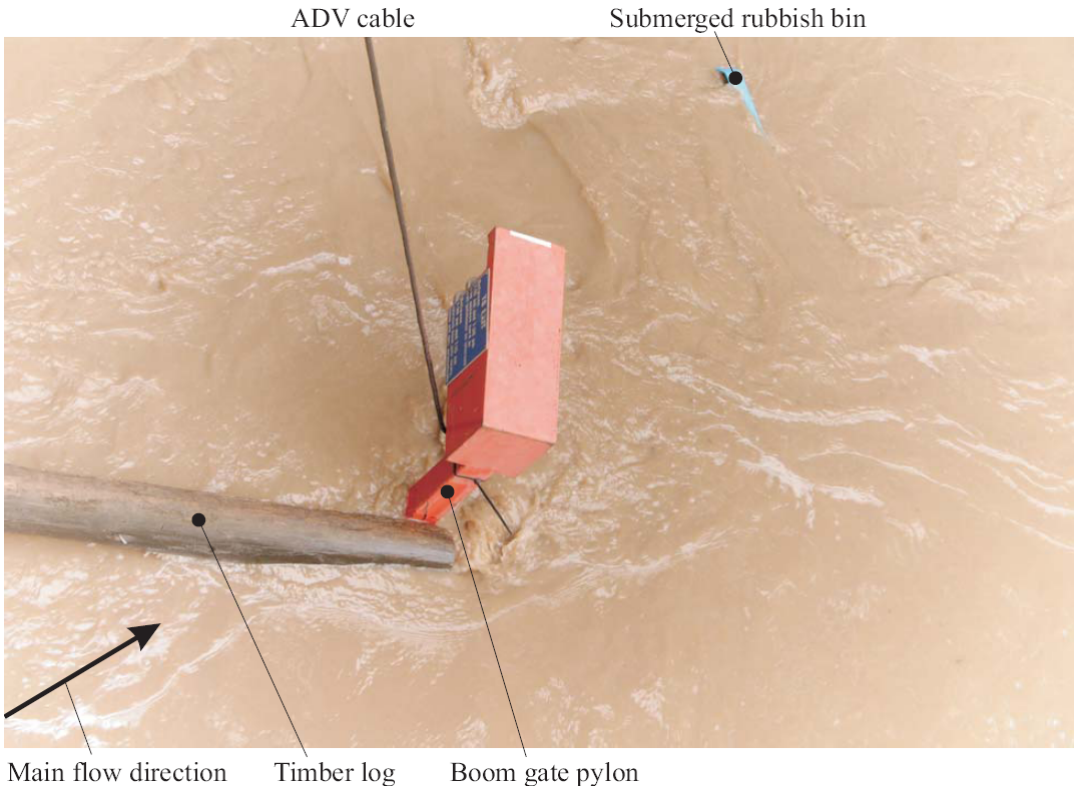

Fig. 2-6 - ADV on 13 January 2011 at 10:40 with the main flow direction from bottom left to top right- Note the timber log jammed in boom gate pylon (left), the stretched ADV cable (middle) and the lid of the plastic 'wheelie' bin barely visible beneath the free-surface (top right)

Fig. 2-7 - ADV on 14 January 2011 at 05:57 after the flood receded - The ADV unit is on the left while the boom gate pylon (white arrow) is seen in the right background, behind the concrete column - The blue arrow shows the main flow direction - Note that the parking concrete slab was

already cleaned up prior to the photograph being taken

On Thursday 13 January 2011, the ADV unit was repositioned to a nearby handrail and mounted vertically (Fig. 2-4B & 2-7). During the fourth deployment (Data file T4, Table 2-1), the ADV unit had to be stopped because the generator was required to assist flood victims whose homes were without electricity. A second, smaller generator was installed and the ADV was restarted two hours later. The fifth deployment (Data file T5, Table 2-1) ended when the flood waters receded and the upper ADV receiver became out of the water (Fig. 2-7).

2.4.3 Comments

After the ADV was dislodged by the impact of a timber log, the ADV unit was inspected and checked. Test T3 was performed specifically to verify the operation of the unit. While the results were successful, an inspection of the ADV system revealed that the stem was very slightly bent. The authors acknowledge that this physical damage might have some effect on the ADV data, although a careful data analysis of tests T3, T4 and T5 showed no obvious problem. Further, the suspended sediment tests were performed with the ADV unit four days later and the results indicated no apparent issue with the ADV operation. Nonetheless the velocity data sets T3, T4 and T5 must be considered with care.

3. SEDIMENT PROPERTIES AND SUSPENDED SEDIMENT CONCENTRATION MEASUREMENTS

3.1 PRESENTATION

The bed sediment material was characterised by a series of laboratory experiments (SHI 2011). The density of the wet sediment samples was about **s** = 1.461. Assuming a sediment density of 2.64 (MORRIS and LOCKINGTON 2002), this would correspond to a sample porosity of 0.72. The particle size distribution data are presented in Figure 3-1 and the results are summarised in Table 3-1. Figure 3-1 includes both the probability distribution functions and cumulative probability distribution functions of the sediment samples (Table 3-1). The results were close considering that they were collected over two different days at four different locations (Table 3-1).

The median particle size was about 25 μm corresponding to some silty materials (GRAF 1971, JULIEN 1995, CHANSON 2004). The sorting coefficient $\sqrt{d_{90} / d_{10}}$ ranged from 21 to 44. The bed material was basically a cohesive mud mixture. The results may be compared with dredged sediment samples collected in the Brisbane River between the city and the river mouth in 2001 (MORRIS and LOCKINGTON 2002, Table 3-1). These samples were collected during a dry period and the particle size data differed substantially from the present observations.

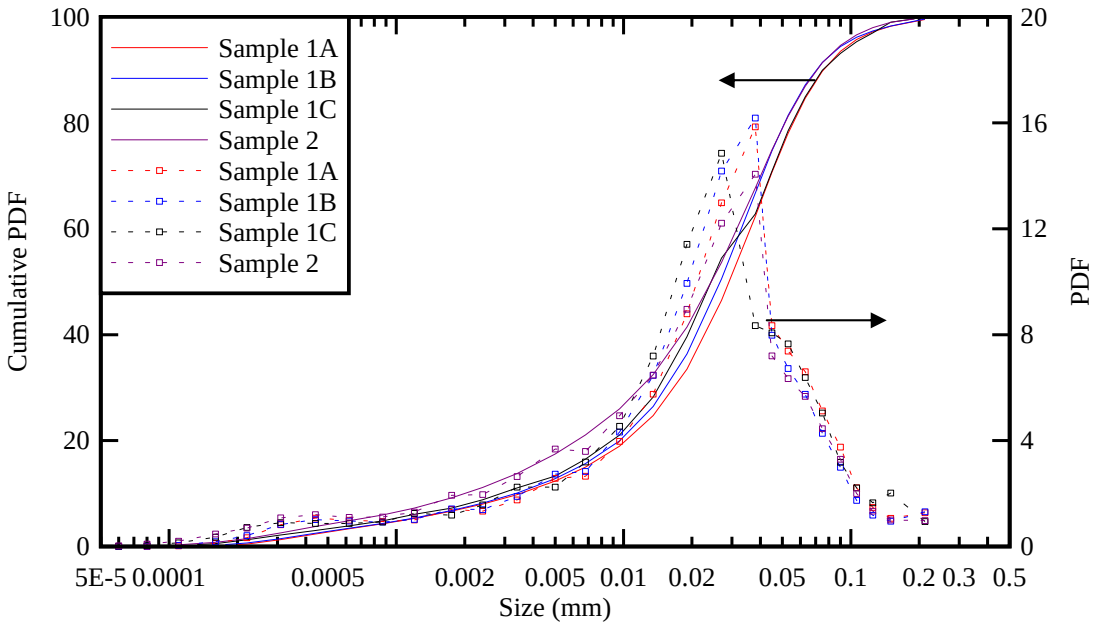

Fig. 3-1 - Particle size distributions of mud samples collected in the QUT Gardens Point campus on 13 and 14 January 2011 (Table 3-1)

Table 3-1 - Characteristics of sediment samples collected in the Brisbane River: flood sediment deposit samples collected along Gardens Point Road next to C Block on 13 and 14 January 2011 (Present study) and dredged sediment samples collected in 2001 (MORRIS and LOCKINGTON 2002)

Sediment deposit	Location	Collection date	Type	d_{50} μm	d_{10} μm	d_{90} μm	d_{90}/d_{10}	% organic carbon %
(1)	(2)	(3)	(4)	(5)	(6)	(7)	(8)	(9)
Flood deposits								
Sample 1A	High waterline at roundabout , end of Gardens Point Rd	13 January 2011	Silt	29.4	3.54	75.9	21.4	8.2
Sample 1B	Concrete footpath beside ADV location B	13 January 2011	Silt	26.7	3.36	88.0	26.2	13.8
Sample 1C	Garden bed beside ADV location B	13 January 2011	Silt	24.6	2.93	91.5	31.2	6.4
Sample 2	B Block parking ramp, Gardens Point Rd	14 January 2011	Silt	24.6	2.02	88.4	43.8	8.6
Dredged sediments								
Sample 1	BP Wharf (AMTD 2 km)	2001	Clayey sand	108.6	--	277.1	--	0.63
Sample 2	Cairncross Dock (AMTD 12.9 km)	2001	Organic silt	< 1.2	--	23.2	--	1.80

Notes: AMTD: adopted middle thread distance, measured upstream from the river mouth; (--): data not available.

The fraction of organic carbon in the sediment samples was determined by loss on ignition. The samples were oven dried at 105 C for 48 hours before being allowed to cool down to room temperature. The subsamples were heated to 300 C for two hours and then to 780 C for 1 hour. The results are listed in Table 3-1 (column 9). On average the fraction of organic carbon was about 8-9%. For comparison, MORRIS and LOCKINGTON (2002) sampled Brisbane River bed materials during a dry period and measured an organic carbon fraction ranging from 0.63 to 1.8%. The 2011 flood sediment data showed comparatively larger organic contents.

The rheometry tests provided some information on the apparent yield stress τ_c of the mud sludge and the effective viscosity μ as functions of the sample density. Note that a more complete characterisation of the rheological behaviour of non-Newtonian mud sludge would require the

determination of further parameters. Within the frame of the present work, we only proceeded to a rapid but also approximate characterisation of the sediment material. It may be expected that, as the solid fraction changes in such silty mixtures, the basic parameters that change are mainly the apparent viscosity and yield stress under given conditions, while the other parameters of the kinetic equation remain more or less constant. The yield stress and apparent viscosity were estimated during the unloading phase to be consistent with earlier studies (ROUSSEL et al. 2004, CHANSON et al. 2006, 2010). The yield stress and apparent viscosity results were derived by fitting the rheometer data with a Herschel-Buckley model. In a Herschel-Bulkley fluid, the relationship between shear stress τ and shear rate $\partial V/\partial z$ is assumed to be:

$$\tau = \tau_c + \mu \times \left(\frac{\partial V}{\partial z} \right)^m \quad (3\text{-}1)$$

where $0 < m \leq 1$ (HUANG and GARCIA 1998, WILSON and BURGESS 1998). For m = 1, Equation (3-1) yields the Bingham fluid behaviour, and a Newtonian behaviour for m=1 and $\tau_c = 0$. The experimental results are presented in Figure 3-2 and Table 3-2. The behaviour of the mud material highlighted some differences between the loading and unloading sequences (Fig. 3-2A). For shear rates $\partial V/\partial z$ larger than 300 s^{-1}, the loading and unloading tests gave close results, suggesting a conservation of the macroscopic structure possibly in the form of particle arrangement into thin layers. For the tests with the undiluted sediment sample (V2A), the apparent viscosity was μ = 8.1 Pa.s, the yield stress was about τ_c = 35.3 Pa and the exponent was m = 0.34. The results are compared with sediment mud samples collected in the Garonne River estuarine zone in Table 3-2. The mud properties differed between the estuarine mud of the Garonne River and the flood deposit mud of the Brisbane River. The latter had a smaller apparent viscosity μ (Table 3-2, column 8).

Table 3-2 - Measured properties of mud/silt samples: Brisbane River flood sediment sample collected along Gardens Point Road next to C Block on 14 January 2011 (Present study) and mud samples collected in the Garonne River estuarine zone (CHANSON et al. 2010)

Study	Sediment sample	Sample ref.	Description	**s**	Solid fraction	τ_c	μ	m
						Pa	Pa.s	
(1)	(2)	(3)	(4)	(5)	(6)	(7)	(8)	(9)
Brisbane River	Sample 2	V2A	Brisbane River sediment	1.461	0.508	35.32	8.10	0.342
		V2B	Diluted (+15 g water)	1.439	0.484	23.36	8.68	0.308
		V2C	Diluted (+30 g water)	1.418	0.470	21.41	4.84	0.347
		V2D	Diluted (+45 g water)	1.400	0.458	14.89	3.13	0.360
Garonne River	Sample 1	Test2	Arcins Channel sediment	1.41	--	49.7	44.7	0.277
	Sample 2	Test3	Arcins Channel sediment	1.41	--	61.4	55.9	0.273

Notes: **s**: wet sediment sample density; (--): data not available.

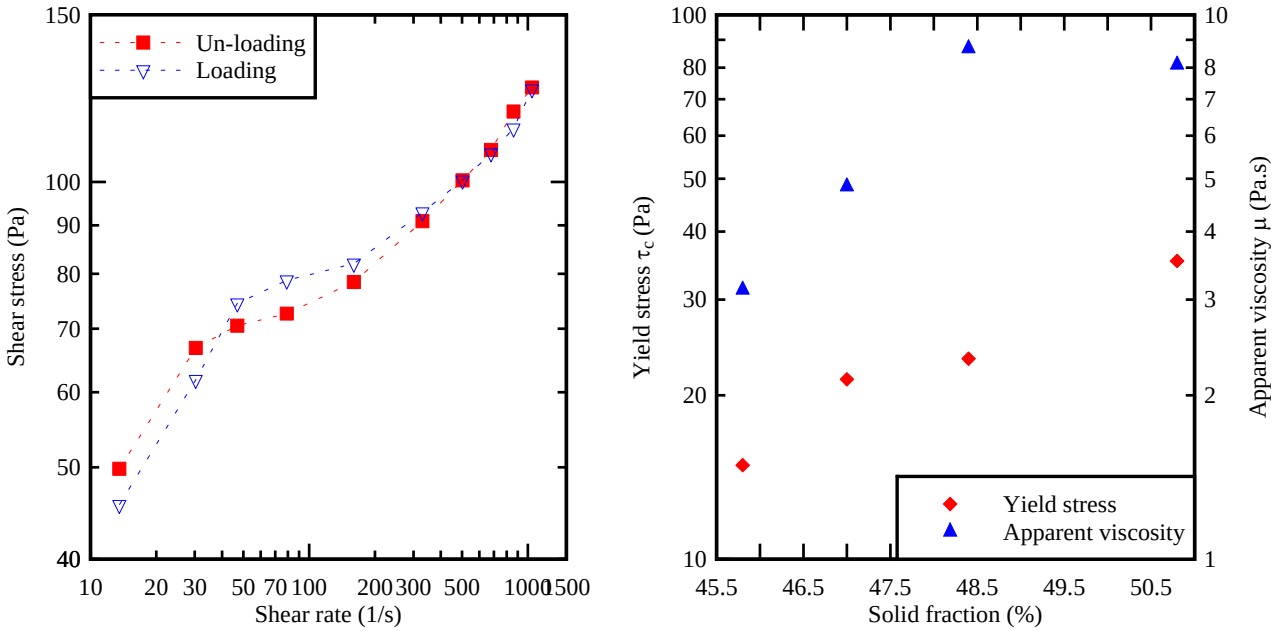

(A, Left) Loading and unloading cycle for sample V2A (original sample)

(B, Right) Effect of the solid fraction on the yield stress and apparent viscosity

Fig. 3-2 - Results of mud/silt sample rheometry tests

3.2 ACOUSTIC BACKSCATTER AMPLITUDE AND SUSPENDED SEDIMENT CONCENTRATION

The acoustic Doppler velocimeter (ADV) is designed to record the instantaneous velocity components at a single-point with relatively high frequency. Additionally the ADV signal strength, or acoustic backscatter strength, may be related to the instantaneous suspended sediment concentration (SSC) with proper calibration (KAWANISI and YOKOSI 1997, FUGATE and FRIEDRICHS 2002). Although the method was initially developed for non-cohesive sediments, it was recently extended successfully to cohesive materials (CHANSON et al. 2008, HA et al. 2009, CHANSON et al. 2010, SALEHI and STROM 2011). Some thorough experiments indicated that the acoustic backscatter intensity increased monotically with increasing SSC for relatively low suspended sediment loads (FUGATE and FRIEDRICHS 2002, CHANSON et al. 2008). For high suspended loads, the ADV backscatter intensity decreased with increasing SSC. The trend is believed to highlight some signal saturation linked to multiple scattering and associated sound absorption (HA et al. 2009, CHANSON et al. 2010).

Within the experimental conditions, the relationships between acoustic backscatter amplitude

(Ampl) and suspended sediment concentrations (SSC) were tested systematically for SSCs between 0 and 98 kg/m^3. The experimental results are summarised in Figure 3-3. The full data sets are reported in Appendix C.

First the data trend was independent of the ADV settings. No difference was observed between the ADV settings on 12 January and 13 January 2011. Second there was a good agreement between all the data showing two characteristic trends. For SSC ≤ 3.2 kg/m^3, the data yielded a monotonic increase in suspended sediment concentration with increasing backscatter signal amplitude. For larger SSCs (i.e. SSC > 3.2 kg/m^3), the experimental results demonstrated a decreasing signal amplitude with increasing SSC.

For the laboratory tests with low suspended loads (SSC ≤ 3.2 kg/m^3), the best fit relationships were:

$$SSC = 1.578 \times 10^{-77} \times (Ampl + 5.076)^{26.865} \qquad SSC \leq 3.2 \text{ kg/m}^3 \quad (3\text{-}2a)$$

$$SSC = 1.916 \times (BSI - 0.21)^{2.463} \qquad SSC \leq 3.2 \text{ kg/m}^3 \quad (3\text{-}2b)$$

where the suspended sediment concentration SSC is in kg/m^3, and the amplitude Ampl is in counts and the acoustic backscatter intensity BSI is deduced from the average amplitude as:

$$BSI = 10^{-5} \times 10^{0.043 \times Ampl} \qquad (3\text{-}3)$$

where the backscatter intensity BSI is dimensionless, the average amplitude Ampl is in counts and the coefficient 10^{-5} is a value introduced to avoid large values of backscatter intensity (NIKORA and GORING 2002, CHANSON et al. 2008). Equations (3-2a) and (3-2b) were correlated with a normalised correlation coefficient of 0.994.

For large suspended sediment concentration within 3.2 < SSC < 98 kg/m^3, the results showed a good correlation between the acoustic backscatter strength and the SSC, although the ADV signal was saturated as observed by CHANSON et al. (2010). For SSC > 3.2 kg/m^3, the data were best correlated by

$$SSC = 81.44 - 0.636 \times Ampl \qquad 40 > SSC > 3.2 \text{ kg/m}^3 \quad (3\text{-}4a)$$

$$SSC = 5.7405 - 8.583 \times Ln(BSI) \qquad SSC > 3.2 \text{ kg/m}^3 \quad (3\text{-}4b)$$

with a normalised correlation coefficient of 0.982 and 0.940 respectively. Equations (3-2) and (3-4) are compared with the data in Figure 3-3.

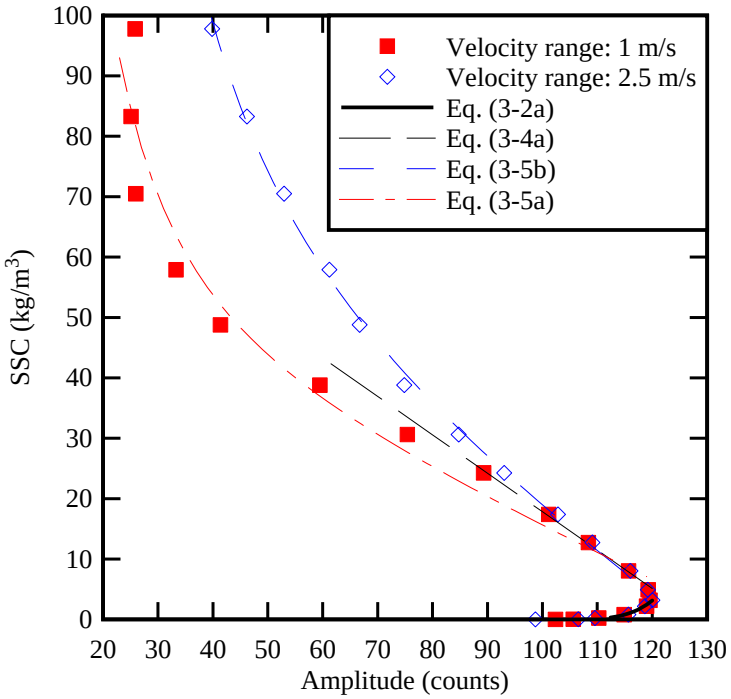

(A) Relationship between suspended sediment concentration (SSC in kg/m^3) and acoustic signal amplitude (Ampl in counts)

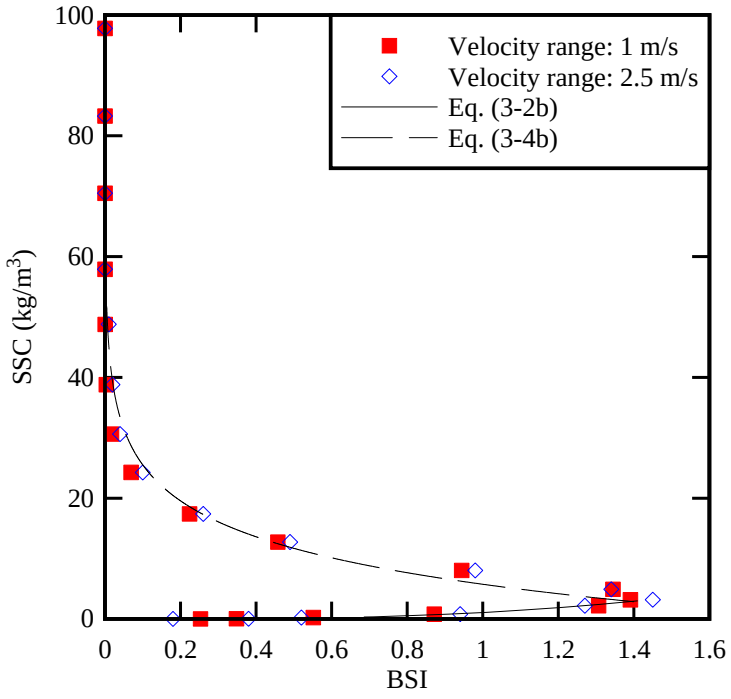

(B) Relationship between suspended sediment concentration (SSC in kg/m^3) and acoustic backscatter intensity (BSI)

Fig. 3-3 - Relationship between suspended sediment concentration, acoustic signal amplitude and acoustic backscatter intensity with the sediment mud collected along Gardens Point Road - Comparison between the data and Equations (3-2), (3-4) and (3-5)

Discussion

The data showed some slight differences between the two ADV settings: namely the velocity range had some impact on the upper calibration curve (Fig. 3-3A). The difference might be linked with the flow conditions. At the highest SSCs (SSC > 55 kg/m^3), the mixer speed was set to 520 rpm to prevent sedimentation and it was likely the velocity in the ADV sampling volume exceeded 1 m/s. As a result, the calibration data at high SSCs must be considered with care with the 1.0 m/s velocity range.

Equation (3-4a) was valid within 3.2 < SSC < 40 kg/m^3. For larger SSCs, the ADV velocity range settings had some impact on the best data fit as seen in Figure 3-3A. For SSC > 3.2 kg/m^3, the data were best correlated by:

$$SSC = 54.23 - 0.4113 \times Ampl + \frac{25518}{Ampl^2} \qquad \text{velocity range: 1.0 m/s} \quad (3\text{-}5a)$$

$$SSC = 72.61 - 0.6174 \times Ampl + \frac{81229}{Ampl^2} \qquad \text{velocity range: 2.5 m/s} \quad (3\text{-}5b)$$

with a normalised correlation coefficient of 0.980 and 0.999 respectively.

During the present field investigations, the authors observed that the Brisbane River water was very turbid. They could not see their fingers below 2-3 cm from the water surface. In the Brisbane River in flood, the current speeds exceed the critical erosion. A number of field observations showed that, during large flood periods similar to the present investigation, the Brisbane River water was murky and its suspended sediment load would exceed 3 kg/m^3 (HORN et al. 1999). Therefore Equations (3-4) and (3-5) were considered to be representative of the relationship between the suspended sediment concentration (SSC), signal amplitude (Ampl) and acoustic backscatter intensity (BSI) in the Brisbane River flood plain at QUT on 12 and 13 January 2011 ([1]).

[1] Herein the SSCs were calculated from the ADV signal amplitude data using Equations (3-5a) and (3-5b).

4. FLOW OBSERVATIONS

4.1 BASIC OBSERVATIONS

During the rising stage of the Brisbane River flood on Tuesday evening and Wednesday, the river swelled and inundated parts of western Gardens Point. The inundated flood plain included the car parks located beneath the South-East Freeway and Captain Cook Bridge (Fig. 4-1A, right), Gardens Point Road and the car parks (level 1) of C Block, S Block and Z Bock of QUT Gardens Point campus (Fig. 4-1 & 4-2). On the left bank, a relatively fast flow motion was observed along Gardens Point Road from Parliament House to the Goodwill Bridge (Fig. 4-1 & 4-2). Figure 4-1 shows the flood flow along Gardens Point Road on Wednesday 12 January 2011 morning. Figure 4-2 presents a series of photographs taken on Thursday 13 January morning at the downstream end of Gardens Point Road in front of C Block. Further photographs are regrouped in Appendix A.

Visual and photographic observations indicated that the free-surface flow in Gardens Point Road was subcritical. That is, the flood flow behaved like a fluvial motion controlled by the downstream conditions (HENDERSON 1966, CHANSON 2004). During the flood, the authors went into the C Block car park (level 1) to install the ADV system and later to re-locate the unit. They observed some very slow fluctuations of the water level, together with some water surges. At times, they felt some faster running water between their legs. The concrete invert was flat and no sediment deposition was felt on the floor. It is believed that the fast flowing water prevented any deposition.

(A) Gardens Point Road on Wednesday 12 January 2011 at 10:07 looking downstream from Z

Block (Photograph courtesy of QUT Facilities Management)

(B) Gardens Point Road on Wednesday 12 January 2011 at 10:08 looking downstream from C Block (Photograph courtesy of QUT Facilities Management)

(C) Roundabout at the southern end of Gardens Point Road on Wednesday 12 January 2011 at 11:49 with C Block on the right, the Brisbane River main channel on the far left (background) and the flood flow from background right to left (Photograph courtesy of QUT Facilities Management)

Fig. 4-1 - Photographs of the flow in Gardens Point Road - Black arrows shows the flow direction

(A) General view of Gardens Point Road viewed from C Block parking level 2 on Thursday 13 January 2011 at 10:39 (Photograph Hubert CHANSON) - Flow from right to left, with Captain Cook Bridge in the background

(B) Main flow in Gardens Point Road looking upstream (NW) on Thursday 13 Jan. 2011 at 11:40 - Flow from background right to foreground left

(C) Submerged ADV system (on foreground right) in operation on Thursday 13 Jan. 2011 at 11:40

Fig. 4-2 - Photographs of the sampling site in Gardens Point Road during the flood (Photographs Hubert CHANSON) - Black arrows shows the flow direction

On Thursday afternoon and evening, the river receded and left a layer of soft mud covering the inundated parts of Gardens Point. On Friday morning, Gardens Point Road and the car parks were covered by a 2-10 cm thick layer of mud and silt. The properties of the mud were tested in a laboratory after the event (section 3).

4.2 WATER ELEVATIONS

The water elevation and fluctuations were recorded manually at the start of three tests and using the ADV pressure sensor during tests T1 and T2 ([1]). The manual observations are summarised in Table 4-1 (columns 5 & 6). The results are reported in Figure 4-3 showing the manual observations expressed in m AHD ([2]) and the instantaneous water level h ([3]) measured above the ADV sensor as a function of the time since 00:00 on Wednesday 12 January 2011. The data are compared with the Brisbane River levels recorded at the City Gauge ([4]) located about 1.55 km downstream of the

[1] For tests T3, T4 and T5, the ADV pressure sensor was out of the water.

[2] Elevation above mean sea level or Australian Height Datum (AHD).

[3] h is the pressure head equal to the water depth above the sensor assuming hydrostatic pressure distribution.

[4] The Brisbane City Gauge is located at the end of Edward Street in the CBD, on the left bank. The Alert

sampling site ([5]).

Both the manual observations and water level fluctuations showed some trends that were close to the Brisbane River record at the City Gauge. The water level rose slightly on Wednesday 12 January evening until the Brisbane River peaked on Thursday morning around 04:00. The water elevation dropped on Thursday 13 January morning and afternoon, and the sampling site was dry about 20:00 in the evening.

The manual observations of water elevation were higher than the City Gauge data on Wednesday evening and Thursday mid-day (0.16 m on average for the two readings). The trend would be consistent with the upstream location of the sampling site and the associated head losses between the two locations. Some differences might also be linked with the different reading techniques and site location: the City Gauge is located in the main river channel while the present readings were taken in the left flood plain. On Thursday afternoon, the last manual reading (t = 145,800 s, Fig. 4-3) was lower than the City Gauge data, possibly because of the drawdown of the Brisbane River and the effects of local topography on the shallow water flow. The water depth was less than 0.26 m at the sampling site at the time.

Table 4-1 - Manual observations of the water depth and elevation in Gardens Point on 12-13 January 2011

Data point	ADV location	Date and time	Time (*)	Water depth d	Water level elevation	Fr	E	M
			s	m	m AHD		m	m^2
(1)	(2)	(3)	(4)	(5)	(6)	(7)	(8)	(9)
1	A	12 Jan. 2011 at 20:00	72,000	0.89	4.31	0.17	0.90	0.42
2	B	13 Jan. 2011 at 11:30	127,800	0.67	4.09	0.22	0.69	0.25
3	B	13 Jan. 2011 at 16:30	145,800	0.26	3.68	0.21	0.27	0.04

Notes: Location A: ADV unit mounted horizontally on boom gate support; Location B: ADV unit mounted vertically on a hand rail; d: water depth measured above the concrete invert; Fr: local Froude number; E: specific energy; M: specific momentum; Fr, M and E were estimated using the mean longitudinal velocity measurements; (*): time since 00:00 on 12 Jan. 2011.

The pressure sensor readings highlighted some large fluctuations of the water level around its mean trend (black thick line, Figure 4-3). While the standard deviation of the fluctuations was 0.1 m on

---

Gauge is slightly below the Thornton Street ferry pier on the right bank.

[5] Distance measured following the main river channel centreline.

average for the entire data set, the authors observed significant fluctuations of the water level with a period about 50 to 60 s when they were in the water to install and later to re-position the ADV unit on 12 January evening and 13 January mid-day respectively. These long-period fluctuations were associated with changes in water elevations of up to 0.1 to 0.2 m (visual observations). A fast Fourier transform (FFT) of the pressure sensor signal is presented in Figure 4-4. Both the raw and smooth-filtered FFT data are shown ([6]). The data highlighted a marked peak with a frequency corresponding to a period of about 60 s. In Figure 4-4, the smoothed-filtered PSD function data peaked at 0.0171 Hz (T = 58.5 s).

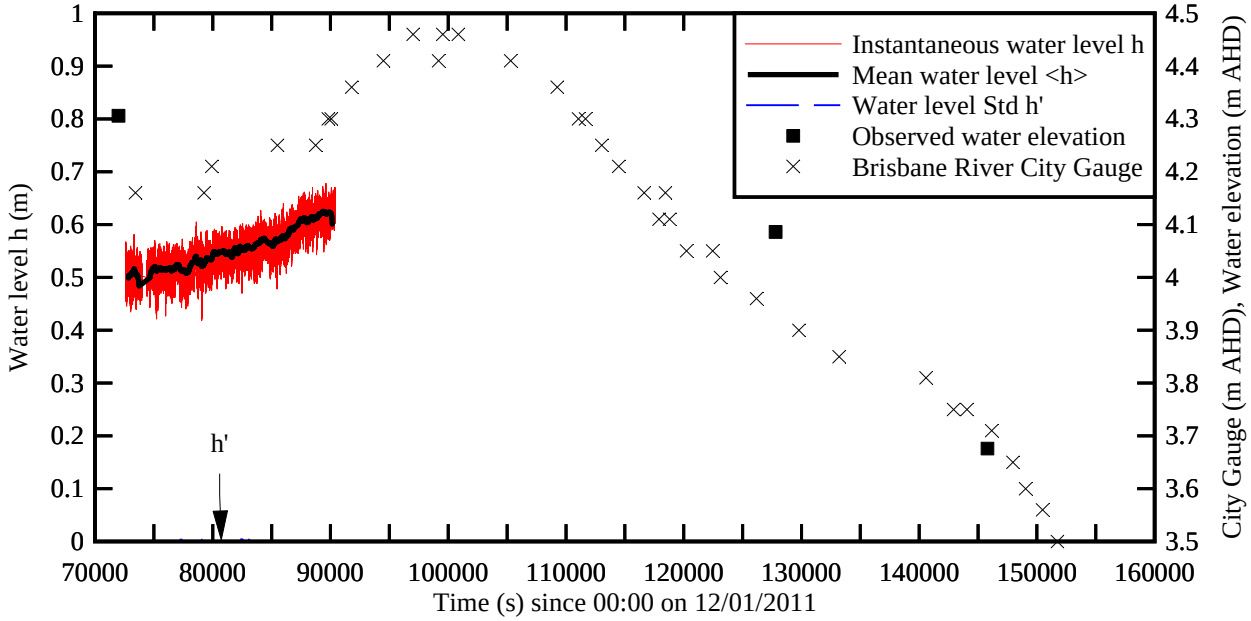

Fig. 4-3 - Fluctuations of instantaneous water level h measured above the ADV pressure sensor - Comparison with the manual observations and the Brisbane River City Gauge data (Source: BOM) - Both the manual observations and Brisbane River City Gauge data are reported in m AHD

[6] FFT of low-pass filtered data (0-5 Hz) smoothed with a window of 20 points.

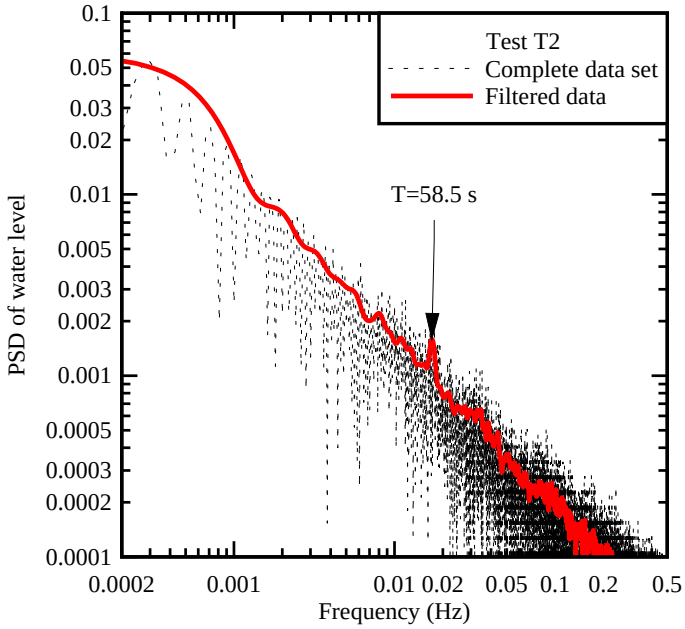

Fig. 4-4 - Spectral analysis of the water level fluctuations: raw FFT (dashed line) and smooth and filtered FFT (thick red line) - Test T2

4.3 DISCUSSION

The visual observations on Wednesday 12 January 2011 evening and Thursday 13 January 2011 highlighted some low-frequency fluctuations in water elevation and longitudinal velocity at both ADV sampling locations. These were confirmed by some spectral analyses of sampled data (Fig. 4-4 & section 5.1). The source of these oscillations was likely linked with the geometry and configuration of the surrounding urban environment, in particular of the C Block (level 1) car park (Fig. 4-5). Figure 4-5 presents a three-dimensional CAD drawing of the C Block level 1. The two ADV locations are shown together with some main flow directions.

In a free-surface flow, the first mode of natural resonance has a period:

$$T_{res} = \frac{2 \times l}{\sqrt{g \times d}} \qquad (4\text{-}1)$$

where T_{res} is the resonance (or sloshing) period, l is the characteristic development length of the sloshing, g is the gravity acceleration and d is the mean flow depth. During the present study, the main direction of the flow at the sampling locations was from C Bock level 1 car park towards Gardens Point Road and Goodwill Bridge (Fig. 2-1 & 4-5). Equation (4-1) was applied to the main horizontal dimensions (length, width) of the building car park (level 1) for the three observed water depths listed in Table 4-1. The results are regrouped in Table 4-2 showing a natural resonance period about 50-80 s linked with the length of the building and consistent with the field observations (section 5).

Table 4-2 - First mode of the sloshing period of the free-surface flow in C Block (level 1) on 12 and 13 January 2011

Depth d m (1)	Sloshing period (s)				Remark (6)
	C Block full length (L=70.2 m) (2)	C Block full width (B=33.6 m) (3)	Length to staircase (L1=29.3 m) (4)	Throat width between staircases (B1=10 m) (5)	
0.89	47	23	20	6.8	12 Jan. 2011 at 20:00
0.67	55	26	23	7.8	13 Jan. 2011 at 11:30
0.26	88	42	37	12	13 Jan. 2011 at 16:30

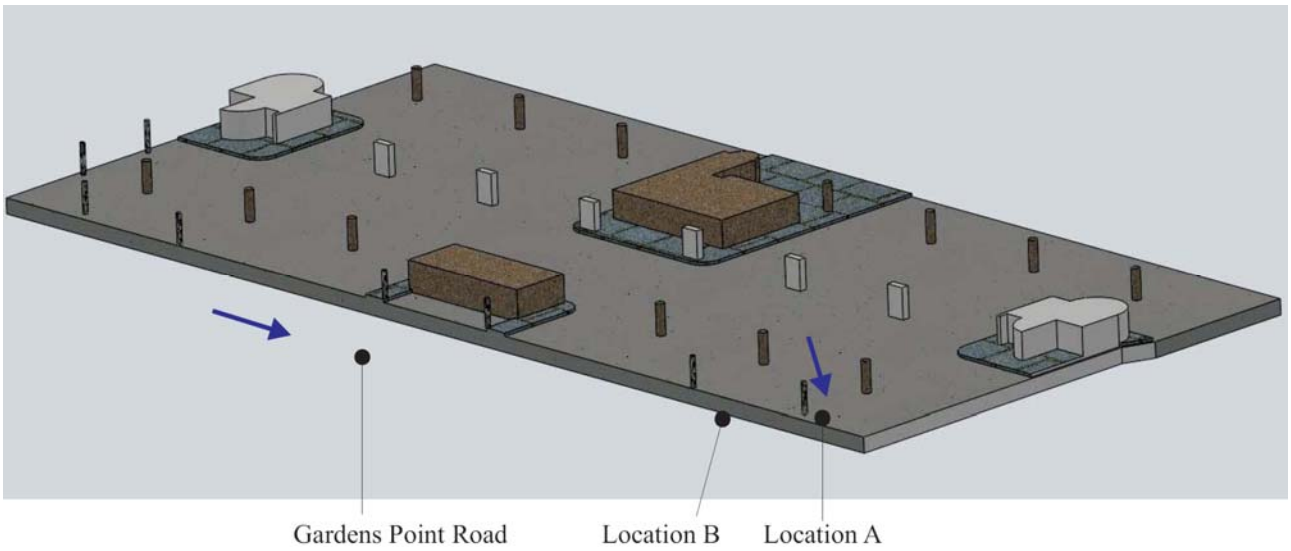

Fig. 4-5 - C Block (level 1) car park - Three-dimensional CAD drawing - The blue arrows show the main flow directions in Gardens Point Road and eastern end of car park - The brown coloured sections are the staircase wells

5. TURBULENT VELOCITY AND SUSPENDED SEDIMENT CONCENTRATION MEASUREMENTS

5.1 PRESENTATION

The measurements of water level h, longitudinal velocity V_x and velocity flux $q = V_x \times h$ showed some low-frequency oscillations with periods of about 50 to 90 s. Figure 5-1 shows some frequency analyses of the water level, longitudinal velocity and velocity flux fluctuations during test T2. Both the raw and smooth-filtered FFT data are shown. The results highlighted the long-period oscillations with periods between 3 s and 500 s, as well as a peak in power spectrum density (PSD) functions at about 50 to 60 s. Some sensitivity analyses (not shown here) were conducted on the data samples T1, T2 and T3 to investigate the effects of the cut-off frequencies on the triple decomposition of the velocity component, depth and velocity flux data. The results indicated that the mean velocity <V> was little affected by a cut-off frequency below 0.002 to 0.005 Hz, while the turbulent component v and its standard deviation were nearly independent of an upper cut-off frequency greater than 0.1 to 0.3 Hz. Note that the power spectrum density (PSD) functions of the longitudinal velocity and velocity flux presented some local minima for frequencies about 0.002-0.005 and 0.1-0.3 Hz (Fig. 5-1).

The triple decomposition of the instantaneous velocity data was applied successfully to periodic flows and turbulent structures in riverine systems (HUSSAIN and REYNOLDS 1972, FOX et al. 2005). In the present study, the instantaneous velocity time-series may be represented as a superposition of three components:

$$V = < V > + [V] + v \qquad (5\text{-}1)$$

where V is the instantaneous velocity, <V> is the mean velocity contribution, [V] is the slow fluctuating component of the velocity and v corresponds to the turbulent motion. Herein <V> is the low-pass filtered data with a cut-off frequency of 0.002 Hz (1/500 s^{-1}). The slow fluctuating component [V] is the band-passed signal with the upper and lower cut-off frequencies set at 0.33 Hz and 0.002 Hz (1/3 s^{-1} and 1/500 s^{-1} respectively). The turbulent component v is the high-pass filtered data with a cut-off frequency of 0.33 Hz (1/3 s^{-1}). All the statistical properties of the turbulent velocity components were calculated over a 500 s interval (25,000 data samples).

The same triple decomposition treatment was applied to the fluctuations of water depth, velocity flux, suspended sediment concentration (SSC) and suspended sediment flux.

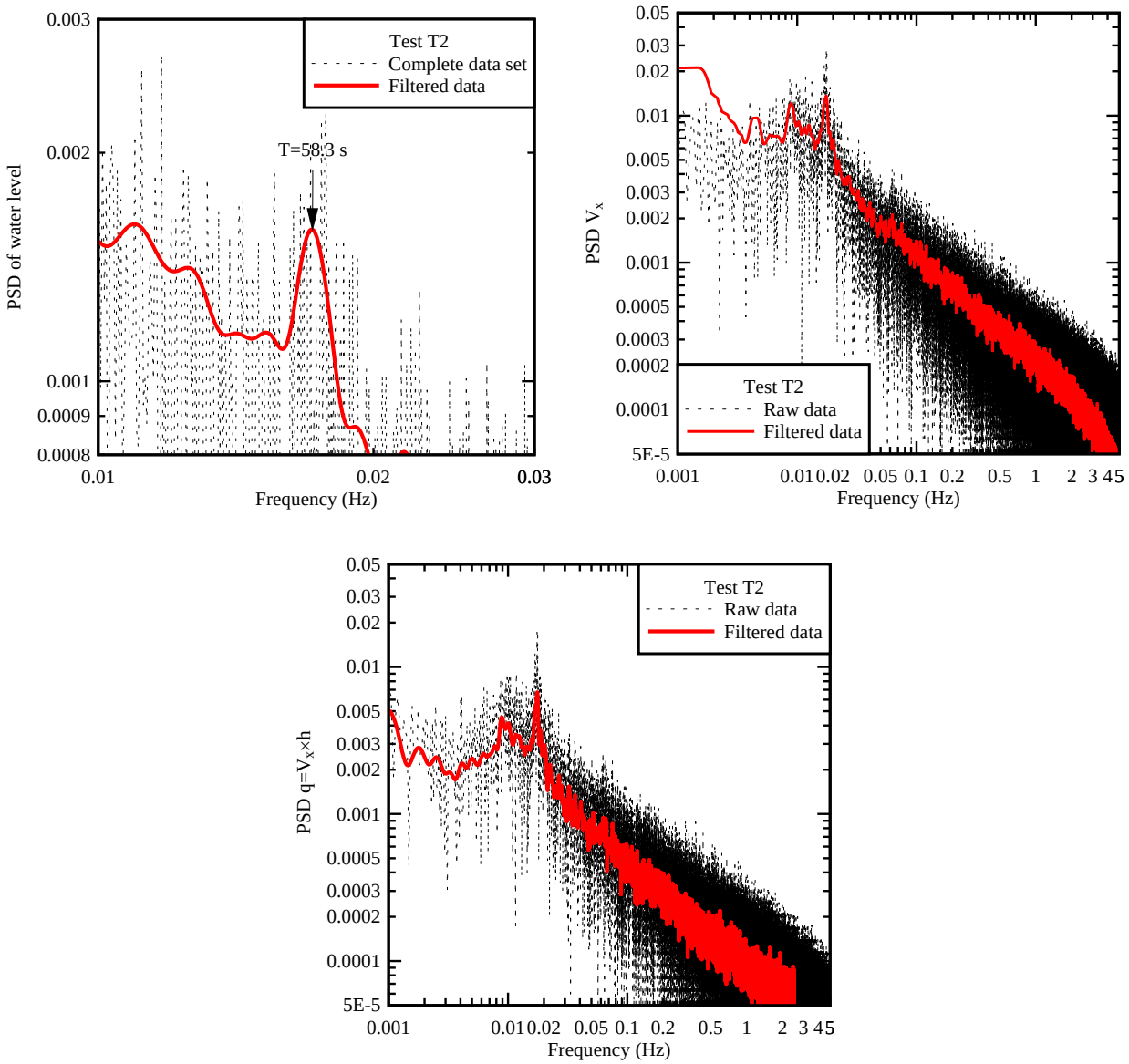

Fig. 5-1 - Spectral analysis of the fluctuations of water level h, longitudinal velocity V_x and velocity flux V_x×h: raw FFT (dashed line), and filtered and smoothed FFT (thick red line) - Test T2

5.2 MEAN FLOW PROPERTIES

5.2.1 Basic results

The time-variations of the pressure head h and velocity flux q = h×V_x are presented in Figures 4-3 and 5-2 respectively. Herein h is the pressure head recorded by the ADV pressure sensor and equal to the water level above the ADV unit assuming a hydrostatic pressure distribution. V_x is the longitudinal velocity component positive downstream and its direction is defined in Table 2-1 (column 8). Each figure includes the instantaneous data, the mean value <h> and <q> (low-pass filtered data with 0.002 Hz cut-off frequency) and the standard deviation h' and q' of the turbulent fluctuation component (high-pass filtered data with 0.33 Hz cut-off frequency). The Brisbane City

Gauge data are shown for comparison.

The water level data presented a mean trend which was close to the Brisbane River record at the City Gauge (Fig. 4-3). That is, the water level rose gently on Wednesday 12 January evening until the Brisbane River peaked on Thursday early morning. The present data showed however a great level of detail because of the high-temporal resolution. The water level fluctuations were significant. On average during test T2, the mean deviation of the instantaneous water level from the mean level was $(h - \langle h \rangle)' = 0.10$ m. The large fluctuations were predominantly caused by relatively long-period oscillations with periods greater than 3 s (sections 4.3 & 5.2.2). The standard deviation of the turbulent fluctuations ([1]) was significantly smaller: $h' = 0.003$ m on average for test T2 (Fig. 4-3).

The velocity flux q is homogeneous to a longitudinal volume discharge per unit width defined herein in terms of the longitudinal velocity measured 0.35 m above the invert and the water level h recorded above the ADV pressure sensor ([2]). The field measurements showed large fluctuations around an almost constant trend line (Fig. 5-2). For tests T1 and T2, $\langle q \rangle = 0.25$ m^2/s on average, and the deviation from the mean flux was $(q - \langle q \rangle)' = 0.10$ m^2/s on average. For comparison, the standard deviation of the turbulent flux fluctuations was significantly smaller: $q' = 0.018$ m^2/s on average. The large and relatively slow fluctuations in velocity flux were consistent with the personal observations by the investigators who could feel some water surges every minute to every couple of minutes when they were in the water beside the ADV unit.

The time-variations of the velocity components are presented in Figure 5-3. Herein V_x is the longitudinal velocity positive downstream with its direction defined in Table 2-1 (column 8), V_y is the horizontal transverse velocity positive towards roughly 71º and 82º for locations A and B respectively, and V_z is the vertical velocity positive upwards. The graphs include the instantaneous data V, the mean value $\langle V \rangle$ and the standard deviation v' of the turbulent fluctuations. The experimental data showed a slow decrease in longitudinal velocity magnitude during tests T1 and T2 (location A) while the water level was increasing gently. The trend in terms of longitudinal velocity was unexpected since the mean velocity would be expected to increase during the rising stage. This might be linked with some local geometry effects. During the receding flood (tests T3, T4 and T5), the velocity magnitude decreased with increasing time and declining water level. The last test (T5) was conducted in very shallow waters. The velocity magnitude was very small $\langle V_x \rangle \sim 0.002$ m/s on average during test T5. The local water depth ranged from about 0.26 m down to 0.10

[1] High-pass filtered data with 0.33 Hz cut-off frequency.

[2] Note that the pressure sensor was about 0.05 m above the ADV sampling volume during tests T1 and T2. That is, it was about 0.40 m above the concrete invert.

m, when some receivers came out of the water. Afterwards the ADV data became meaningless and the record was terminated.

The transverse velocity data fluctuated around zero (Fig. 5-3B). The fluctuations were smaller than the fluctuations of the horizontal and vertical velocity components. On average, the standard deviation of transverse velocity fluctuations about the mean was 0.4 times the standard deviation of the longitudinal velocity fluctuations about the mean: i.e., $(V_y-<V_y>)'/(V_x-<V_x>)' \approx 0.4$. The lesser transverse velocity fluctuations seemed to be a feature to the flood flow motion because the same trend was observed at both locations with two different ADV settings and mountings.

While the transverse velocity data were about zero on average, the vertical velocity data were typically non-zero and positive in particular at location A. For tests T1 and T2, the ADV was positioned above a small traffic island (Fig. 5-4). The geometry was close to a forward-facing step investigated by TACHIE et al. (2004) and SHERRY et al. (2009). The forward-facing step induced a significant modification of the streamlines with the likely formation of a recirculation bubble redirecting upwards the streamlines and mean flow (Fig. 5-4B). Figure 5-4B shows an idealised recirculation bubble for a turbulent flow past a forward-facing step. The exact flow pattern was complicated by the skewed flow direction with the island kerb (Fig. 5-4A) as well as by the presence of surrounding obstacles including some upstream structural column.

The instantaneous and mean velocity data indicated some unusual event during test T4 about t = 136,000 to 140,000 s (Fig. 5-3 & 5-5). That is, on Thursday 13 January 2011 between 13:40 and 14:45. During this event, the mean flow direction shifted by up to 12º to the left when looking downstream (Fig. 5-5B) while the transverse turbulent fluctuation increased sharply (Fig. 5-5A). The same event was also associated with a sharp increase in suspended sediment concentration (see below). The exact causes of this unusual flow pattern are unknown, but its impact on the flow in Gardens Point Road was clearly recorded.

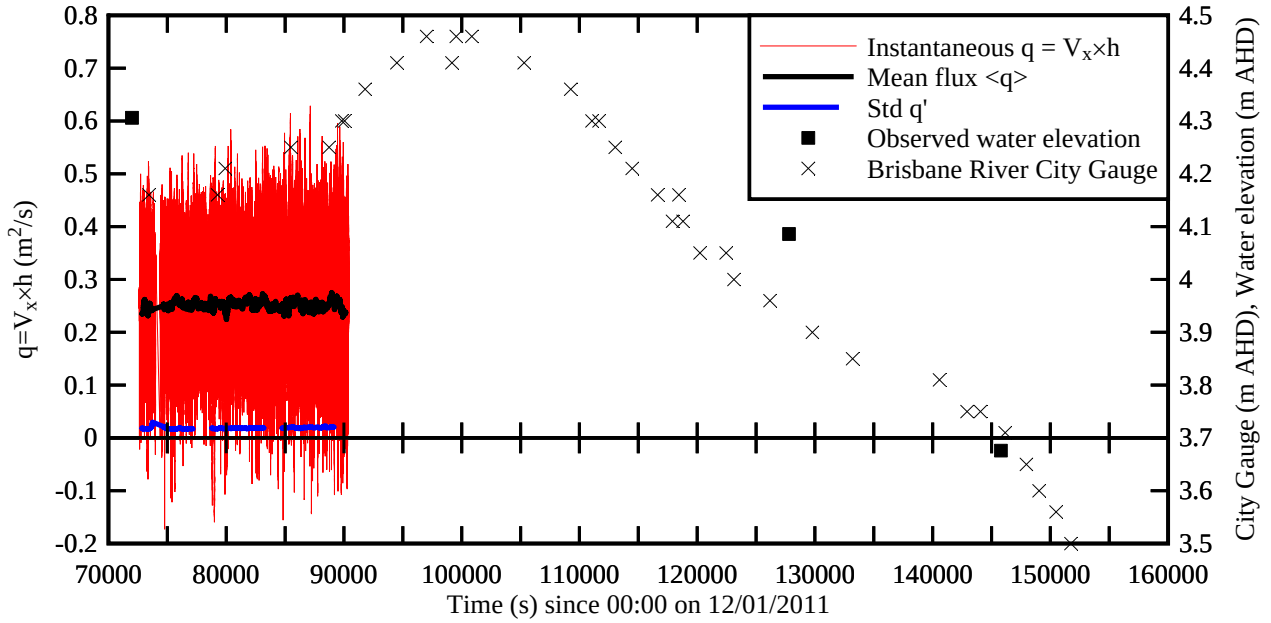

Fig. 5-2 - Time variations of the velocity flux q = h×V_x: instantaneous flux q, mean velocity flux <q> and standard deviation q' of the turbulent fluctuation component (high-pass filtered data with 0.33 Hz cut-off frequency) - Comparison with the manual observations and Brisbane River City Gauge data (Source: BOM) - Both manual observations and Brisbane River City Gauge data are reported in m AHD

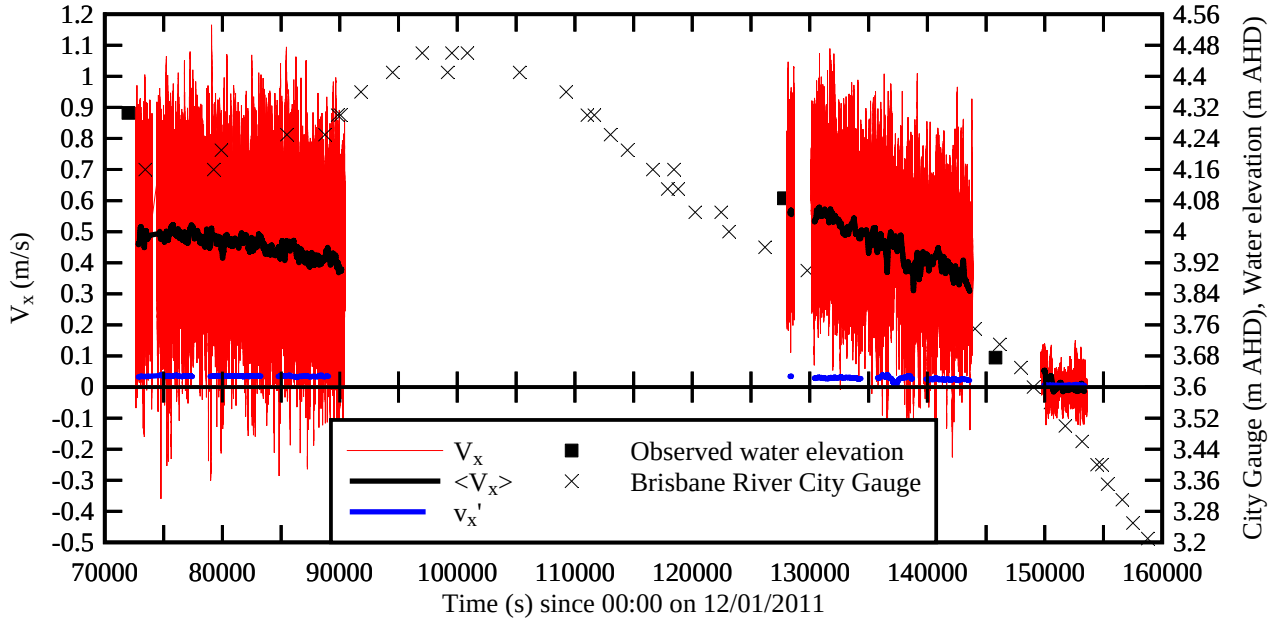

(A) Longitudinal velocity component V_x - Note that the direction of the longitudinal velocity is defined in Table 2-1

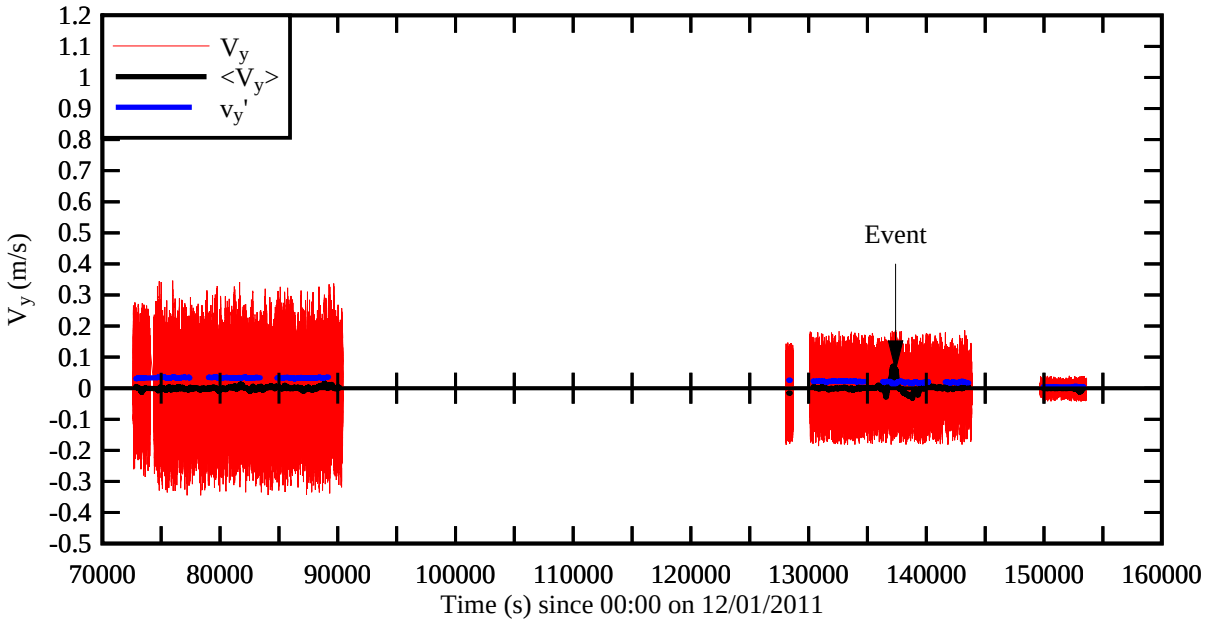

(B) Horizontal transverse velocity component V_y

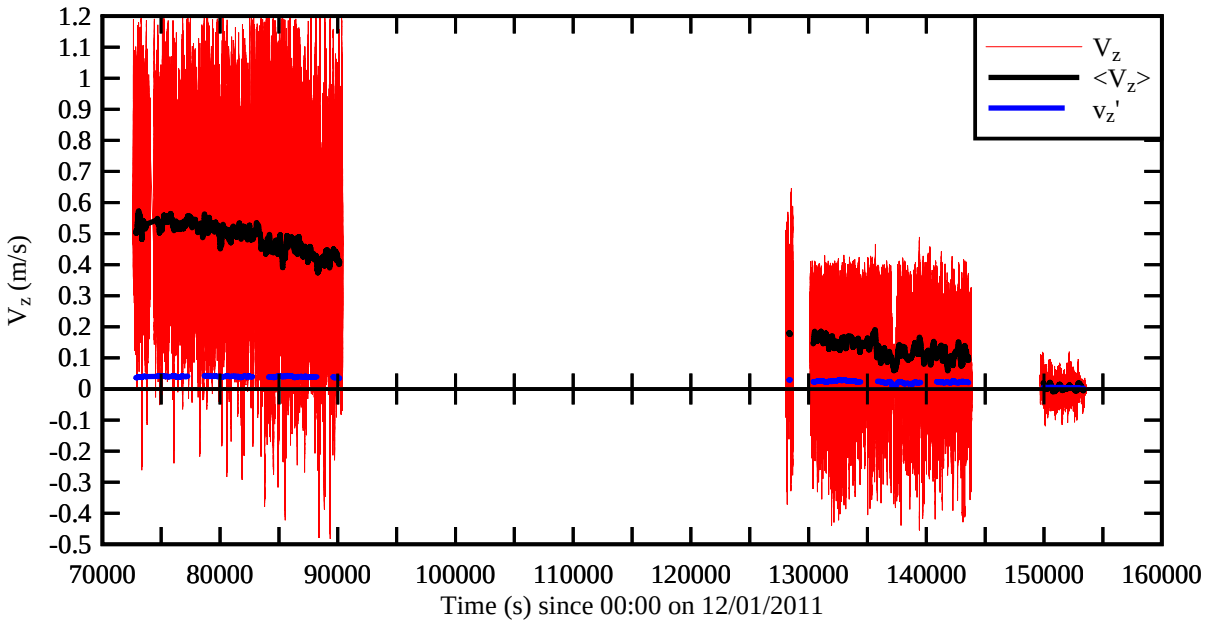

(C) Vertical velocity component V_z

Fig. 5-3 - Time variations of the velocity components: instantaneous velocity V, mean velocity <V> and standard deviation v' of the turbulent fluctuation component

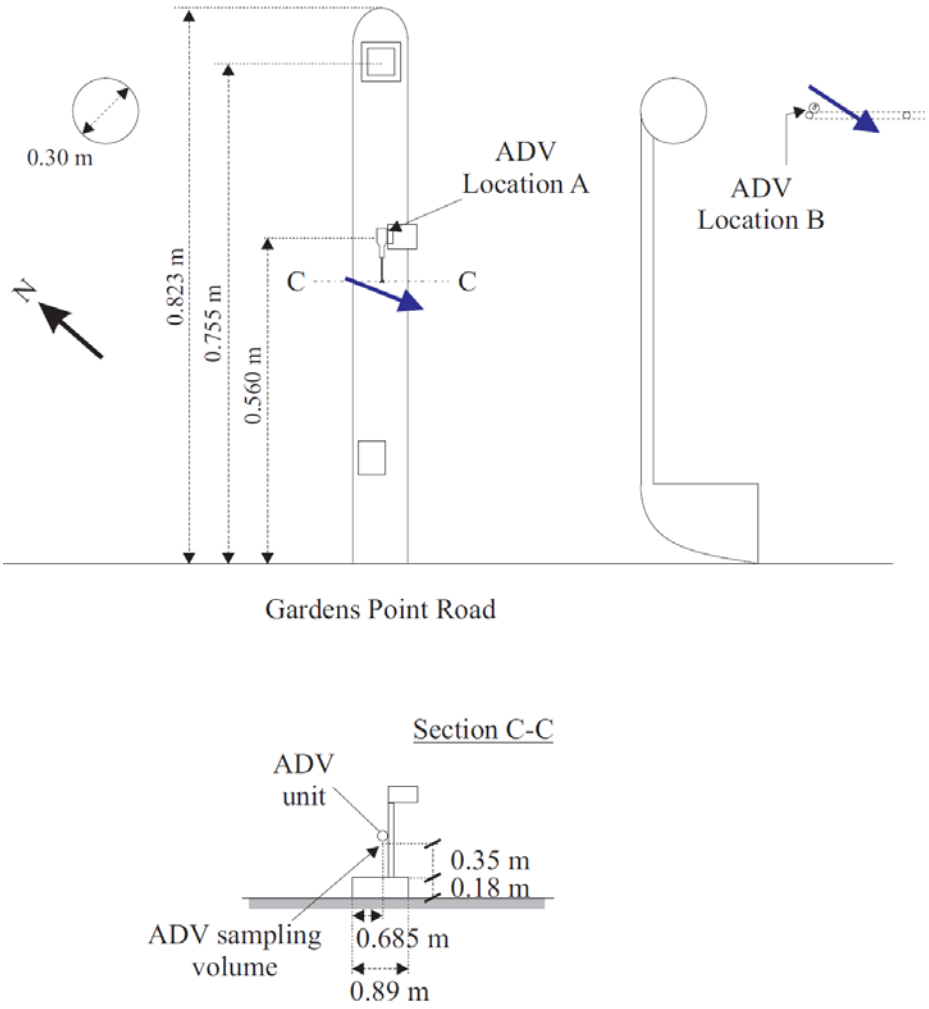

(A) ADV mounting at location A with the forward facing step geometry created by kerb (not to scale) - Top: View in elevation; blue arrows show mean flow direction during tests T1 & T2 (location A) and tests T3, T4 & T5 (location B) - Bottom: Side view looking from Gardens Point Rd

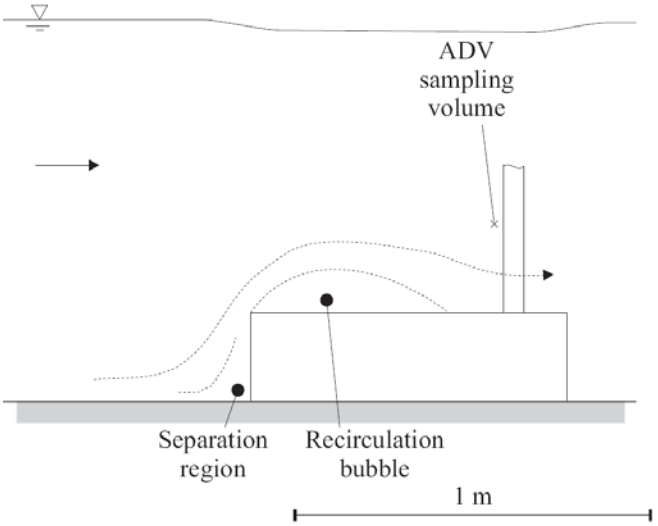

(B) Streamline pattern around the kerb (dimensioned sketch)

Fig. 5-4 - ADV mounting at location A on a traffic island

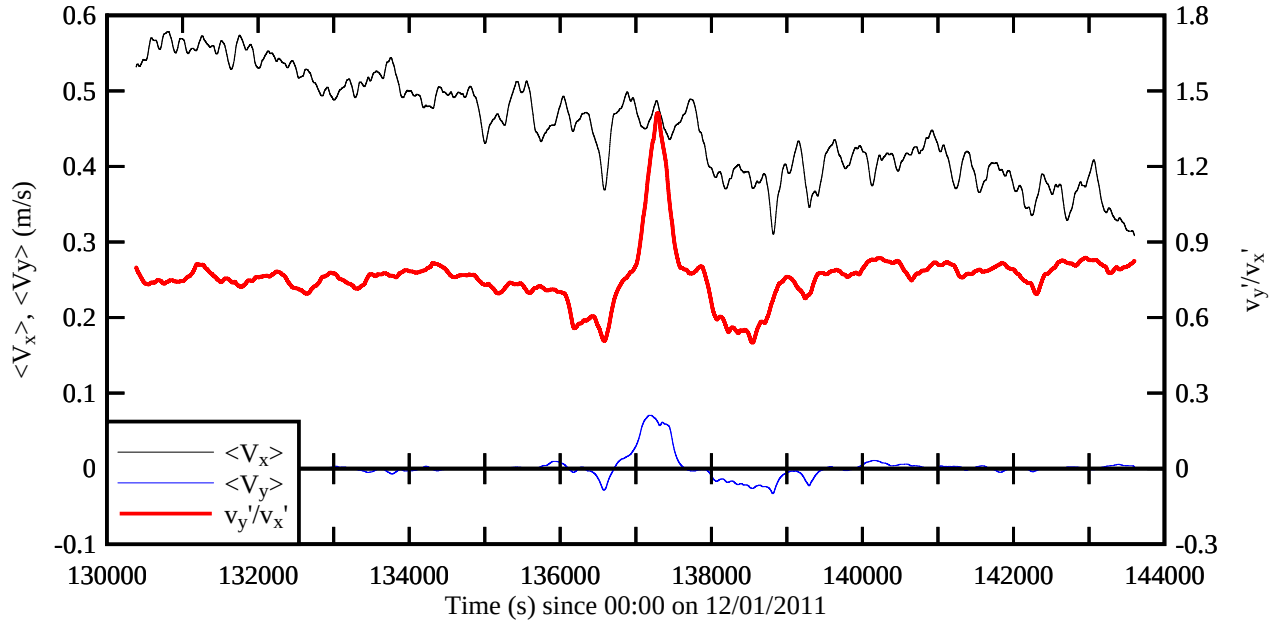

(A) Longitudinal and transverse velocity components and dimensionless ratio v_y'/v_x'

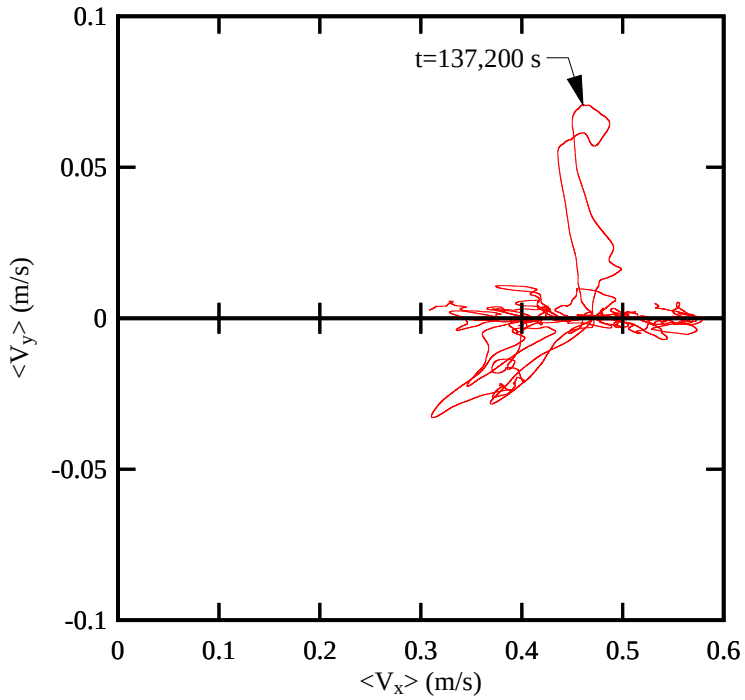

(B) Horizontal velocity amplitude and direction

Fig. 5-5 - Longitudinal and transverse velocities during test T4

5.2.2 Discussion

The present data set was recorded during both the rising and receding stages of the Brisbane River flood. Tests T1 and T2 were conducted during the rising stage and tests T3, T4 and T5 were performed during the receding stage. While some form of hysteresis between depth and velocity has

been documented in river floods (HENDERSON 1966, MONTES 1998), it is believed that a comparison between the rising and receding stages of the flood is meaningless in the present study for a number of reasons. These included the different locations of the ADV, the different ADV mountings, the strong influence of the surrounding urban environment (section 3) and the unknown upstream boundary conditions including sediment wash load. For example, the Brisbane River flood caused some massive soil erosion in the Brisbane Valley and in particular in the Lockyer Valley (Fig. 1-2). The flood hydrograph of Lockyer Creek at Rifle Range Road ([3]) showed a broad flood peak between Tuesday 11 January 2011 afternoon and Thursday 13 January early morning (CHANSON 2011). As a result, the influence of Lockyer Creek runoff might have been felt in Brisbane during most of the field study.

Figure 5-6 presents the probability distribution functions of the longitudinal velocity fluctuation around the mean V_x-$\langle V_x \rangle$. The data are presented in dimensionless form as $(V_x-\langle V_x \rangle)/(V_x-\langle V_x \rangle)'$. Further results in terms of the transverse and vertical velocity fluctuations are reported in Appendix D. The results indicated that the velocity fluctuations around the mean followed a pseudo-Gaussian distribution. Some basic statistical properties are summarised in Table 5-1. These include the mean flow data (e.g. $\langle V \rangle$) averaged over the sampling period and the average standard deviation of the fluctuations around the mean flow properties (e.g. $(V-\langle V \rangle)'$). In Table 5-1, the data for tests T1 and T3 were shaded to highlight the relatively small number of samples. The results indicate that the velocity magnitude was about 0.4 to 0.5 m/s for tests T1 to T4. During the last test (T5), the velocity amplitude was much lower: $\langle V_x \rangle$ = 0.0018 m/s on average. It is likely that test T5 corresponded to the final stage of the flood water recession associated with some suspended sediment accretion.

The local Froude number defined in terms of the water depth and mean longitudinal velocity was about 0.2 at the time of water depth observations (Table 4-1, column 7). That is, the flow motion was subcritical at the sampling site and the calculations were consistent with visual and photographic observations (section 4). Within the car park (C Block level 1), the flow was affected by some constriction induced by the two stairwells located upstream of the sampling site (Fig. 5-7). The gap between the stairwells was 10 m compared to the C Block car park width of 33.6 m. Based upon the water depth and mean longitudinal velocity data, some simple hydraulic calculations (HENDERSON 1966) show that the constricted flow could reach transcritical flow conditions associated with choking, especially during test T4. For a given specific energy and discharge, choking may occur when the channel constriction is too narrow, and additional specific energy is required to maintain the flow rate (HENDERSON 1966, MONTES 1988).

[3] The Rifle Range Road gauge is located about 150 km upstream of Gardens Point.

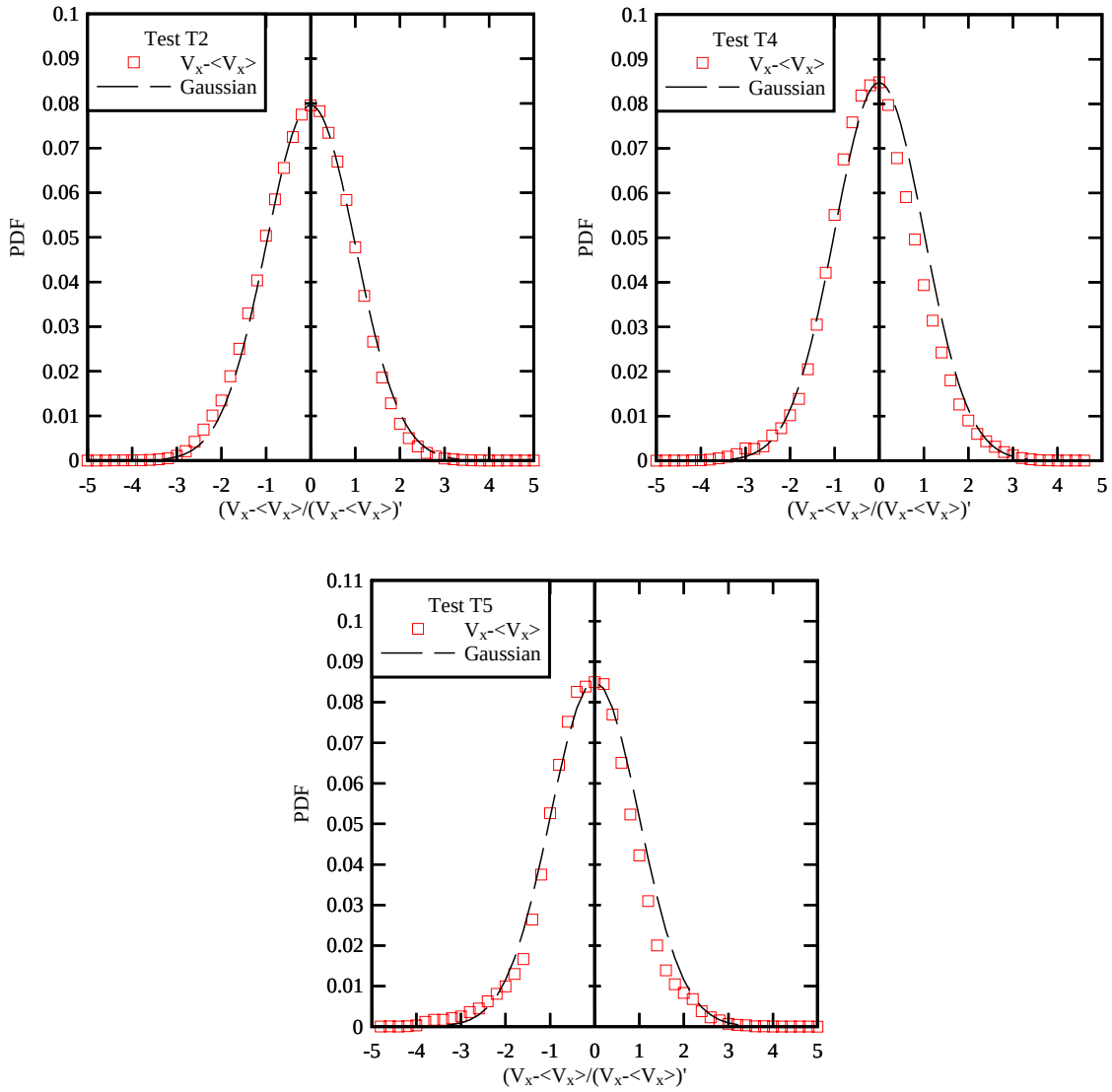

Fig. 5-6 - Probability distribution functions (PDFs) of the longitudinal velocity fluctuations around the mean V_x - $\langle V_x \rangle$ during tests T2, T4 and T5 (12-13 January 2011)

The channel constriction might further be considered as a thick orifice flow. The narrowing of the flow cross-section leads to a convergence of the streamlines associated with some regions of flow separation immediately downstream of the sharp-edged contraction. Further regions of flow separation may occur in the downstream channel expansion. The maintenance of the recirculation in these separated flow regions would require some energy loss through the contraction. Some simple energy considerations show that the total head loss in the stairwell contraction may be estimated as:

$$\Delta E = k \times \frac{V_1^2}{2 \times g} \left(1 - \frac{B_1}{B} \right) \qquad (5\text{-}1)$$

where ΔE is the energy loss, k is an energy loss coefficient close to unity for B_1/B about unity, B is the upstream channel width and B_1 is the contraction width. For the present investigation, Equation (5-1) yields some head loss as large as 0.05 to 0.15 m during the study period.

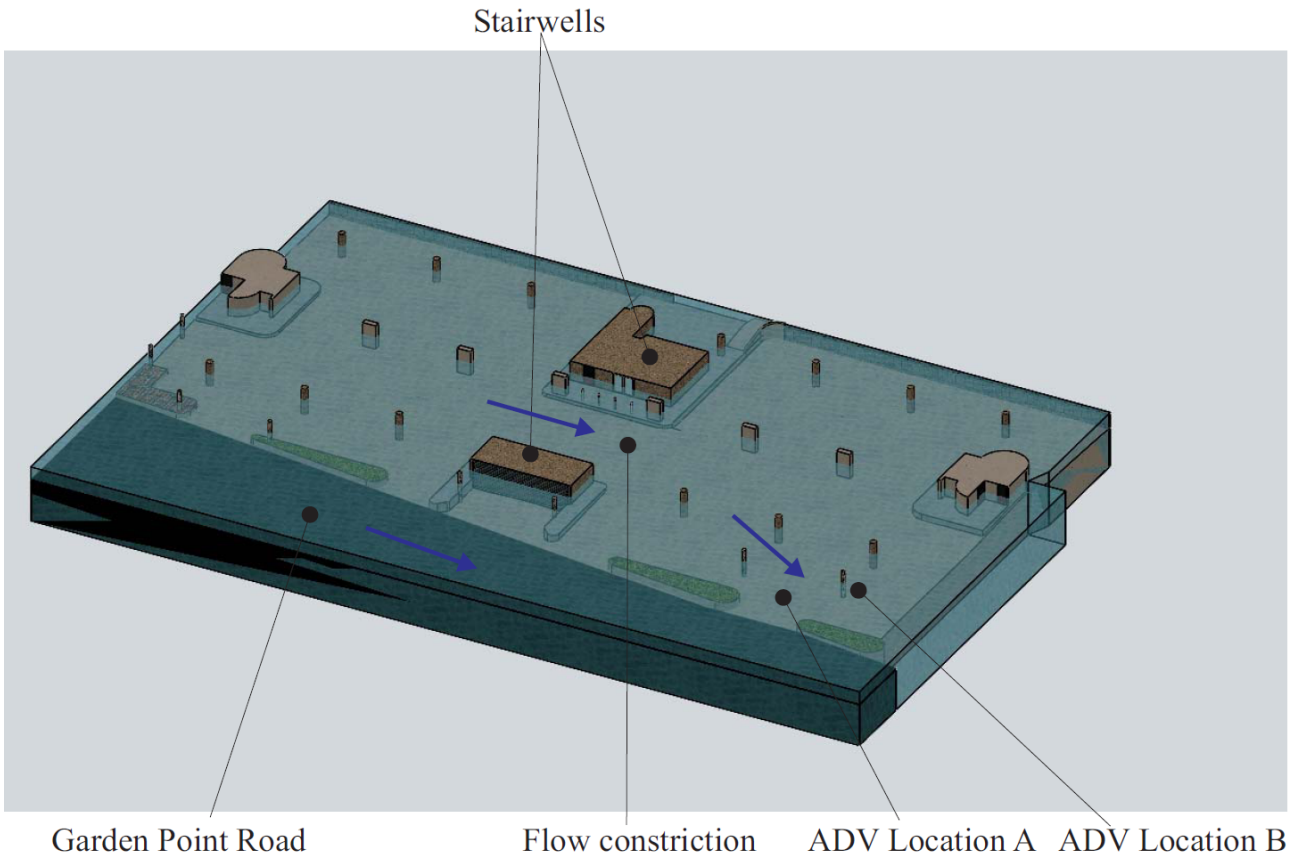

Fig. 5-7 - CAD drawing of the submerged car park (C Block level 1) with the constriction induced by the stairwells - Blue arrows indicate the main flow direction

When the flow in the stairwell contraction reached near-critical conditions (transcritical), choking would take place, and additional energy would be required to maintain the flow rate inducing additional head losses. The energy losses in the contraction could become substantially larger than the rate of energy loss of the main river flow, and the inundation flow would redirect around the stairwells to achieve a minimum energy path. The pattern could be responsible for some flow oscillation next to the stairwells with a period close to the natural sloshing period of the building car park (Table 4-2) and correspond to the long-period fluctuations in depth and velocity observed at the sampling site (Fig. 5-1).

A frequency analysis was performed to characterise the dominant period of the slow fluctuations in terms of the water level, velocity flux, velocity components, suspended sediment concentration and suspended sediment flux. The results are summarised in Table 5-2. They showed the presence of some slow fluctuations with periods between 50 and 100 s for all tests for the water depth, velocity flux and velocity components. The dominant period increased with decreasing water depths and it was close to the first mode of sloshing resonance linked with the length of the C Block car park (section 4.3). During the tests T4 and T5, the suspended sediment concentration and suspended sediment load data exhibited some slightly different oscillation periods (section 5-4).

Table 5-1 - Turbulent velocity measurements in the flood plain (QUT car park) of the Brisbane River in flood on 12-13 January 2011

Data file	ADV location	Sampling rate Hz	Velocity range m/s	z m	Start time	Nb of samples
(1)	(2)	(3)	(4)	(5)	(6)	(7)
T1	A	50	2.5	0.350	12/01/2011 at 20:10:31	70,162
T2	A	50	2.5	0.350	12/01/2011 at 20:40:08	800,000
T3	B	50	2.5	0.083	13/01/2011 at 11:34:28	31,171
T4	B	50	1.0	0.083	13/01/2011 at 12:08:55	685,884
T5	B	50	1.0	0.083	13/01/2011 at 17:34:40	196,762

Data file	z m	Avg <h> m	Avg <h×V_x> m^2/s	Avg <V_x> m/s	Avg <V_y> m/s	Avg <V_z> m/s	Avg <SSC> kg/m^3	Avg <SSC×V_x> $kg/m^2/s$
(1)	(5)	(8)	(9)	(10)	(11)	(12)	(13)	(14)
T1	0.350	0.5055	0.2479	0.487	-0.0024	0.533	5.45	2.67
T2	0.350	0.5579	0.2521	0.455	0.00053	0.486	6.03	2.73
T3	0.083	--	--	0.565	-0.0159	0.179	19.81	11.57
T4	0.083	--	--	0.452	0.001	0.129	22.1	9.18
T5	0.083	--	--	0.00176	-0.0002	0.00438	27.28	0.085

Data file	z m	Avg (h-<h>)' m	Avg (h×V_x-<h×V_x>)' m^2/s	Avg (V_x-<V_x>)' m/s	Avg (V_y-<V_y>)' m/s	Avg (V_z-<V_z>)' m/s	Avg (SSC-<SSC>)' kg/m^3	Avg (SSC×V_x-<SSC×V_x>)' $kg/m^2/s$
(1)	(5)	(15)	(16)	(17)	(18)	(19)	(20)	(21)
T1	0.350	0.242	0.145	0.176	0.0687	0.227	1.037	1.072
T2	0.350	0.1014	0.0988	0.163	0.0757	0.228	1.351	1.113
T3	0.083	--	--	0.116	0.044	0.107	1.276	2.544
T4	0.083	--	--	0.123	0.0409	0.121	4.922	2.705
T5	0.083	--	--	0.03059	0.0098	0.0277	3.422	0.6866

Notes: Avg: time-average over the test sampling duration; Location A: ADV unit mounted horizontally on boom gate support; Location B: ADV unit mounted vertically on a hand rail; SSC: suspended sediment concentration; <V>: mean velocity contribution after triple decomposition; [V]: slow fluctuating component after triple decomposition; (V)': standard deviation of V calculated over 500 s; z: vertical elevation above the invert; Shaded data: data set with relatively small number of samples.

Table 5-2 - Dominant period of the slow fluctuations during the field study on 12-13 January 2011 in Gardens Point

Test	Period (s)						
	h	$h \times V_x$	V_x	V_y	V_z	SSC	$SSC \times V_x$
(1)	(2)	(3)	(4)	(5)	(6)	(7)	(8)
T2	58	57	57	56	57	56	57
T4	--	--	88	92	89	N/A	73 & 101
T5	--	--	101	105	59 & 101	61	134

Note that a further influence of the flow contraction in between the stairwells might be the development of large scale eddies in the developing shear layers of the expansion flow. It is believed however that the time scale of these eddies was noticeably shorter than a minute.

In summary, the dominant periods of slow fluctuations in water level, velocity components and velocity flux were close to the natural sloshing period of the car park (C Bock level 1) based upon its length (Tables 4-2 & 5-2). It is believed that the excitation source was some choking in the flow contraction between stairwells (Fig. 5-7) and associated energy losses.

5.3 TURBULENT PROPERTIES AND REYNOLDS STRESSES

In the previous section, the velocity data indicated some large fluctuations around the mean values. These included the slow fluctuating component and the turbulent motion. Herein the focus is on the true turbulent motion calculated as the high-pass filtered data with a cut-off frequency of 0.33 Hz (1/3 s^{-1}) over a 500 s interval (25,000 data samples). Some basic results are summarised in Table 5-3 in terms of the standard deviation of depth, velocity flux, velocity component, suspended sediment concentration and suspended sediment flux (Table 5-3, columns 3-11), and skewness and kurtosis of the turbulent velocity data (Table 5-3, columns 12-17).

First, the average standard deviations of fluctuations in depth, velocity flux and turbulent velocity components were one order of magnitude lower than the average standard deviation of the fluctuation about the mean: e.g., v'/(V-<V>)' ~ 0.1. The finding was consistent through the study, except possibly during test T5. It implies that the slow fluctuating components were associated with the main energy of fluctuating velocity.

Table 5-3 - Statistical properties of the turbulent motion data during Gardens Point field measurements in the flood plain (QUT car park) of the Brisbane River in flood on 12-13 January 2011

Data file	z	Avg h'	Avg $(v_x \times h)'$	Avg v_x'	Avg v_y'	Avg v_z'	Avg ssc'	Avg $(ssc \times v_x)'$	Avg $(v_y/v_x)'$	Avg $(v_z/v_x)'$
	m	m	m^2/s	m/s	m/s	m/s	kg/m^3	$kg/m^2/s$		
(1)	(2)	(3)	(4)	(5)	(6)	(7)	(8)	(9)	(10)	(11)
T1	0.350	0.00321	0.0184	0.034	0.0328	0.0388	0.764	0.361	0.964	1.139
T2	0.350	0.00308	0.0187	0.035	0.0337	0.0399	0.796	0.367	0.962	1.14
T3	0.083	--	--	0.0347	0.0257	0.02897	0.821	0.796	0.74	0.833
T4	0.083	--	--	0.0273	0.0203	0.0226	0.756	0.627	0.76	0.836
T5	0.083	--	--	0.00613	0.00467	0.00419	0.967	0.139	0.763	0.685

Data file	z	Avg Skew(v_x)	Avg Skew(v_y)	Avg Skew(v_z)	Avg Kurto(v_x)	Avg Kurto(v_y)	Avg Kurto(v_z)
	m						
(1)	(2)	(12)	(13)	(14)	(15)	(16)	(17)
T1	0.350	-0.248	0.271	-0.0436	9.576	7.943	9.318
T2	0.350	-0.382	-0.315	0.0783	11	9.246	10.188
T3	0.083	-0.1367	-0.1289	0.01317	9.934	8.6367	10.441
T4	0.083	-22.52	-0.1963	-0.9039	20.13	17.54	28.47
T5	0.083	-0.136	0.0529	-1.0979	19.448	16.359	22.954

Notes:

Avg: time-average over the test sampling duration; Kurto: Fisher kurtosis calculated over 500 s; Skew: Fisher skewness calculated over 500 s; ssc: turbulent fluctuation of suspended sediment concentration after triple decomposition; v: turbulent velocity component after triple decomposition; v': standard deviation of v calculated over 500 s; z: vertical elevation above the invert; Shaded data: data set with relatively small number of samples.

Second, the longitudinal turbulent intensity $v_x'/\langle V_x \rangle$ was on average 5 to 6% for tests T1 to T4. The results were close to laboratory measurements in open channels although possibly slightly larger (NEZU and NAKAGAWA 1993, XIE 1998, KOCH and CHANSON 2005). The horizontal and vertical turbulence intensities v_y'/v_x' and v_z'/v_x' showed some difference between locations A and B. On average for tests T1 to T4, v_y'/v_x' was equal to 0.96 and 0.75 at z = 0.35 and 0.083 m respectively, while v_z'/v_x' equalled 1.14 and 0.83 at z = 0.35 and 0.083 m respectively. At z = 0.35 m, the results suggested that the turbulence was about isotropic: $v_x' \approx v_y' \approx v_z'$. At z = 0.083 m, the findings indicated some anisotropy and the overall results tended to ratios v_y'/v_x' and v_z'/v_x' close to those observed in laboratory studies with straight prismatic rectangular channels (NEZU and

NAKAGAWA 1993, NEZU 2005, KOCH and CHANSON 2009).

Third the Fisher skewness and Fisher kurtosis of turbulent velocity components showed some deviation from a Gaussian distribution, associated with non unity values of anisotropy and implying that the turbulence was not homogeneous. With one exception, the skewness of all velocity components for tests T1 to T5 was relatively close to 0 implying that the skewness is approximately Gaussian. The exception was the skewness of v_x in test T2 which was negatively skewed indicating that the tail on the left side of velocity PDF was longer than that on the right. Inspection of the corresponding PDF showed the non-symmetrical nature of the distribution (App. D, Fig. D-5). In most PDFs of velocity components from laboratory data, values close to the mean are normally symmetric but in this study a comparison with the corresponding Gaussian values shows that they were not. It is notable that the skewness of v_x was different to that of the other two velocity components. The reason for this behaviour is not clear. It might be related to the heavy sediment load, though this would be expected to effect all velocity components. Unlike the approximately Gaussian behaviour of most skewness, the excess kurtosis of all tests and all velocity components was consistently higher than the Gaussian value (zero), indicating a sharper peak and longer, fatter tails. Tests T4 and T5 had consistently higher kurtosis than tests T1, T2 and T3. The reasons for these differences were not clear but suggested possibly some significant variations of turbulence during the duration of the flood.

The turbulent Reynolds stress tensor components were calculated (App. E). The basic statistical properties are summarised in Table 5-4 for the normal and tangential stresses. Both the average mean values and standard deviations are reported ([4]). The shear stress correlation coefficients (e.g. $\overline{v_x v_z} / \sqrt{\overline{v_x^2}\ \overline{v_z^2}}$) are reported in columns 9 to 11 (Table 5-4). The dimensionless Reynolds stresses were low compared to those reported in the literature in developing boundary layers in open channels and fully-developed open channel flows (XIE 1998, TACHIE 2001).

[4] The minimum and maximum values are presented in Appendix E.

Table 5-4 - Statistical properties of the turbulent Reynolds stresses during the Gardens Point field measurements in the flood plain (QUT car park) of the Brisbane River in flood on 12-13 January 2011

Data file	z	Avg $\overline{\rho v_x^2}$	Avg $\overline{\rho v_y^2}$	Avg $\overline{\rho v_z^2}$	Avg $\overline{\rho v_x v_z}$	Avg $\overline{\rho v_x v_y}$	Avg $\overline{\rho v_y v_z}$	Avg $\frac{\overline{v_x v_z}}{\sqrt{\overline{v_x^2}\,\overline{v_z^2}}}$	Avg $\frac{\overline{v_x v_y}}{\sqrt{\overline{v_x^2}\,\overline{v_y^2}}}$	Avg $\frac{\overline{v_y v_z}}{\sqrt{\overline{v_y^2}\,\overline{v_z^2}}}$
	m	Pa	Pa	Pa	Pa	Pa	Pa			
(1)	(2)	(3)	(4)	(5)	(6)	(7)	(8)	(9)	(10)	(11)
T1	0.350	1.983	1.805	2.555	-0.0807	-0.1823	-0.0323	-0.0328	-0.0954	0.01371
T2	0.350	2.158	1.958	2.782	-0.064	0.1401	0.0229	-0.02659	0.06817	0.009502
T3	0.083	2.166	1.179	1.54	-0.080	-0.1365	0.0716	-0.0629	-0.0867	0.05405
T4	0.083	1.445	0.7881	1.007	-0.0734	-0.0249	0.03362	0.04224	-0.02558	-0.06443
T5	0.083	0.07086	0.04078	0.03184	0.00379	0.00107	-0.0002	0.07823	0.02573	0.07823

Data file	z	Avg $(\rho v_x^2)'$	Avg $(\rho v_y^2)'$	Avg $(\rho v_x^2)'$	Avg $(\rho v_x v_z)'$	Avg $(\rho v_x v_y)'$	Avg $(\rho v_y v_z)'$
	m	Pa	Pa	Pa	Pa	Pa	Pa
(1)	(5)	(12)	(13)	(14)	(15)	(16)	(17)
T1	0.350	1.998	1.826	2.595	1.449	1.221	1.391
T2	0.350	2.156	1.956	2.781	1.556	1.313	1.495
T3	0.083	1.718	0.9704	1.2498	0.946	0.8322	0.7108
T4	0.083	1.4458	0.7895	1.0068	0.7541	0.68098	0.5631
T5	0.083	0.0696	0.04012	0.03141	0.02835	0.03537	0.02097

Notes: Avg: time-average over the test duration; v: turbulent velocity component after triple decomposition; z: vertical elevation above the invert; $\overline{\rho v^2}$: time-averaged Reynolds stress component calculated over 500 s; (ρv^2): standard deviation of Reynolds stress component calculated over 500 s; Shaded data: relatively small number of data samples.

5.4 SUSPENDED SEDIMENT PROPERTIES

The time-variations of suspended sediment concentration SSC and longitudinal suspended sediment flux q_s = SSC×V_x are presented in Figures 5-8 and 5-9 respectively. The suspended sediment concentrations were calculated from the measured acoustic backscatter amplitude data using Equation (3-5). Both the suspended sediment concentration and longitudinal velocity V_x data were measured simultaneously in the same control volume located 5 cm away from the ADV emitter. Each figure includes the instantaneous data, the mean value <SSC> and <q_s> (low-pass filtered data with 0.002 Hz cut-off frequency) and the standard deviation ssc' and q_s' of the turbulent fluctuation component (high-pass filtered data with 0.33 Hz cut-off frequency). The Brisbane City gauge data are shown for comparison.

The suspended sediment concentration data showed a general trend with an increase in mean concentration <SSC> from about 6 kg/m^3 to more than 20 kg/m^3 during the entire study period (Fig. 5-8). The trend might be linked with the change in ADV sampling volume elevation between locations A and B. However, during test T5 with shallow waters, it is likely that the data trend reflected an increase in SSC prior to mud deposition on the concrete invert. During test T4, the suspended sediment concentration measurements highlighted two key features. First some large suspended sediment concentrations and large fluctuations in SSC about the mean trend were observed between t = 135,600 and 140,800 s (Thursday 13 January between 13:40 and 15:10). The period corresponded to the unusual flow pattern discussed in section 5.2, and it is likely that the development of large-scale vortical structures could have enhanced turbulent mixing and re-suspended some deposited sediment materials. Another feature of test T4 was the existence of long-period oscillations of the mean suspended sediment concentration data <SSC> with a period of about 1,100 s (18 minutes) (Fig. 5-8). Such oscillations were not seen in the velocity data, and the authors do not have any explanation to date.

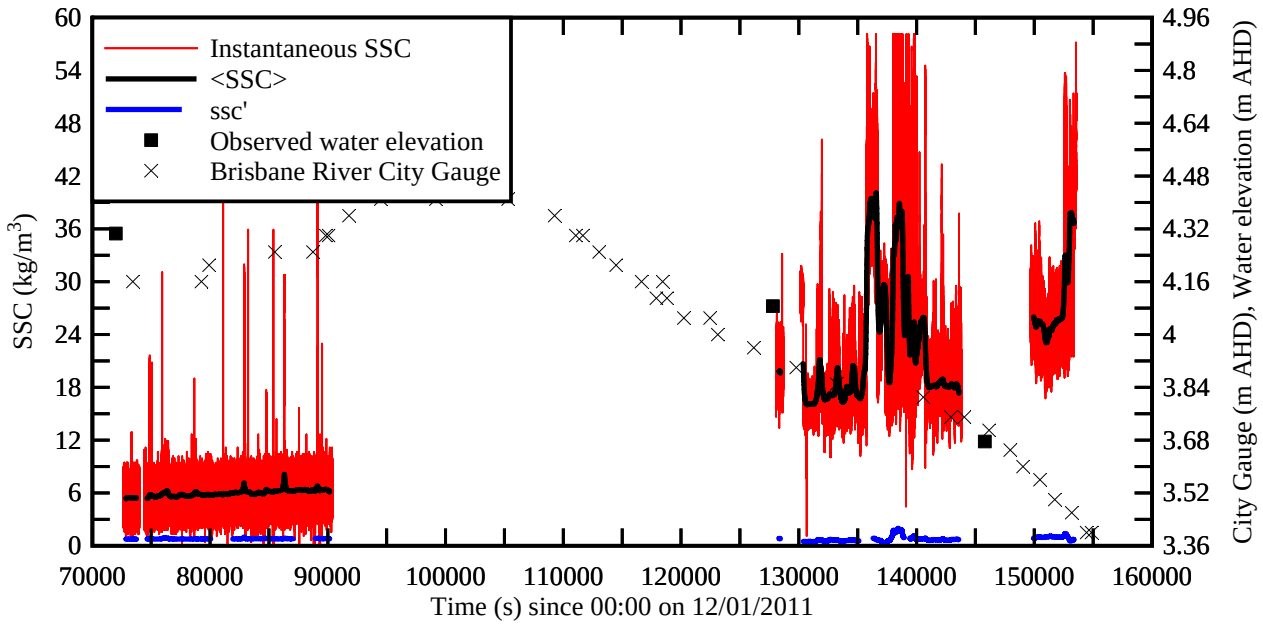

Fig. 5-8 - Time variations of the suspended sediment concentration: instantaneous suspended sediment concentration SSC, mean suspended sediment concentration <SSC> and standard deviation ssc' of the turbulent fluctuation component - Comparison with the manual observations and Brisbane River City Gauge data (Source: BOM) - Both manual observations and Brisbane River City Gauge data are reported in m AHD

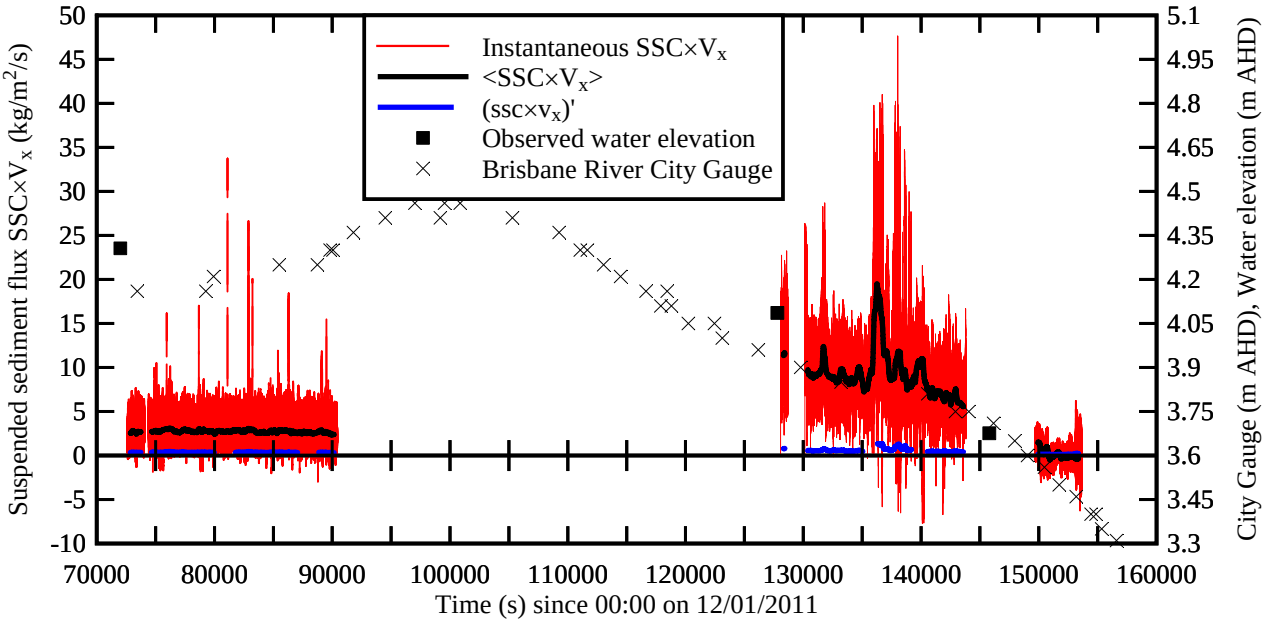

Fig. 5-9 - Time variations of the longitudinal suspended sediment flux $SSC \times V_x$: instantaneous suspended sediment flux $SSC \times V_x$, mean suspended sediment flux $\langle SSC \times V_x \rangle$ and standard deviation $(ssc \times v_x)'$ of the turbulent fluctuation component - Comparison with the manual observations and Brisbane River City Gauge data (Source: BOM) - Both manual observations and Brisbane River City Gauge data are reported in m AHD

The longitudinal suspended sediment flux data q_s showed some substantial sediment flux values which would be consistent with the murky colour of the Brisbane River. Herein q_s represents a sediment flux per unit area. The data highlighted a major increase in sediment flux about t = 136,263 s (Thursday 13 January 13:51) (Fig. 5-9). It is believed to be linked with the high values of observed SSC and velocity during a major flow episode. During test T5, the data indicated some low mean sediment flux despite some large SSCs. This test corresponded to a period of very sluggish flow motion (Table 5-1, columns 10 to 12) likely associated with suspended sediment deposition on the invert.

Comments

Some statistical properties in terms of the suspended sediment concentration and flux are presented in Table 5-1 (columns 13-14 & 20-21) and Table 5-3 (columns 8-9). The results suggested that most fluctuations in SSC were relatively rapid with periods less than 3 s. The data indicated some distinctively different time scales compared to the velocity and SSC fluctuations. The finding might suggest that the velocity fluctuations were linked with local effects and features of the urban environment, while the suspended sediment concentration and flux were affected predominantly by

the upstream catchment runoff characteristics including the sediment wash load.

5.5 DISCUSSION

The flow conditions at the sampling sites corresponded to a specific momentum between 0.2 to 0.5 m^2 during tests T1 to T4. Figure 5-10 presents further the time-variations of the instantaneous specific momentum at location A during tests T1 and T2 (Fig. 5-10A) and the probability distribution function of the momentum function during test T2 (Fig. 5-10B). The specific momentum was calculated as:

$$M = \frac{d^2}{2} + d \times \frac{V_x^{\,2}}{g} \qquad (5\text{-}2)$$

where d and V_x were respectively the instantaneous water depth and longitudinal velocity. The specific momentum observations would be near the upper end of the scale of the criteria for safe evacuation of individuals in flooded areas developed by ASAI et al. (2010). But the authors experienced first hand the force of the flood flow in the car park (C Block level 1) and Gardens Point Road. They would not describe the flow conditions as safe for evacuation ([5]) because of the intense turbulent mixing and the water surges which were felt at irregular intervals. It is suggested that any criterion solely based upon the flow velocity, water depth or specific momentum cannot account for the hazards caused by the velocity and water depth fluctuations. These considerations ignore further the risks associated with large debris entrained by the flow motion (Fig. 2-6).

[5] The authors used secured safety ropes and safety handrails to work safely in the flood waters. However no published guidance/procedures directly relevant to this flood study have been found. As in any field work risk assessment should be undertaken by a competent person taking into account all of the foreseen hazards. Swift water flood rescue material (http://www.rescuetraininggroup.com.au/) does exist. Appropriate selection of equipment can be aided by the requirements of AS4488, Industrial Rope Access, - applicable for certain situations of static and dynamic loading including fall arrest, and does not directly apply to moving flood waters. Guidance for cleaning up after the floods is available from Workplace Health and Safety Queensland (http://www.deir.qld.gov.au/workplace/subjects/floods/index.htm). This lack of appropriate guidance for working in floodwaters highlights a need for development in this field.

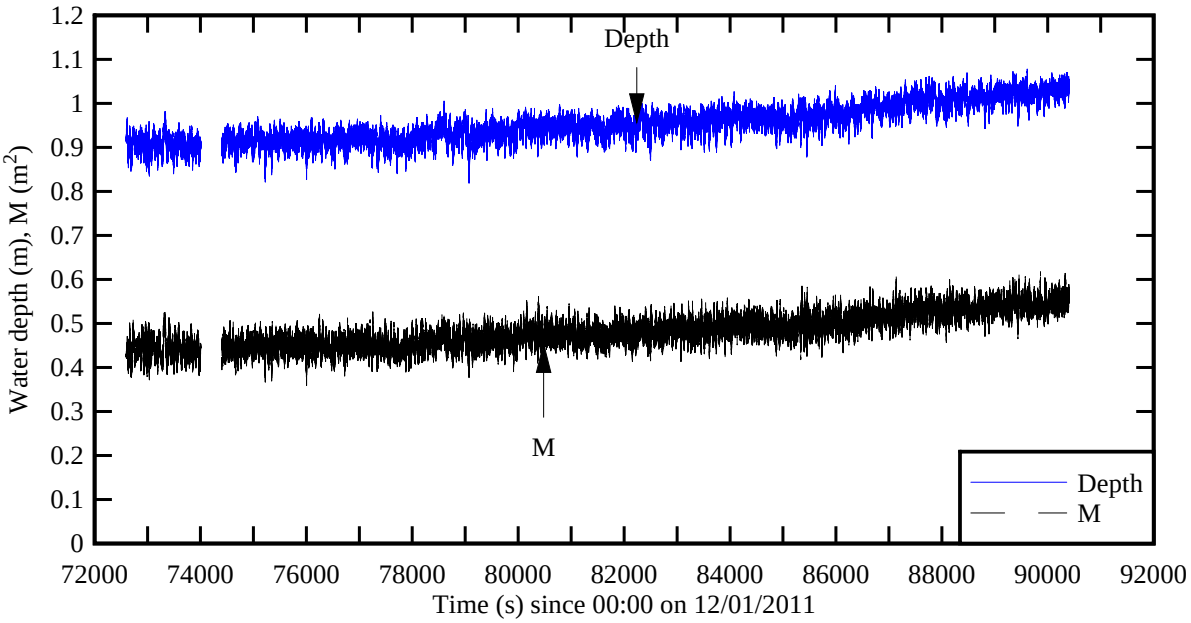

(A) Time variations of instantaneous water depth and specific momentum at location A during tests T1 and T2

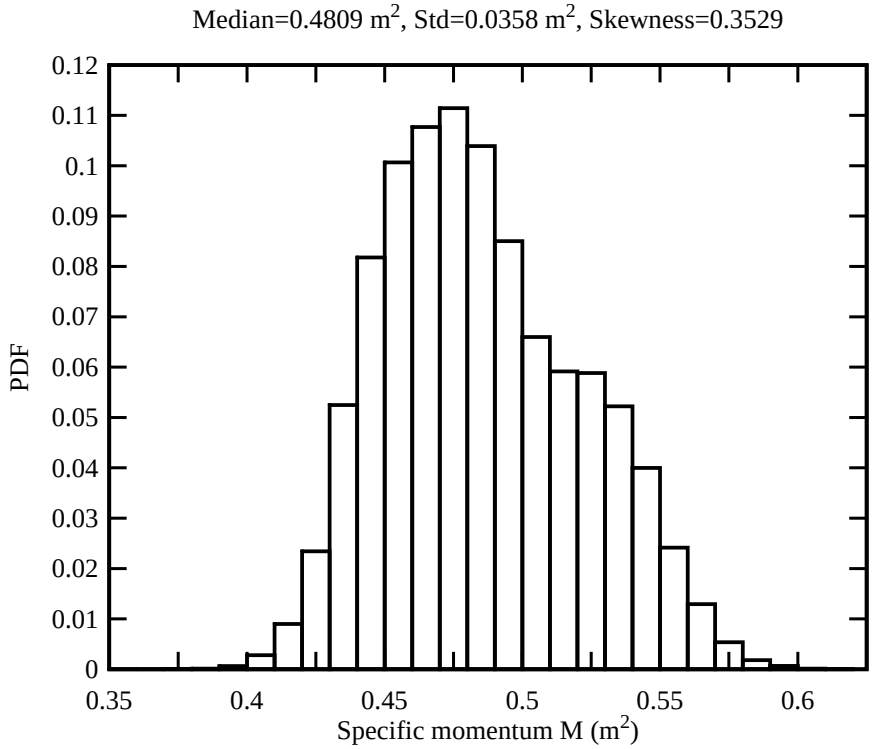

(B) Normalised probability distribution function of instantaneous specific momentum at location A during test T2

Fig. 5-10 - Instantaneous specific momentum M during tests T1 and T2 at location A

Table 5-5 - Local friction slope estimates based upon the water depth observations and mean velocity measurements in Gardens Point on 12-13 January 2011

Data point	ADV location	Date	Time	Water depth d m	$<V_x>$ m/s	Fr	Re	S_f
(1)	(2)	(3)	(4)	(5)	(6)	(7)	(8)	(9)
1	A	12 Jan. 2011	20:00	0.89	0.49	0.17	1.7×10^5	0.000071
2	B	13 Jan. 2011	11:30	0.67	0.57	0.22	1.4×10^5	0.00014
3	B	13 Jan. 2011	16:30	0.26	0.33	0.21	3.4×10^4	0.00016

Notes: Location A: ADV unit mounted horizontally on boom gate support; Location B: ADV unit mounted vertically on a hand rail; d: water depth measured above the concrete invert; Fr: local Froude number; E: specific energy; M: specific momentum.

The local friction slope S_f was deduced from the measured flow depth d and mean longitudinal velocity $<V_x>$:

$$S_f = \frac{f \times < V_x >^2}{8 \times g \times d} \quad (5\text{-}3)$$

where f is the Darcy-Weisbach friction factor. S_f is the longitudinal slope of the total head line. The results showed that the local friction slope was about 1×10^{-4} (Table 5-5, column 9). For comparison the difference in water elevations between Gardens Point and City Gauge on Wednesday evening and Thursday mid-day gave a free-surface slope of about 1×10^{-4}, while the average friction slope of the Brisbane River between Chelmer and the CBD was $S_f = 2.3\times10^{-4}$ on average (App. F). The comparative results might suggest that the friction slope was smaller around the CBD.

The last test (T5) took place in very shallow waters. The turbulent velocity data showed a flow pattern very different from the other tests. The very slow flow motion suggested that the flow in the car park was disconnected from the main channel. The disconnection might be caused by the concrete blocks and traffic islands between the car park and Gardens Point and between Gardens Point Road and the river bank. An alternative might be the stoppage of the flow into the C Block level 1 at the north-western end of the building.

6. CONCLUSION

During the 12-13 January 2011 flood of the Brisbane River, some field measurements were conducted in an inundated urban environment on the river left bank (Fig. 6-1). Turbulent velocity data were collected at relatively high frequency (50 Hz) using acoustic Doppler velocimetry in Gardens Point Road next to Brisbane's central business district (CBD). The properties of the sediment flood deposits were characterised. The sediment samples were some cohesive mud sludge with a median particle size of about 25 μm and a sorting coefficient between 21 and 44. The organic carbon content was about one order of magnitude larger than those recorded during dry periods. The acoustic Doppler velocimeter unit was calibrated to obtain the relationship between the acoustic backscatter amplitude and the suspended sediment concentration. Using the calibration results, the ADV outputs comprised the simultaneous measurements of the three velocity components and the suspended sediment concentration in the same sampling volume with the same temporal resolution.

Despite some field incidents, the field deployment showed some unusual features of the flood flow in the urban environment. The flow motion in Gardens Point Road was subcritical (Fig. 6-1). The water elevations and velocities fluctuated with a distinctive period between 50 and 80 s. These low frequency fluctuations of velocity and water depth were likely linked with some local topographic effects. It is believed that these oscillations were induced by some local choke induced by the constriction between stairwells upstream of the sampling location. The high energy loss associated with choking would cause a flow re-direction around the stairwells and some slow oscillations with a period close to the natural sloshing period of the car park length.

The instantaneous velocity data were analysed using a triple decomposition, whereby the instantaneous velocity component is equal to a mean velocity <V> plus a slow fluctuating component [V] and a turbulent motion component v. The same triple decomposition analysis was applied to the water depth, velocity flux, suspended sediment concentration and suspended sediment flux data. The velocity fluctuation data showed a large energy component in the slow fluctuation range, while the turbulent motion components were much smaller: v'/(V-<V>)' ~ 0.1. During the first two tests at z = 0.35 m (location A), the turbulence data suggested some isotropy with $v_x' \approx v_y' \approx v_z'$. At location B (z = 0.083 m), the findings indicated some anisotropy and the overall ratios v_y'/v_x' and v_z'/v_x' were close to those observed in laboratory studies with straight prismatic rectangular channels.

The suspended sediment concentration (SSC) data presented a general trend with increasing SSC for decreasing water depth. During test T4, some long-period oscillations were observed with a period about 18 minutes. The cause of these oscillations remains unknown to the authors. The last test (T5) took place in very shallow waters and high suspended sediment concentrations. It is

suggested that the flow in the car park was disconnected from the main channel, and the flow properties were affected by the interactions between the suspended sediment deposition process and the flow turbulence.

Overall the flow conditions at the sampling sites corresponded to a specific momentum between 0.2 to 0.4 m^2 which would be near the upper end of the scale for safe evacuation of individuals in flooded areas (ASAI et al. 2010). But the authors experienced the force of the flood flow in the car park caused by the intense turbulent mixing and the surge of waters. They believe that any criterion for safe evacuation solely based upon the flow velocity, water depth or specific momentum cannot account for the hazards caused by the turbulent velocity and water depth fluctuations, nor by large debris.

The local friction slope S_f was deduced from the measured flow depth d and mean longitudinal velocity. The results showed that the local friction slope was about 1×10^{-4} in the inundated zone The results compared well with the longitudinal free-surface slope between Gardens Point and City Gauge on Wednesday evening and Thursday mid-day, although the average friction slope of the Brisbane River between Chelmer and the CBD was $S_f = 2.3\times10^{-4}$ on average. The findings would suggest that the friction slope of the Brisbane River was smaller around the CBD.

Fig. 6-1 - Inundated Gardens Point Road (left), C Block car park level 1 (right) and ADV system (arrow) on Thursday 13 Jan. 2011 at 11:39 - Flow from background right to left

7. ACKNOWLEDGEMENTS

The authors thank Dr Frédérique LARRARTE (IFSTTAR, Bouguenais, France) for her detailed review of the report and valuable comments.

The writers acknowledge Jon JAMES (QUT Technical Services Unit, Faculty of Built Environment and Engineering), Gary WOODS (QUT Facilities Management Group) and QUT Security for access to tools, instrumentation and generators and site access during the stressful and busy period of the flood. They acknowledge Dr Frank SHI (Juius Kruttschnitt Mineral Research Centre), Nathaniel RAUP (QUT Technical Services Unit of the Faculty of Built Environment and Engineering) for sediment organic content measurements and A/Profs Les DAWES and Godwin AYOKO for access to associated instrumentation. They thank all people who participated in the field works, in particular Tony COOPER and Darielle BROWN and those who assisted in the post-field work calibration of the ADV sediment concentration, in particular Nic SURAWSKI, and in the preparation of building plans, in particular Ken TAN. The first writer also acknowledges the financial support of the QUT Faculty of Built Environment and Engineering through a special project grant. The authors acknowledge some discussions with Dr Mark TREVETHAN and Professor Laurent DAVID. Lastly the authors thank their respective families for their support during the difficult period of the flood in Brisbane.

APPENDIX A - PHOTOGRAPHIC OBSERVATION DURING THE FIELD MEASUREMENTS ON 12-14 JANUARY 2011

A.1 PHOTOGRAPHS DURING THE FLOOD

Fig. A-1 - Gardens Point Road looking NW (upstream) with the Captain Cook Bridge on the left and C Block on the right on Thursday 13 Jan. 2011 at 11:39 (Photograph Hubert CHANSON) - ADV unit on right handside - Pentax™ K-7 with Pentax™ DA18-250mm f3.5-6.3 ED AL lens

Fig. A-2 - Upstream end of Gardens Point Road on Wednesday 12 Jan. 2011 at 10:28 (Photograph courtesy of QUT Facilities Management) - Canon™ 5D Mk II with Canon™ EF24-105mm F4L IS

USM lens - Flow direction from right to left background

Fig. A-3 - Gardens Point Road looking NW (upstream) from Z Block on Wednesday 12 Jan. 2011 at 10:07 (Photograph courtesy of QUT Facilities Management) - Canon™ 5D Mk II with Canon™ EF24-105mm F4L IS USM lens - Flow direction from top right to bottom left

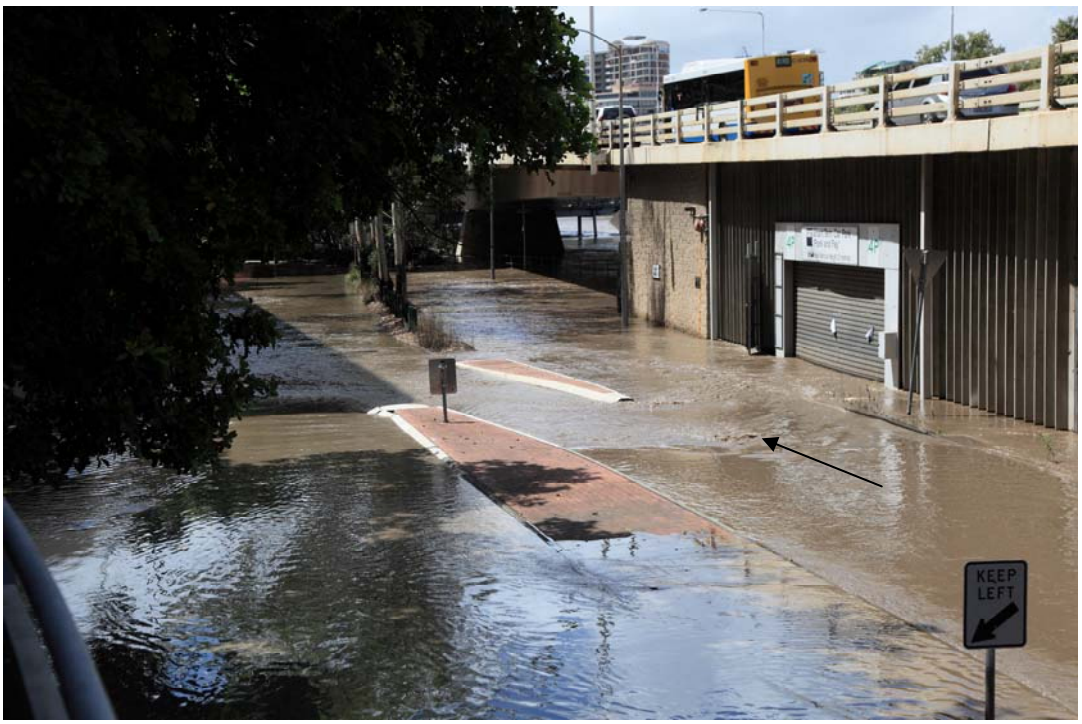

Fig. A-4 - Gardens Point Road looking SE (downstream) from Z Block on Wednesday 12 Jan. 2011 at 10:07 (Photograph courtesy of QUT Facilities Management) - Canon™ 5D Mk II with Canon™ EF24-105mm F4L IS USM lens - Flow direction (arrow) from bottom right to background, towards the sampling site (in the left background)

Fig. A-5 - Gardens Point Road looking SE (downstream) from C Block on Wednesday 12 Jan. 2011 at 10:08 (Photograph QUT Facilities Management) - Canon™ 5D Mk II with Canon™ EF24-105mm F4L IS USM lens - Flow direction from bottom right to background; the main channel of

the Brisbane River is seen in the background beneath the Captain Cook Bridge

Fig. A-6 - Parking beneath C Block with Gardens Point Road in the background on Wednesday 12 Jan. 2011 at 10:18 (Photograph courtesy of QUT Facilities Management) - Canon™ 5D Mk II with Canon™ EF24-105mm F4L IS USM lens - Flow direction (arrow) from right to left

Fig. A-7 - Roundabout at the SE (downstream) end of Gardens Point Road on Wednesday 12 Jan. 2011 at 10:18 (Photograph courtesy of QUT Facilities Management) - Canon™ 5D Mk II with

Canon™ EF24-105mm F4L IS USM lens - Flow direction from top right to left; the ADV sampling site (arrow) was behind and slightly to the right of the large tree beside C Block

Fig. A-8 - Roundabout at the SE (downstream) end of Gardens Point Road on Wednesday 12 Jan. 2011 at 11:48 (Photograph courtesy of QUT Facilities Management) - Canon™ 5D Mk II with Canon™ EF24-105mm F4L IS USM lens - Flow direction from right to left

(A) General view of Gardens Point Road

(B) Panoramic shot made from several photographs - Note the timber log jammed in the boom gate pylon and the stretched ADV cable (see arrows)

Fig. A-9 - Gardens Point Road viewed from C Block parking level 2 on Thursday 13 Jan. 2011 at 10:39 (Photograph Hubert CHANSON) - Pentax™ K-7 with Pentax™ DA18-250mm f3.5-6.3 ED AL lens - Flow from right to left, with Captain Cook Bridge in the background

(A) General view with Gardens Point Road in the background

(B) Zoom into the boom gate pylon and the handrail supporting the ADV system (arrow)

Fig. A-10 - Roundabout at the SE (downstream) end of Gardens Point Road on Thursday 13 Jan. 2011 at 11:38 (Photographs Hubert CHANSON) - Pentax™ K-7 with Pentax™ DA18-250mm f3.5-6.3 ED AL lens - Flow from right to left, with the Captain Cook Bridge in the background and C Block building and car park on the right

Fig. A-11 - View of the boom gate pylon and the handrail supporting the ADV system on Thursday 13 Jan. 2011 at 11:39 (Photograph Hubert CHANSON) - Pentax™ K-7 with Pentax™ DA18-250mm f3.5-6.3 ED AL lens - Flow from background right to left

(A) Submerged ADV system in operation (arrow)

(B) Main flow looking upstream

Fig. A-12 - Gardens Point Road looking NW (upstream) on Thursday 13 Jan. 2011 at 11:40 (Photographs Hubert CHANSON) - Pentax™ K-7 with Pentax™ DA18-250mm f3.5-6.3 ED AL lens - Flow from background right to left

(A) Looking upstream - Note ADV unit (arrow)

(B) View from Gardens Point Road, downstream of the ADV system (arrow)

Fig. A-13 - Flow in the inundated parking, level 1, C Block of Gardens Point campus on Thursday 13 Jan. 2011 at 11:40 (Photographs Hubert CHANSON) - Pentax™ K-7 with Pentax™ DA18-250mm f3.5-6.3 ED AL lens

Fig. A-14 - Fast flowing waters around two pylons in Gardens Road on Thursday 13 Jan. 2011 at 11:42 (Photograph Hubert CHANSON) - Pentax™ K-7 with Pentax™ DA18-250mm f3.5-6.3 ED AL lens - Flow from top right to bottom left

A.2 PHOTOGRAPHS AFTER THE FLOOD

Fig. A-15 - Gardens Point Road looking NW (upstream) with the Captain Cook Bridge on the left and C Block on the right on Friday 14 Jan. 2011 at 06:00 (Photograph Hubert CHANSON) - Pentax™ K-7 with Pentax™ FA31mm f1.8 AL Ltd lens

(A) General view with the ADV on the left, Gardens Point Road in the background, and the boom gate pylon (card reader) on the right of the concrete column

(C) Views of the ADV head location with a measuring tape for scale

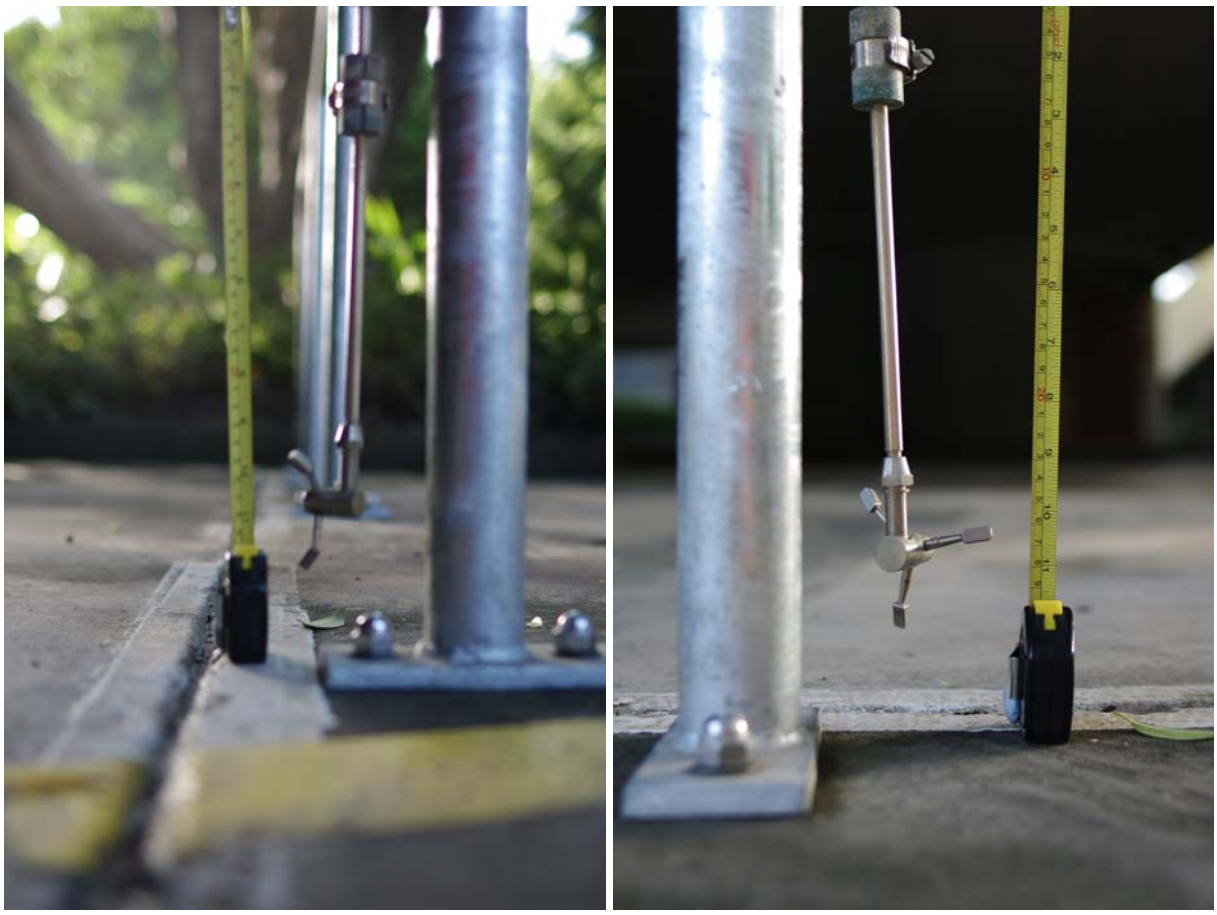

(C) Details of the ADV head location with a measuring tape for scale

Fig. A-16 - ADV unit mounted at the second location (second series of data sets) on Friday 14 Jan. 2011 at 06:00 (Photographs Hubert CHANSON) - Pentax™ K-7 with Pentax™ FA31mm f1.8 AL Ltd lens

APPENDIX B - PHOTOGRAPHS OF GARDENS POINT, BRISBANE

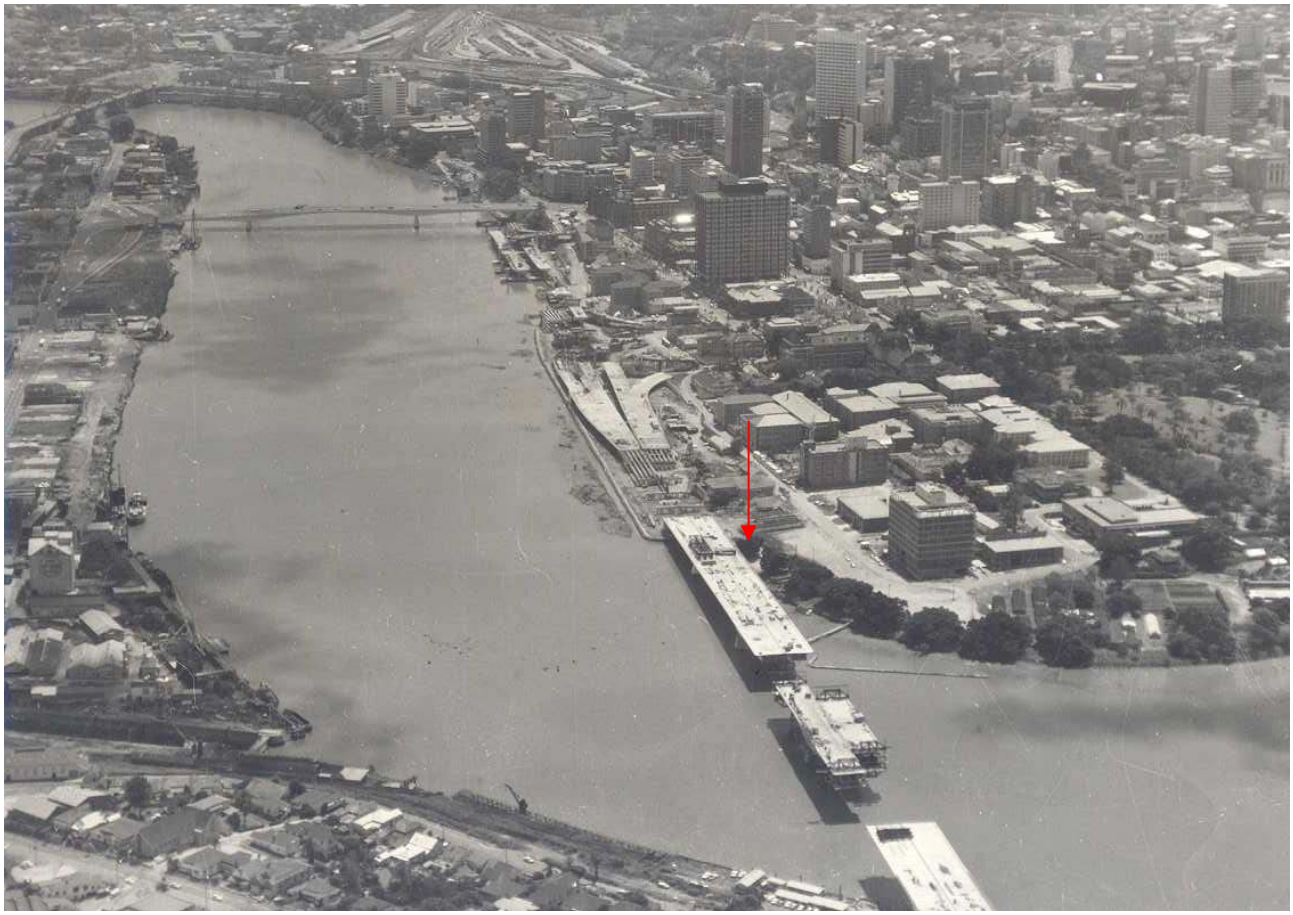

Fig. B-1 - Gardens Point in the early 1970s during the construction of the Captain Cook Bridge (Copyright QUT) - Brisbane River flow from top left to bottom right - the red arrow points to the ADV location

(A) General view of the city centre North of the River, with the Victoria Bridge on the top left and the Captain Cook Bridge on the lower part - The black arrows show the river flow direction

Fig. B-2 - Aerial photograph of Gardens Point during the 1990s (?) (Copyrights QUT) - Brisbane River flow from top left to top right - The red arrow points to the ADV location and the white arrow shows the City Gauge location

(B) Details of the QUT Gardens Point campus

Fig. B-2 - Aerial photograph of Gardens Point during the 1990s (?) (Copyrights QUT) - Brisbane River flow from top left to top right - The red arrow points to the ADV location and the white arrow shows the City Gauge location

Fig. B-3 - Aerial photograph of Gardens Point during construction in 2001 (Copyrights QUT) - Brisbane River flow from top left to bottom right - The black arrow points to Gardens Point Road between Captain Cook Bridge and the C-Z-S Blocks, while the red arrow points to the ADV location - Note the Goodwill Bridge under construction

APPENDIX C - ADV CALIBRATION FOR SUSPENDED SEDIMENT CONCENTRATION MEASUREMENT

C.1 PRESENTATION

Some sediment material was collected in Gardens Point Road next to the high water line on Thursday 13 January 2011 mid-morning and in a nearby flooded car park on Friday 14 January 2011 early morning. The soil samples consisted of fine mud and silt materials collected on the bed within 100 m from the sampling location ([1]). A series of laboratory tests were conducted to characterise the bed material: some particle size distribution and acoustic backscatter experiments.

The soil sample granulometry was measured with a Malvern^{TM} laser sizer with duplicate measurements (SHI 2011). The calibration of the ADV for suspended sediment concentration measurement was accomplished by measuring the signal amplitude of known, artificially produced concentrations of material obtained from the bed material sample, diluted in tap water and thoroughly mixed. All the experiments were conducted on Tuesday 18 January 2011. The laboratory experiments were conducted with the same Sontek^{TM} microADV Sontek 3D-microADV (16 MHz, serial A843F) system using the same settings as for the field observations on 12 and 13 January 2011. Two ADV settings were used: the main difference between the two configurations was the velocity range: 2.5 m/s on 12 and 13 January 2011 and 1 m/s on 13 January 2011.

For each laboratory test, a known mass of sediment was introduced in a water tank which was continuously stirred with a paint mixer (Fig. C-1). The mixer speed was adjusted during the most turbid water tests to prevent any sediment deposition on the tank bottom. The mass of wet sediment was measured with a Kern^{TM} PCB2000-1 (Serial WD080016381) balance, and the error was less than 0.1 g. The mass concentration was deduced from the measured mass of wet sediment and the measured water tank volume. During the tests, the suspended sediment concentrations ranged from less than 0.03 kg/m^3 to 98 kg/m^3.

The acoustic backscatter amplitude measurements were conducted with the ADV (16 MHz) system using the same configuration employed in the field (pulse length, scan rate, velocity range) ([2]). The ADV signal outputs were scanned at 50 Hz for 60 s for each test. The average amplitude measurements represented the average signal strength of the three ADV receivers. For low SSCs, the ADV data were post-processed with the removal of average signal to noise ratio data less than 15 dB, average correlation values less than 40%, and communication errors. For SSC > 8 kg/m^3, the

[1]The parking lot adjacent to the ADV sampling locations was cleaned in the night of 13-14 January 2011 and mud samples could not be collected there after the flood receded. The mud samples taken on 14 January 2011 were collected in the parking lot of B Block.

[2]The tank was strongly agitated by the mixer.

signal processing included the removal of communication errors and average signal to noise ratio data less than 15 dB. For SSC > 48 kg/m^3, unfiltered data were used since both the SNRs and correlations dropped drastically because of signal attenuation.

(A) Test for SSC = 70.5 kg/m^3 - The ADV system is in the background with the water mixers slightly in the right

(B) Details of the mixer blade (right) with ADV head on the left

Fig. C-1 - Photographs of the laboratory experiments

C.2 EXPERIMENTAL RESULTS

C.2.1 Particle size distributions and organic content

The bed sediment material was characterised by a series of laboratory experiments. The density of the wet sediment samples was about **s** = 1.461. Assuming a sediment density of 2.64 (MORRIS and

LOCKINGTON 2002), this would correspond to a porosity of 0.72. The bed material was a cohesive mud mixture and the particle size distribution data are presented in Figure C-2. Figure C-2 includes both the probability distribution functions and cumulative probability distribution functions of the sediment samples (Table C-1). The results were close considering that they were collected over two different days at four different locations (Table C-1). The median particle size was about 25 µm corresponding to some silty materials (GRAF 1971, JULIEN 1995, CHANSON 2004). The sorting coefficient $\sqrt{d_{90} / d_{10}}$ ranged from 21 to 44.

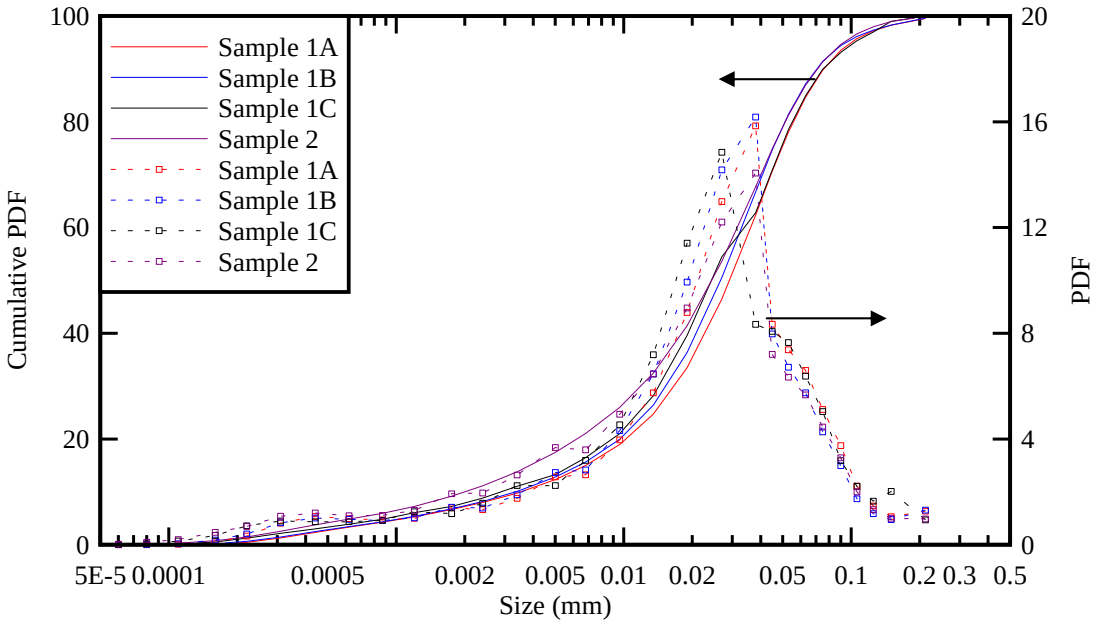

Fig. C-2 - Particle size distributions of mud samples collected in the QUT Gardens Point campus on 13 and 14 January 2011 (Table C-1)

The fraction of organic carbon in the sediment samples was determined by Loss on Ignition. The samples were oven dried at 105 C for 48 hours before being allowed to cool down to room temperatures. The subsamples were heated to 300 C for two hours and then to 780 C for 1 hours. The results are listed in Table C-1 (column 9). On average the fraction of organic carbon was about 8-9%. For comparison, some bed materials dredged from the Brisbane River during a dry period yielded an organic carbon fraction ranging from 0.63 to 1.8% (MORRIS and LOCKINGTON 2002). The 2011 flood sediment data showed comparatively a larger organic content.

Table C-1 - Characteristics of sediment samples collected in the Brisbane River: flood sediment deposit samples collected along Gardens Point Road next to C Block on 13 and 14 January 2011 (Present study)

Sediment deposit	Location	Collection date	Type	d_{50}	d_{10}	d_{90}	d_{90}/d_{10}	% organic carbon
				µm	µm	µm		%
(1)	(2)	(3)	(4)	(5)	(6)	(7)	(8)	(9)
Sample 1A	High waterline at roundabout , end of Gardens Point Rd	13 Jan. 2011	Silt	29.4	3.54	75.9	21.4	8.2
Sample 1B	Concrete footpath beside ADV location B	13 Jan. 2011	Silt	26.7	3.36	88.0	26.2	13.8
Sample 1C	Garden bed beside ADV location B	13 Jan. 2011	Silt	24.6	2.93	91.5	31.2	6.4
Sample 2	B Block parking ramp, Gardens Point Rd	14 Jan. 2011	Silt	24.6	2.02	88.4	43.8	8.6

Notes: AMTD: adopted middle thread distance, measured upstream from the river mouth; (--): data not available.

C.2.2 Acoustic backscatter intensity versus suspended sediment concentration

Location :	Queensland University of Technology, MERF (Prince Charles Hospital)
Dates :	18 January 2011
Experiments by :	R. BROWN, H. CHANSON, D. McINTOSH, J. MADHANI
Data processing by:	H. CHANSON
Soil and water samples :	Tap water. Mud samples collected along Gardens Point Road on 13 and 14 January 2011.
Instrumentation :	Sontek™ microADV (16 MHz, serial A843F) with a three-dimensional side-looking head scanned at 50 Hz for 60 s for each test. ADV settings: 12 January 2011 & 13 January. 2011.
Comments :	All the samples were kept in sealed, water tight containers until testing. Test conducted in a temperature controlled room Water temperature: 25 to 26 C.

Laboratory tests - MicroADV system measurements - Velocity range: 1.0 m/s

Run	Velocity range	Speed	Water temp.	Avg Ampl	SSC	Avg SNR	Avg COR
	cm/s	rpm	Celsius	Counts	g/l	dB	%
(1)	(2)	(3)	(4)	(5)	(6)	(7)	(8)
2	100	290	--	102.4	0.00	35.78	79.46
3	100	290	--	105.62	0.03	37.08	80.33
6	100	290	--	110.27	0.23	39.42	80.30
7	100	290	--	114.89	0.79	41.00	81.35
10	100	290	--	118.98	2.19	32.42	78.44
11	100	290	--	119.61	3.18	34.00	61.17
14	100	290	--	119.27	4.90	41.25	62.14
15	100	290	26.5	115.7	8.04	39.72	60.27
18	100	390	26.5	108.38	12.73	36.43	52.77
19	100	390	--	101.16	17.39	33.18	54.71
22	100	390	--	89.3	24.26	28.22	52.91
23	100	430	27	75.4	30.61	22.10	41.01
26	100	430	--	59.47	38.79	15.25	37.79
27	100	430	26	*41.38*	48.78	7.61	28.97
30	100	520	--	33.28	57.90	4.14	23.50
31	100	520	--	*25.95*	70.49	0.84	25.06
34	100	520	26	*25.09*	83.28	0.62	28.00
35	100	520	--	*25.83*	97.79	0.79	28.84

Run	Avg V_x	Avg V_y	Avg V_z	Std v_x'	Std v_y'	Std v_z'
	cm/s	cm/s	cm/s	cm/s	cm/s	cm/s
(1)	(9)	(10)	(11)	(12)	(13)	(14)
2	6.08	-8.61	-4.33	14.79	10.82	10.81
3	5.21	-9.23	-4.50	13.99	10.16	11.53
6	5.36	-9.41	-5.54	13.85	10.22	11.68
7	4.54	-10.67	-3.38	12.95	9.66	11.73
10	6.79	-8.93	-3.57	15.22	10.71	11.09
11	6.38	-6.67	-5.75	14.61	10.76	11.66
14	4.96	-11.39	-8.97	12.52	9.73	10.74
15	4.59	-11.32	-7.66	14.34	9.73	11.19
18	3.59	-3.19	-7.16	19.19	13.32	11.24
19	2.53	-3.30	-4.53	18.49	12.43	10.25
22	3.25	-2.05	-4.71	19.43	12.88	9.64
23	-9.29	2.55	1.82	29.31	21.79	10.49
26	-8.82	6.43	0.20	31.63	19.72	7.81
27	2.60	3.68	-2.73	31.34	28.15	6.67
30	4.58	3.42	-1.87	39.39	37.42	7.19
31	2.24	1.77	-0.58	31.68	31.22	5.61
34	0.99	0.44	-0.05	23.86	23.46	4.20
35	0.29	-0.29	-0.02	21.72	22.40	3.92

Notes: microADV data scanned at 50 Hz for 60 s; Ampl: acoustic backscatter amplitude (counts); Avg: time-averaged; COR: correlation; SNR: signal to noise ratio; SSC: suspended sediment concentration; Std: standard deviation; *Italic data*: suspicious data with low SNR. Post-processing: low SSCs = removal of Avg SNR < 15 dB, Avg < 40%, & communication errors; intermediate

SSCs = removal of communication errors & Avg SNR < 15 dB; high SSCs = removal of communication errors.

Laboratory tests - MicroADV system measurements - Velocity range: 2.5 m/s

Run	Velocity range	Speed	Water temp.	Avg Ampl	SSC	Avg SNR	Avg COR
	cm/s	rpm	Celsius	Counts	g/l	dB	%
(1)	(2)	(3)	(4)	(5)	(6)	(7)	(8)
1	250	290	--	98.73	0.00	35.39	60.96
4	250	290	--	106.55	0.03	37.38	60.96
5	250	290	--	109.58	0.23	39.37	60.97
8	250	290	--	115.67	0.79	40.98	62.30
9	250	290	--	118.68	2.19	41.40	62.13
12	250	290	--	120.04	3.18	41.44	80.92
13	250	290	--	119.21	4.90	41.23	80.71
16	250	290	26.5	116.03	8.04	39.57	78.86
17	250	390	26.5	109.11	12.73	36.60	74.16
20	250	390	--	102.85	17.39	34.05	71.47
21	250	390	--	93.05	24.26	29.69	62.22
24	250	430	--	84.76	30.61	26.41	43.99
25	250	430	--	74.84	38.79	22.00	33.17
28	250	430	--	66.72	48.78	18.51	27.23
29	250	520	--	61.2	57.90	15.99	24.67
32	250	520	--	*52.96*	70.49	12.59	25.86
33	250	520	--	*46.2*	83.28	9.69	27.27
36	250	520	--	*39.85*	97.79	6.82	30.89

Run	Avg V_x	Avg V_y	Avg V_z	Std v_x'	Std v_y'	Std v_z'
	cm/s	cm/s	cm/s	cm/s	cm/s	cm/s
(1)	(9)	(10)	(11)	(12)	(13)	(14)
1	6.48	-8.36	-5.01	13.24	9.61	11.19
4	6.47	-8.17	-4.75	13.32	9.83	10.78
5	5.44	-8.49	-5.47	12.88	10.14	11.20
8	4.35	-10.14	-6.66	13.45	10.13	11.06
9	4.81	-12.23	-10.34	12.03	9.17	10.63
12	4.18	-12.95	-7.23	13.14	10.43	10.59
13	3.09	-11.94	-6.53	13.63	10.02	10.97
16	3.82	-12.71	-7.29	14.39	10.62	10.80
17	3.48	-4.35	-5.23	19.30	11.57	10.81
20	1.71	-3.11	-4.50	22.52	11.57	10.56
21	2.45	-2.16	-4.40	29.27	12.39	9.07
24	-8.52	2.14	0.19	40.36	21.28	11.01
25	-3.69	2.60	-2.12	46.57	36.43	10.08
28	3.06	-0.48	-4.76	56.80	51.65	10.55
29	5.81	0.00	-3.71	62.95	60.37	11.77
32	3.60	0.47	-1.85	54.08	52.99	9.55
33	2.05	1.61	-1.13	46.59	45.66	8.20
36	1.11	-0.59	-0.02	39.12	39.43	6.94

Notes: microADV data scanned at 50 Hz for 60 s; Ampl: acoustic backscatter amplitude (counts);

Avg: time-averaged; COR: correlation; SNR: signal to noise ratio; SSC: suspended sediment concentration; Std: standard deviation; *Italic data*: suspicious data with low SNR. Post-processing: low SSCs = removal of Avg SNR < 15 dB, Avg < 40%, & communication errors; intermediate SSCs = removal of communication errors & Avg SNR < 15 dB; high SSCs = removal of communication errors.

C.2.3 Discussion

Within the experimental conditions, the relationship between acoustic backscatter amplitude (Ampl) and suspended sediment concentrations (SSC) was tested for SSCs between 0 and 98 kg/m^3. The experimental results are summarised in Figure C-3.

The data trend was independent of the ADV settings. No difference was observed between the ADV velocity ranges. There was a good correlation between all the data showing two distinctive trends. For SSC ≤ 3.2 kg/m^3, a monotonic increase in suspended sediment concentration with increasing signal amplitude was observed. For the laboratory tests with low suspended loads (SSC ≤ 3.2 kg/m^3), the best fit relationship was:

$$SSC = 1.578 \times 10^{-77} \times (Ampl + 5.076)^{26.865} \qquad SSC \leq 3.2 \text{ kg/m}^3 \quad \text{(C-1)}$$

where the suspended sediment concentration SSC is in kg/m^3, and the amplitude Ampl is in count. Equation (C-1) was correlated with a normalised correlation coefficient of 0.994.

For larger SSCs (i.e. SSC > 3.2 kg/m^3), the experimental results demonstrated a decreasing backscatter amplitude with increasing SSC. The data showed some slight differences between the two ADV settings: namely the velocity range had some impact on the calibration curve for high SSCs. The results showed overall some good correlation between the acoustic backscatter strength and the SSC, although the ADV signal was saturated, as observed by CHANSON et al. (2010). For SSC > 3.2 kg/m^3, the data were best correlated by:

$$SSC = 54.23 - 0.4113 \times Ampl + \frac{25518}{Ampl^2} \qquad \text{velocity range: 1.0 m/s} \quad \text{(C-2a)}$$

$$SSC = 72.61 - 0.6174 \times Ampl + \frac{81229}{Ampl^2} \qquad \text{velocity range: 2.5 m/s} \quad \text{(C-2b)}$$

with a normalised correlation coefficient of 0.980 and 0.999 respectively.

The difference might be linked with the flow conditions. At the highest SSCs (SSC > 55 kg/m^3), the mixer speed was set to 520 rpm to prevent sedimentation and it was likely the velocity in the ADV sampling volume exceeded 1 m/s. As a result, the calibration data at high SSCs must be considered with care with the 1.0 m/s velocity range. Further the ADV operation for large SSCs (SSC > 50 kg/m^3) was associated with low averaged signal to noise ratios (SNRs). The results implied that the

ADV system did not operate in optimum conditions.

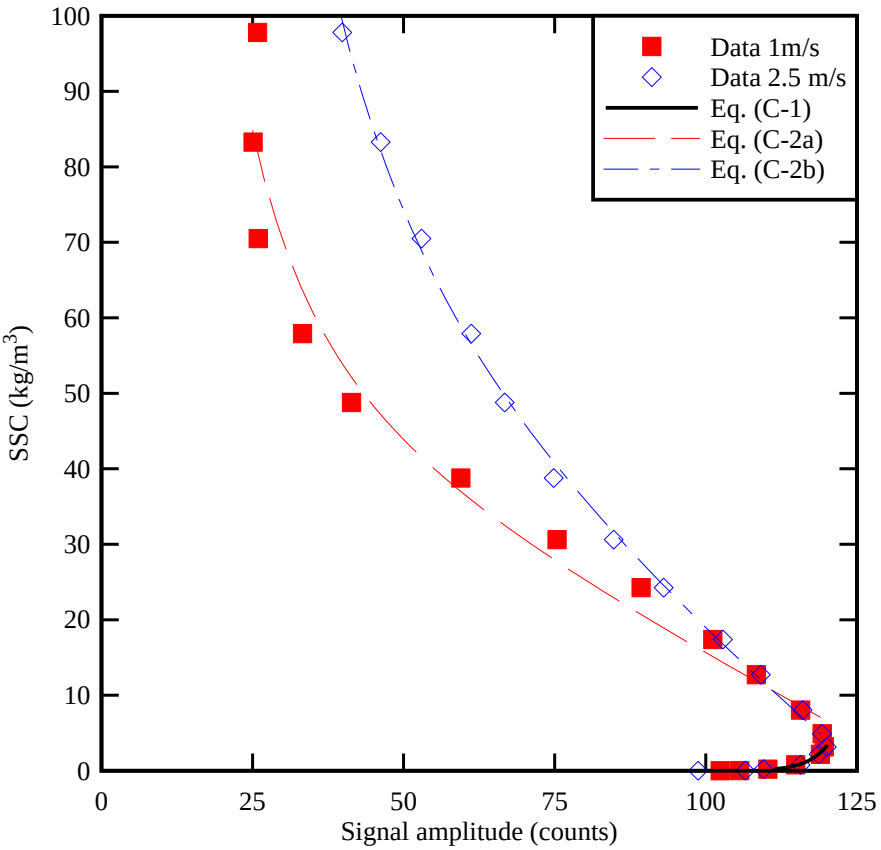

Fig. C-3 - Relationship between suspended sediment concentration and acoustic signal amplitude with the sediment mud samples collected in Gardens Point Road - Comparison between the data and Equations (C-1) and (C-2)

APPENDIX D - TIME-VARIATIONS OF THE FLUCTUATIONS OF WATER LEVEL, VELOCITY COMPONENTS, SUSPENDED SEDIMENT CONCENTRATION AND SUSPENDED SEDIMENT FLUX

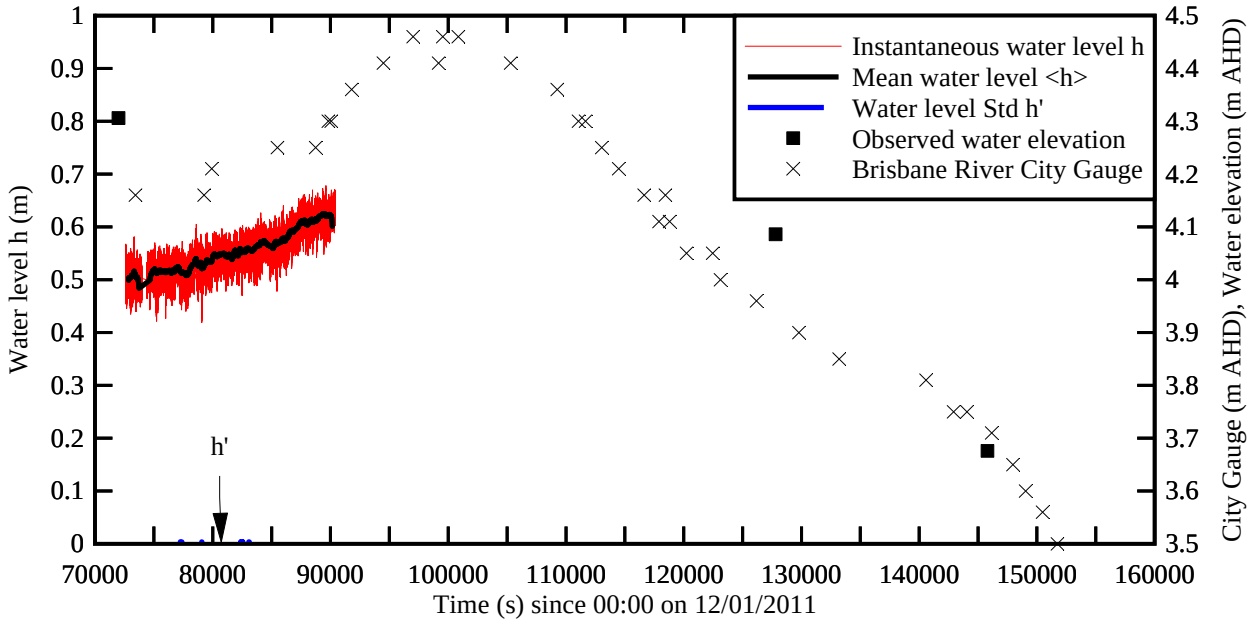

Fig. D-1 - Time-variations of the water level long-term mean value <h> and standard deviation h' of the turbulent motion - Comparison with the manual observations and the Brisbane River City Gauge data (Source: BOM) - Both the manual observations and Brisbane River City Gauge data are reported in m AHD

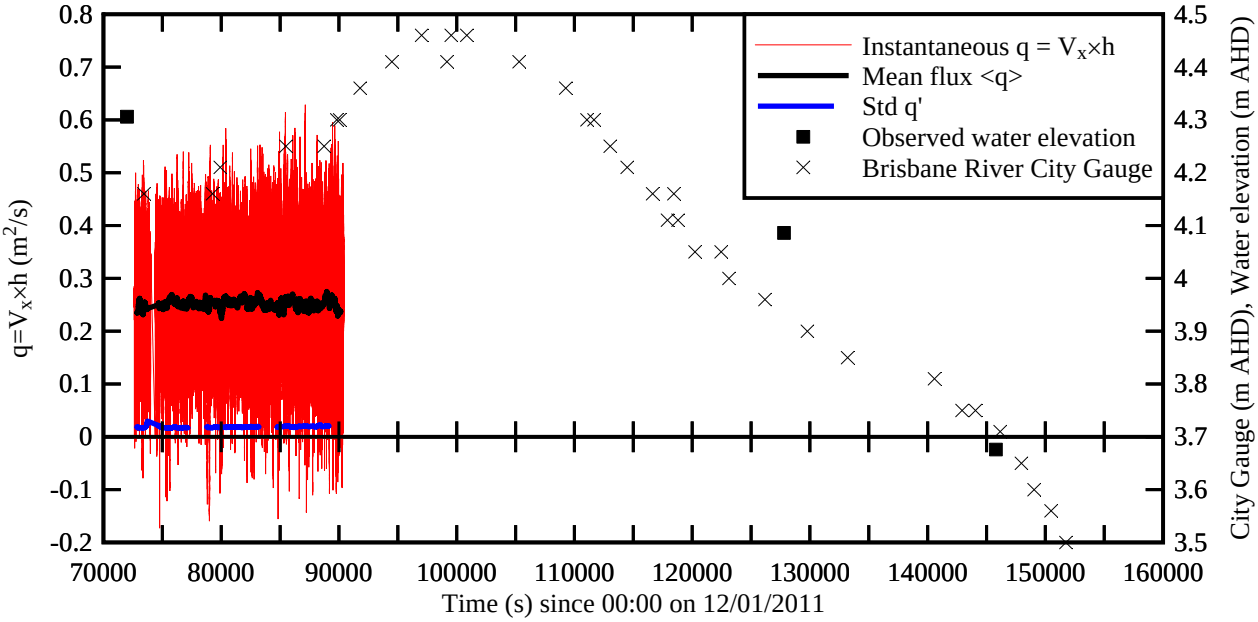

Fig. D-2 - Time-variations of the velocity flux long-term mean value <q> and standard deviation q'

of the turbulent motion - Comparison with the manual observations and the Brisbane River City Gauge data (Source: BOM) - Both the manual observations and Brisbane River City Gauge data are reported in m AHD

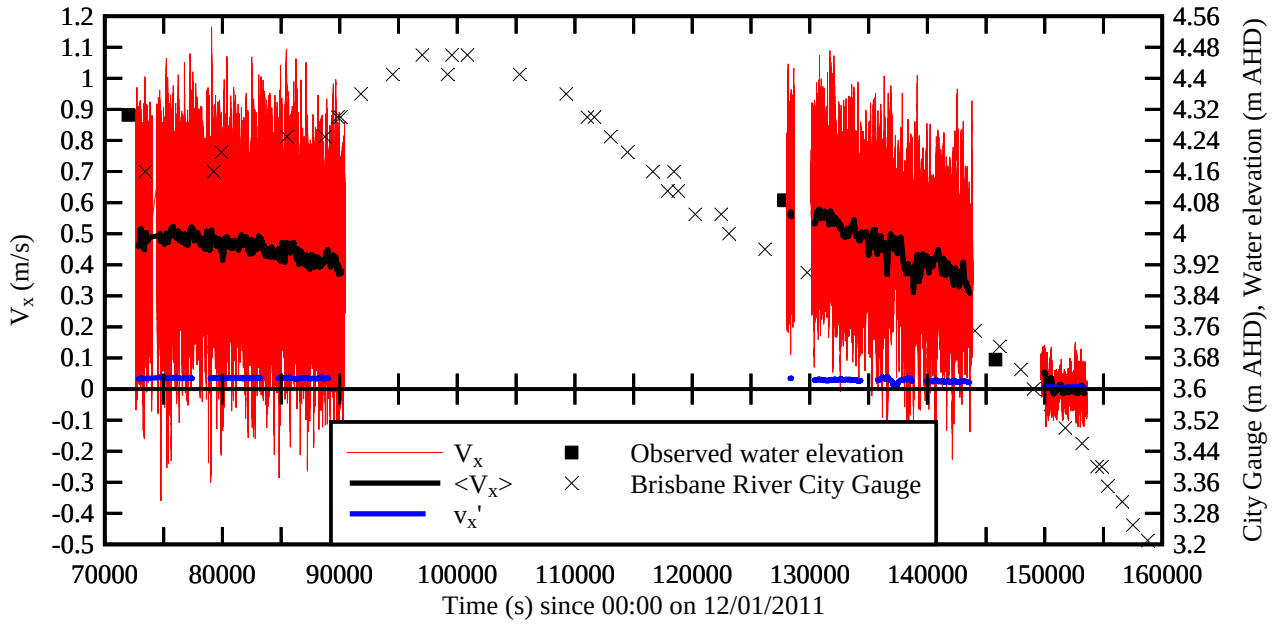

(A) Longitudinal velocity component V_x

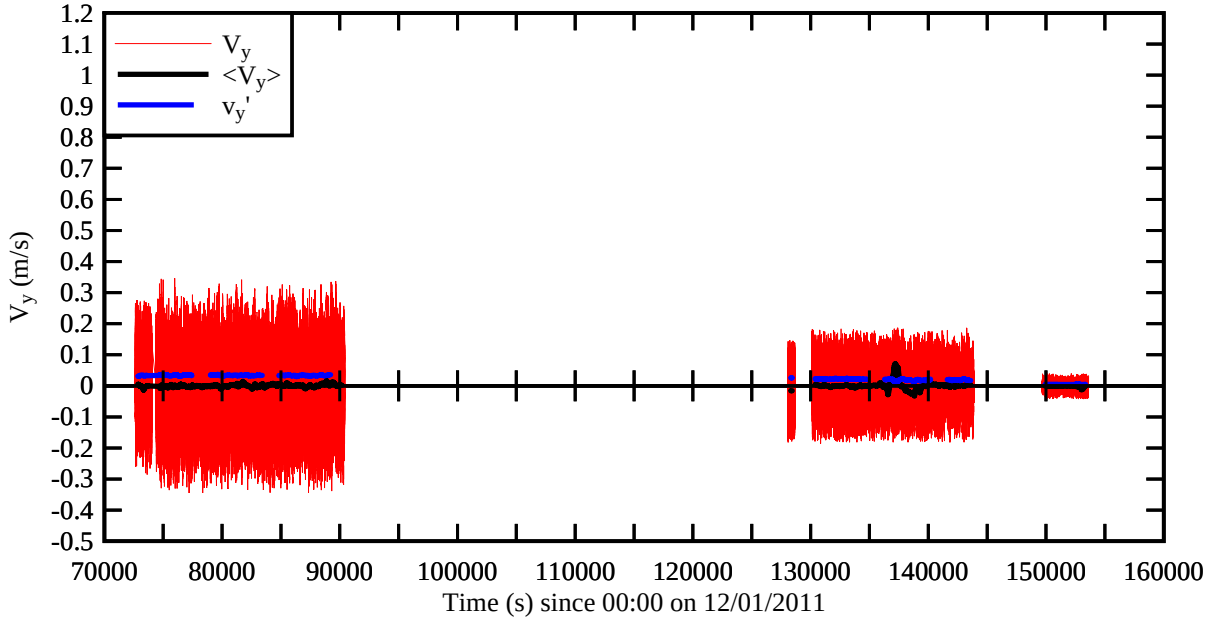

(B) Transverse velocity component V_y

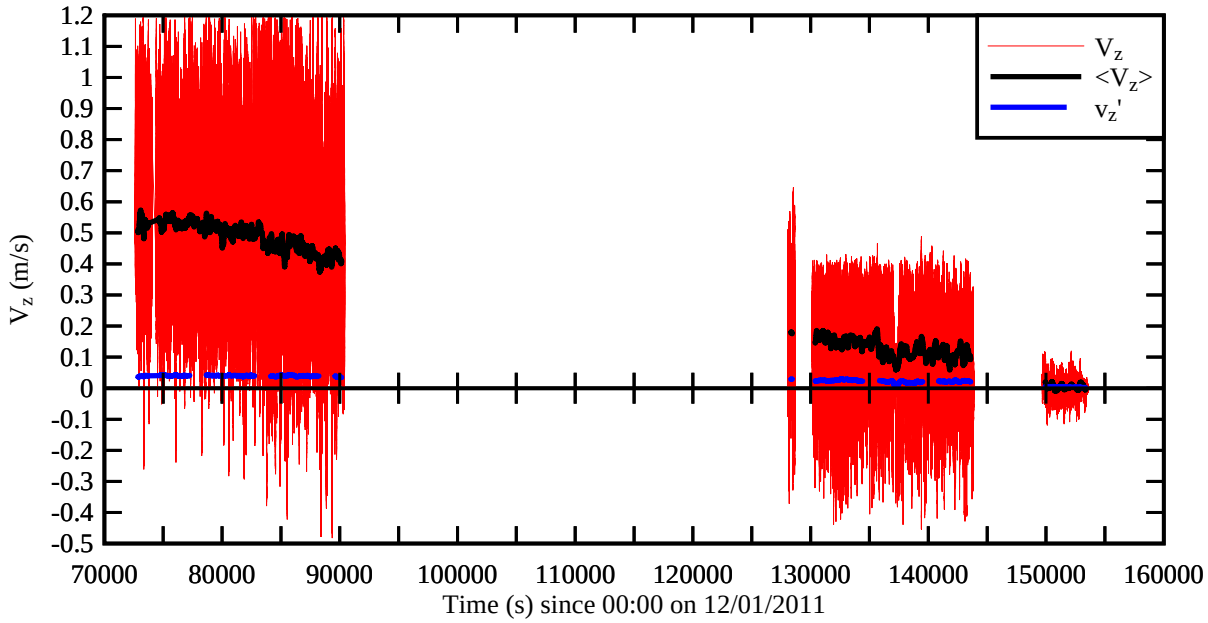

(B) Vertical velocity component V_z

Fig. D-3 - Time-variations of the velocity mean value <V> and standard deviation v' of turbulent motion - Comparison with the manual observations and the Brisbane River City Gauge data (Source: BOM) - Both the manual observations and Brisbane River City Gauge data are reported in m AHD

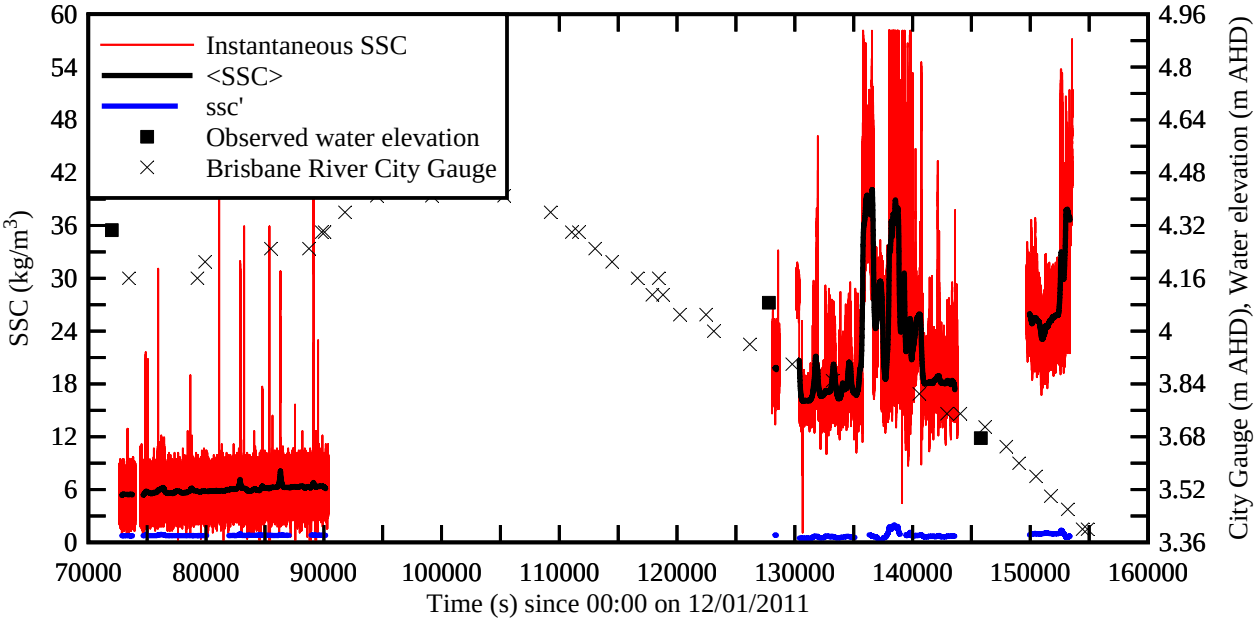

Fig. D-4 - Time-variations of the suspended sediment concentration mean value <SSC> and standard deviation ssc' of turbulent motion - Comparison with the manual observations and the Brisbane River City Gauge data (Source: BOM) - Both the manual observations and Brisbane River City Gauge data are reported in m AHD

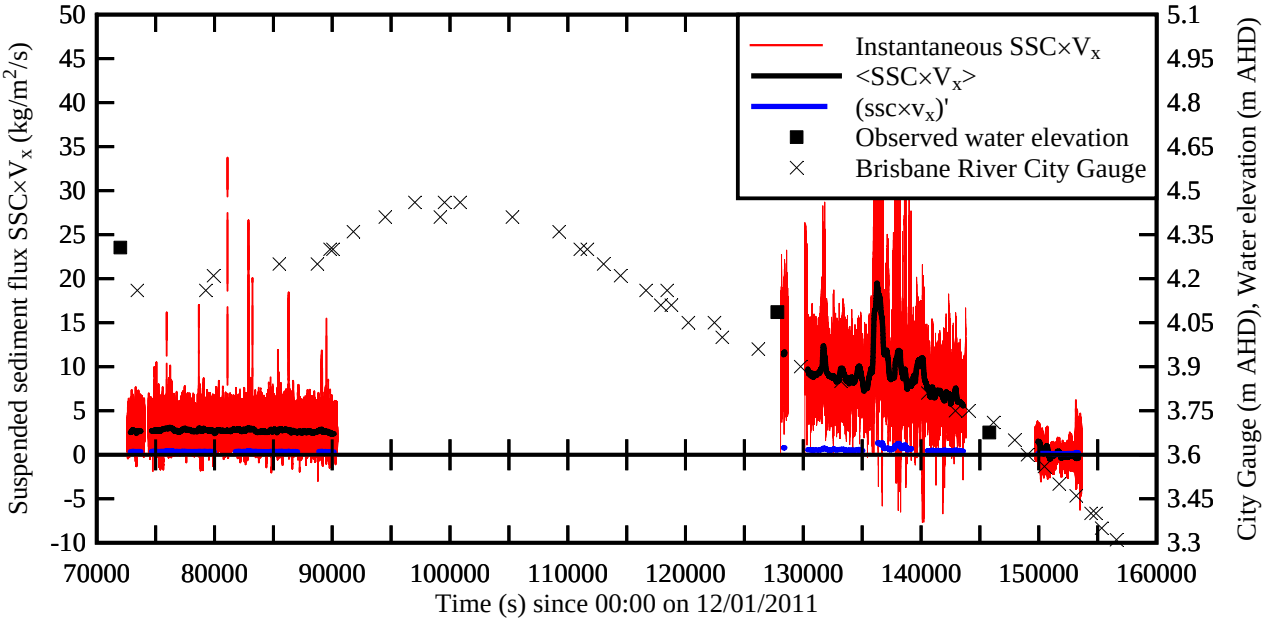

Fig. D-5 - Time-variations of the suspended sediment flux mean value $<SSC \times V_x>$ and standard deviation $(ssc \times v_x)'$ of turbulent motion - Comparison with the manual observations and the Brisbane River City Gauge data (Source: BOM) - Both the manual observations and Brisbane River City Gauge data are reported in m AHD

Probability distribution functions (PDFs) of the velocity fluctuations around the mean V - <V>

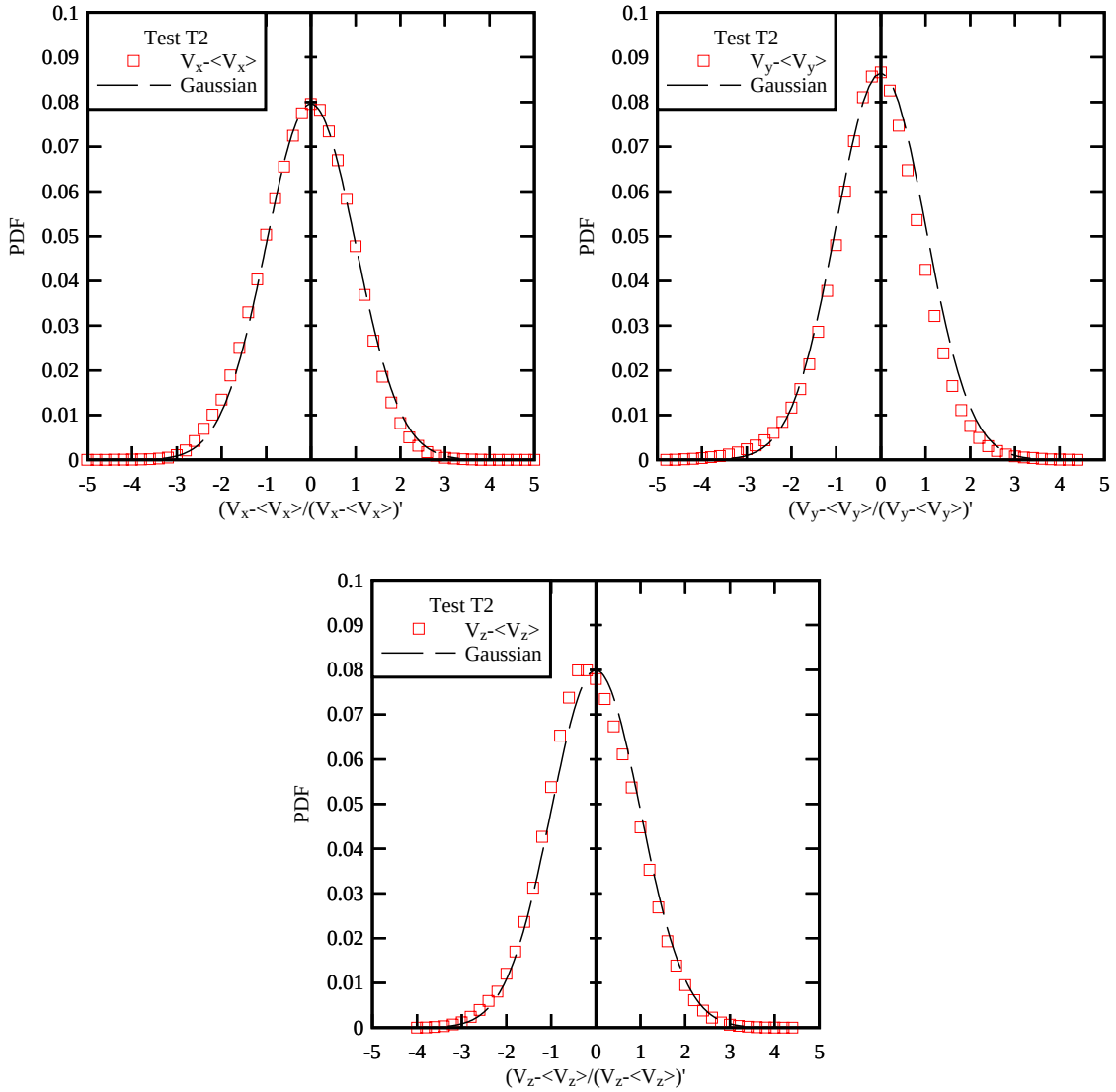

Fig. D-5 - Probability distribution functions (PDFs) of the velocity fluctuations around the mean V - <V> during test T2 (12-13 January 2011)

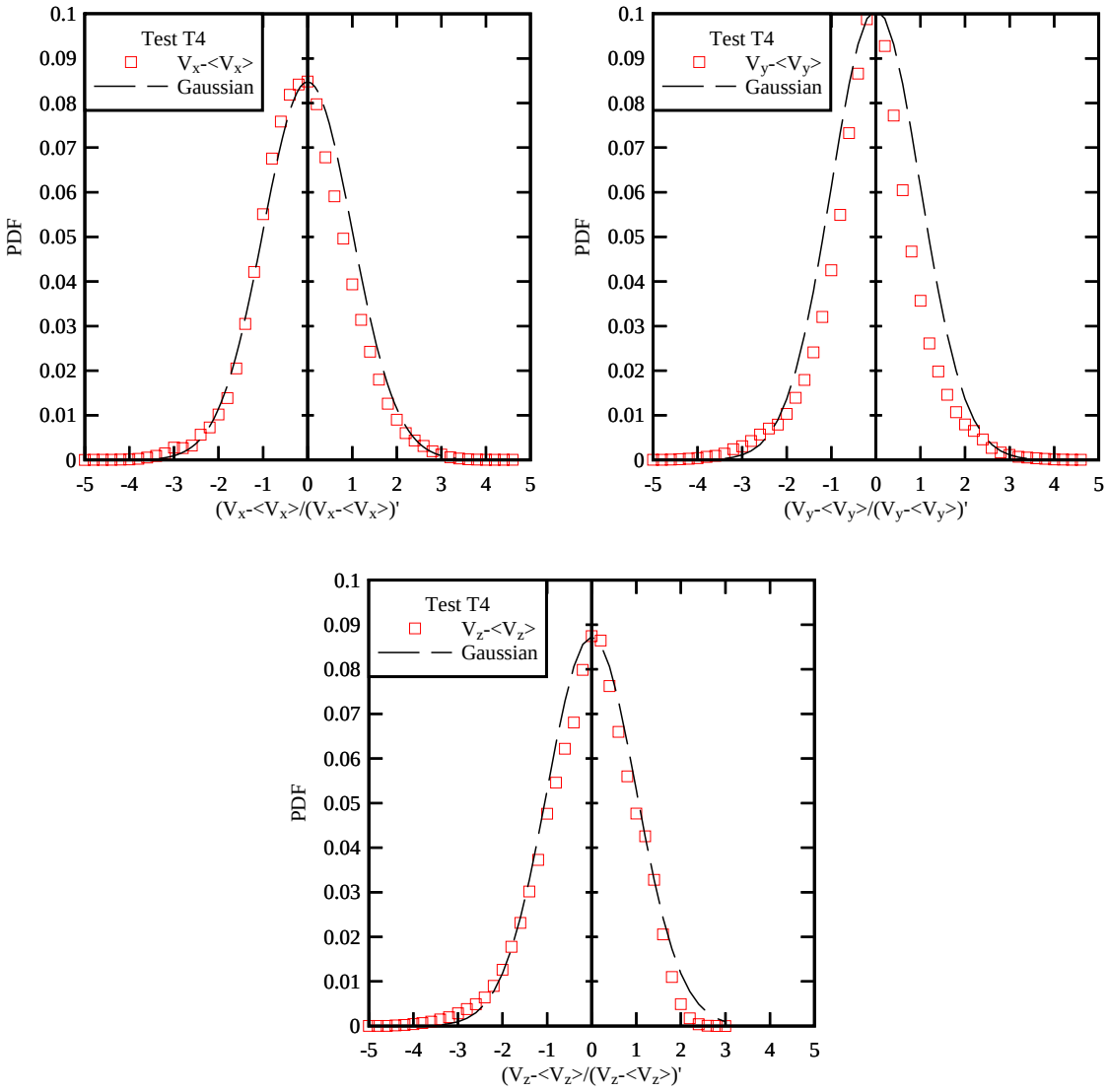

Fig. D-5 - Probability distribution functions (PDFs) of the velocity fluctuations around the mean V - <V> during test T4 (13 January 2011)

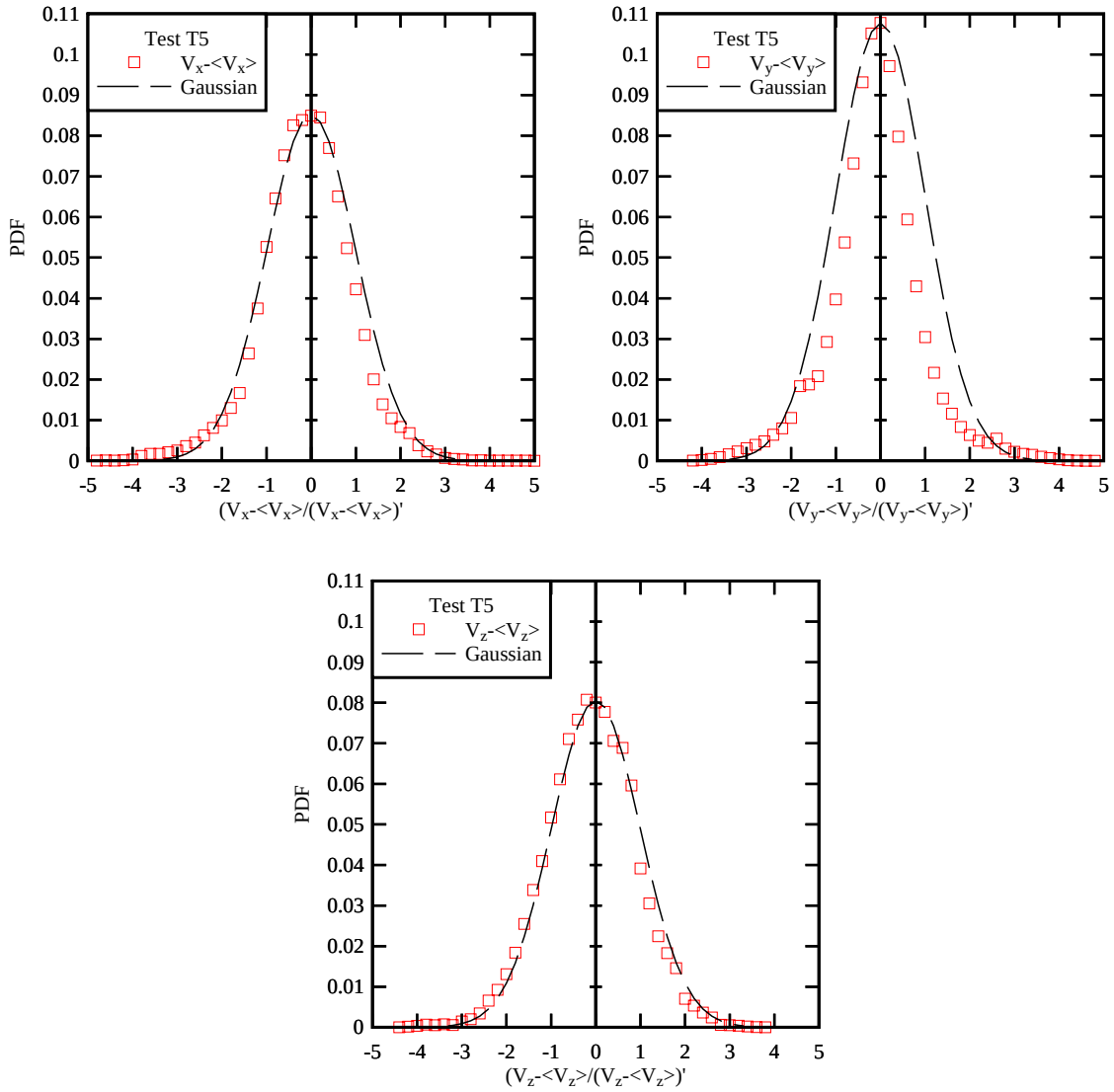

Fig. D-5 - Probability distribution functions (PDFs) of the velocity fluctuations around the mean V - <V> during test T5 (13 January 2011)

APPENDIX E - TIME-VARIATIONS OF THE TURBULENT REYNOLDS STRESSES

Table E-1 - Turbulent Reynolds stress measurements in the flood plain (QUT car park) of the Brisbane River in flood on 12-13 January 2011

Data file	ADV location	Sampling rate Hz	Velocity range m/s	z m	Start time	Nb of samples
(1)	(2)	(3)	(4)	(5)	(6)	(7)
T1	A	50	2.5	0.350	12/01/2011 at 20:10:31	70,162
T2	A	50	2.5	0.350	12/01/2011 at 20:40:08	800,000
T3	B	50	2.5	0.083	13/01/2011 at 11:34:28	31,171
T4	B	50	1.0	0.083	13/01/2011 at 12:08:55	685,884
T5	B	50	1.0	0.083	13/01/2011 at 17:34:40	196,762

Data file	z	$\overline{\rho v_x^2}$	$\overline{\rho v_y^2}$	$\overline{\rho v_z^2}$	$\overline{\rho v_x v_z}$	$\overline{\rho v_x v_y}$	$\overline{\rho v_y v_z}$	$\frac{\overline{v_x v_z}}{\sqrt{\overline{v_x^2}\,\overline{v_z^2}}}$	$\frac{\overline{v_x v_y}}{\sqrt{\overline{v_x^2}\,\overline{v_y^2}}}$	$\frac{\overline{v_y v_z}}{\sqrt{\overline{v_y^2}\,\overline{v_z^2}}}$
	m	Pa	Pa	Pa	Pa	Pa	Pa			
(1)	(5)	(8)	(9)	(10)	(11)	(12)	(13)	(14)	(15)	(16)
T1	0.350	1.983	1.805	2.555	-0.0807	-0.1823	-0.0323	-0.0328	-0.0954	0.01371
T2	0.350	2.158	1.958	2.782	-0.064	0.1401	0.0229	-0.02659	0.06817	0.009502
T3	0.083	2.166	1.179	1.54	-0.080	-0.1365	0.0716	-0.0629	-0.0867	0.05405
T4	0.083	1.445	0.7881	1.007	-0.0734	-0.0249	0.03362	0.04224	-0.02558	-0.06443
T5	0.083	0.07086	0.04078	0.03184	0.00379	0.00107	-0.0002	0.07823	0.02573	0.07823

Data file	z	Avg $(\rho v_x^2)'$	Avg $(\rho v_y^2)'$	Avg $(\rho v_x^2)'$	Avg $(\rho v_x v_z)'$	Avg $(\rho v_x v_y)'$	Avg $(\rho v_y v_z)'$
	m	Pa	Pa	Pa	Pa	Pa	Pa
(1)	(5)	(17)	(18)	(19)	(20)	(21)	(22)
T1	0.350	1.998	1.826	2.595	1.449	1.221	1.391
T2	0.350	2.156	1.956	2.781	1.556	1.313	1.495
T3	0.083	1.718	0.9704	1.2498	0.946	0.8322	0.7108
T4	0.083	1.4458	0.7895	1.0068	0.7541	0.68098	0.5631
T5	0.083	0.0696	0.04012	0.03141	0.02835	0.03537	0.02097

Data file	Min $\overline{\rho v_x^2}$	Max $\overline{\rho v_x^2}$	Min $\overline{\rho v_y^2}$	Max $\overline{\rho v_y^2}$	Min $\overline{\rho v_z^2}$	Max $\overline{\rho v_z^2}$	Min $\overline{\rho v_x v_z}$	Max $\overline{\rho v_x v_z}$	Min $\overline{\rho v_x v_y}$	Max $\overline{\rho v_x v_y}$	Min $\overline{\rho v_y v_z}$	Max $\overline{\rho v_y v_z}$
(1)	Pa (23)	Pa (24)	Pa (25)	Pa (26)	Pa (27)	Pa (28)	Pa (29)	Pa (30)	Pa (31)	Pa (32)	Pa (33)	Pa (34)
T1	3.0E-10	290.6	2.1E-9	56.5	3.4E-10	688.7	-48.7	423.0	-30.8	86.5	-33.0	133.5
T2	1.9E-12	228.0	3.1E-15	84.2	3.4E-14	155.1	-96.4	110.7	-43.3	49.1	-77.5	89.9
T3	1.5E-8	204.7	9.4E-11	24.1	2.8E-11	47.0	-28.2	98.1	-27.2	22.4	-17.9	19.6
T4	6.9E-17	166.7	2.5E-16	44.3	1.3E-17	201.5	-39.1	90.8	-32.2	43.6	-30.8	27.2
T5	1.3E-18	9.0	1.6E-17	1.6	3.5E-19	4.6	-4.61	2.19	-1.74	1.71	-1.37	1.20

Notes:

Avg: time-average over the test duration;

Location A: ADV unit mounted horizontally on boom gate support;

Location B: ADV unit mounted vertically on a hand rail;

Max: maximum value;

Min: minimum value;

v: turbulent velocity component after triple decomposition;

z: vertical elevation above the invert;

$\overline{\rho v^2}$: time-averaged Reynolds stress component calculated over 500 s;

(ρv^2): standard deviation of Reynolds stress component calculated over 500 s;

Shaded data: relatively small number of data samples.

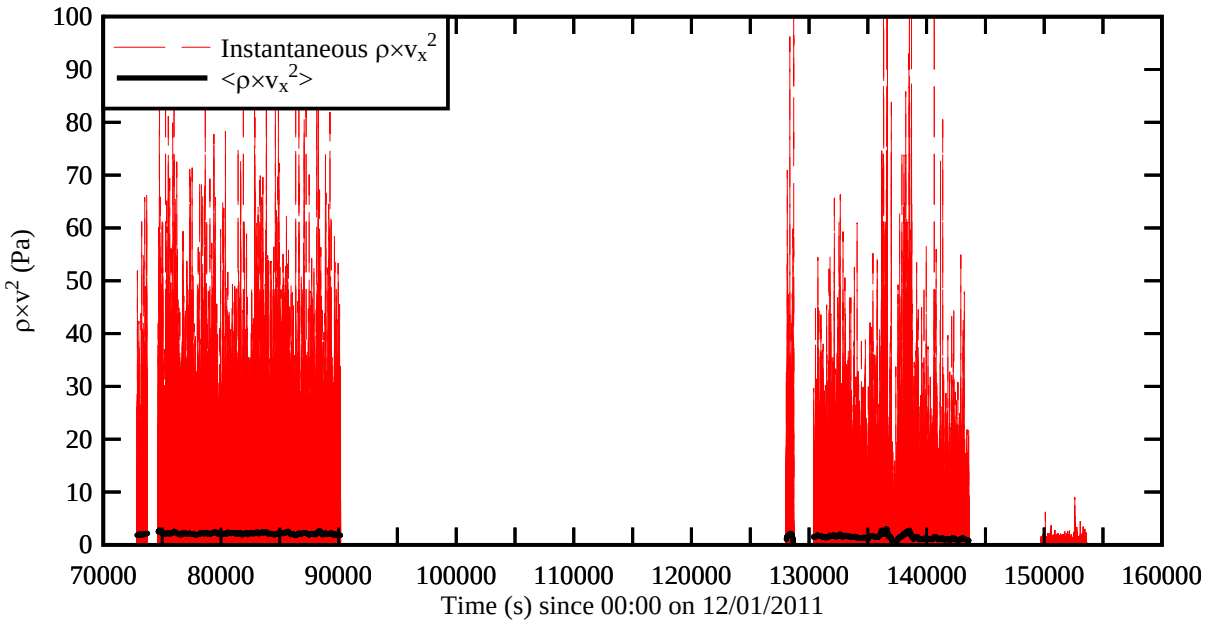

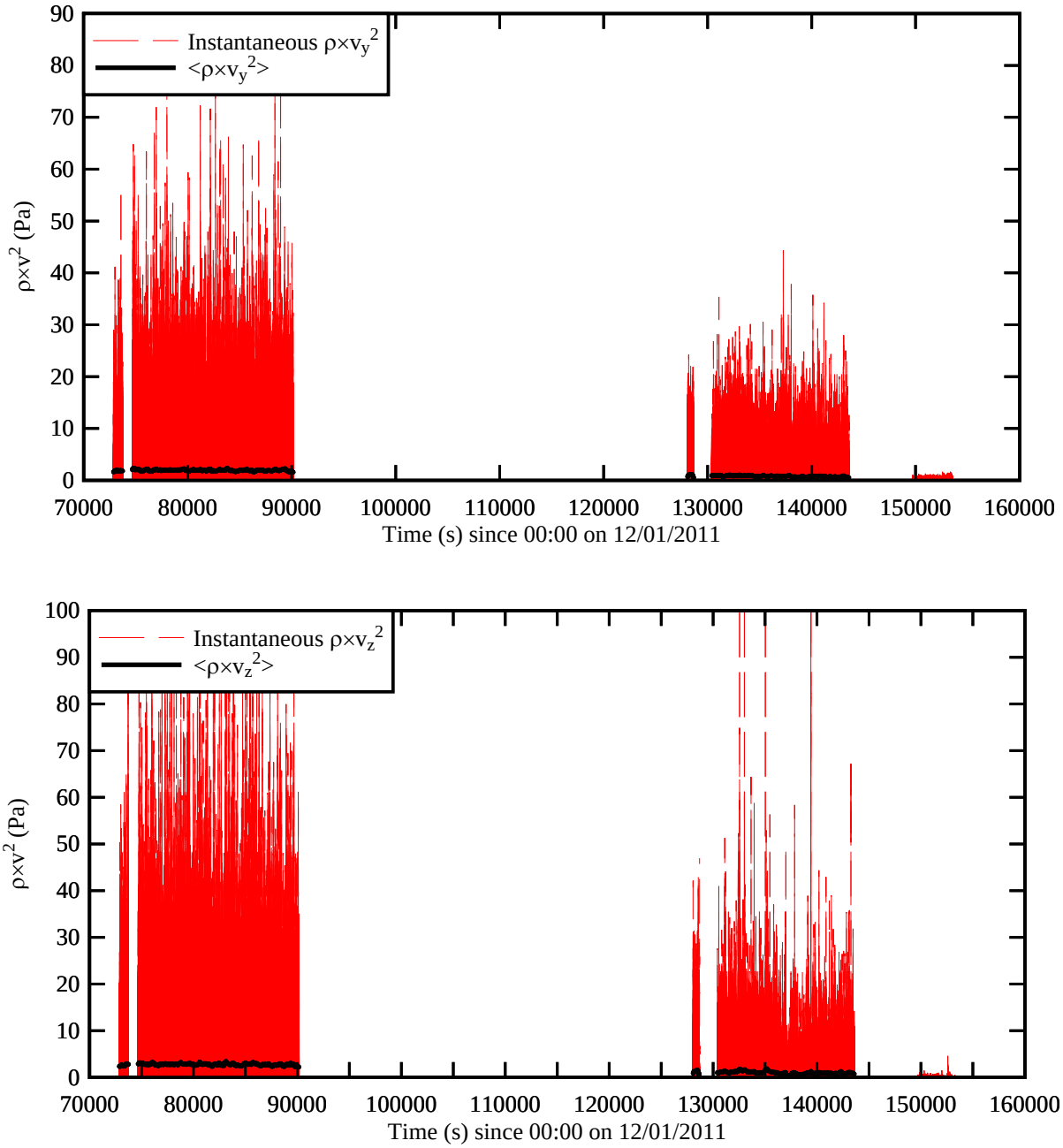

Fig. E-1 - Time-variations of the normal stresses - All turbulent stresses were calculated after triple decomposition based upon the turbulent velocity components

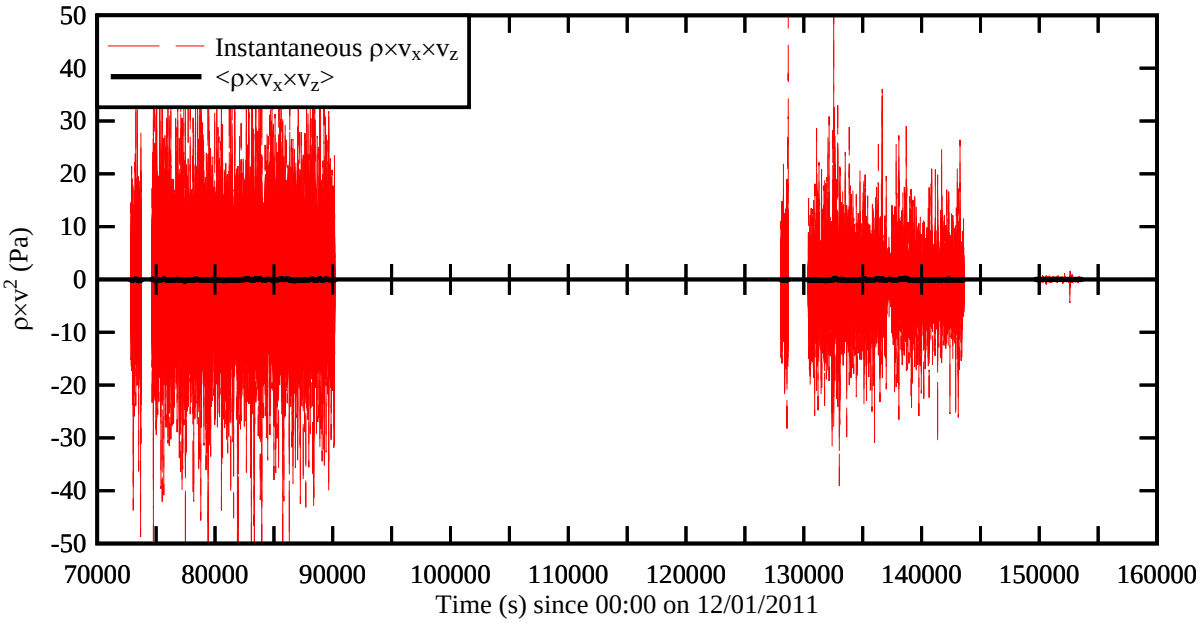
Instantaneous ρ×v_x×v_z
<ρ×v_x×v_z>
ρ×v^2 (Pa)
50
40
30
20
10
0
-10
-20
-30
-40
-50
70000
80000
90000
100000
110000
120000
130000
140000
150000
160000
Time (s) since 00:00 on 12/01/2011

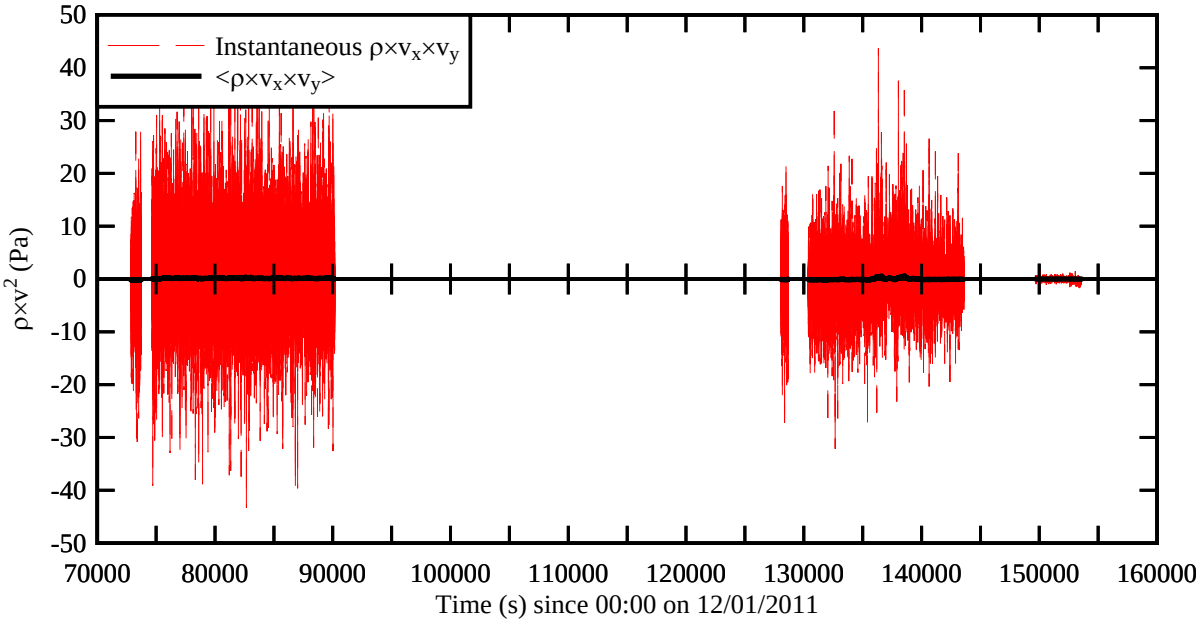
Instantaneous ρ×v_x×v_y
<ρ×v_x×v_y>
ρ×v^2 (Pa)
50
40
30
20
10
0
-10
-20
-30
-40
-50
70000
80000
90000
100000
110000
120000
130000
140000
150000
160000
Time (s) since 00:00 on 12/01/2011

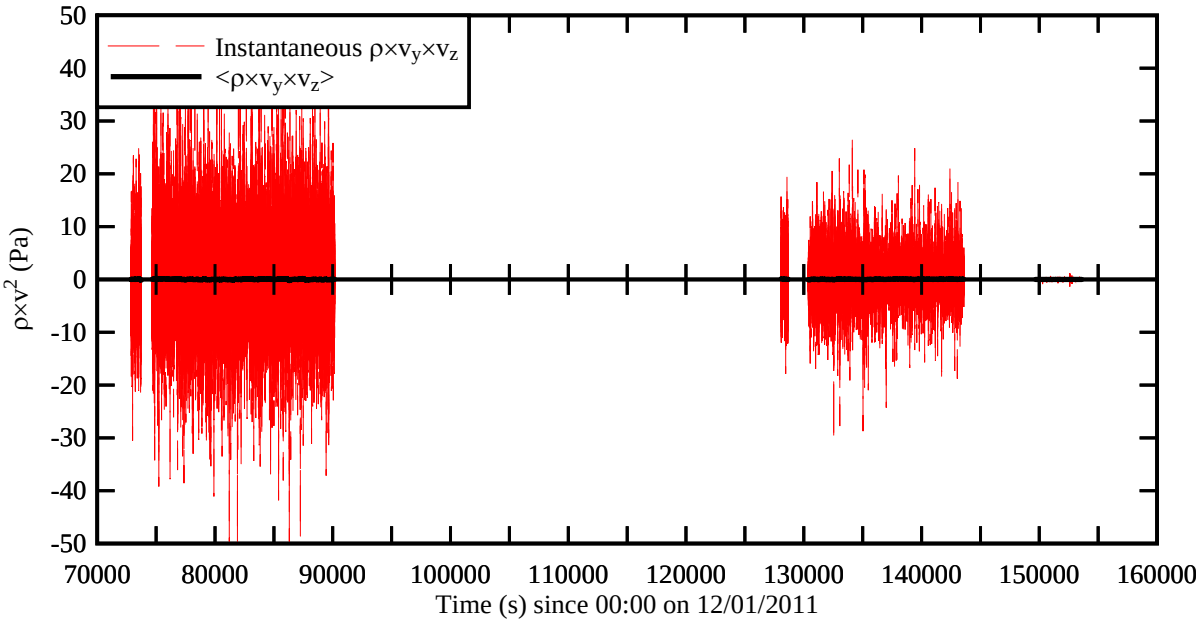

Fig. E-3 - Time-variations of the tangential stresses - All turbulent stresses were calculated after triple decomposition based upon the turbulent velocity components

APPENDIX F - SURVEYED WATER LEVELS OF THE BRISBANE RIVER IN BRISBANE DURING THE JANUARY 2011 FLOOD (BY HUBERT CHANSON)

F.1 PRESENTATION

Some high-resolution photographs of the Brisbane River flood were taken in January 2011 between Jindalee and the Brisbane Central Business District (CBD) (CHANSON 2011,2011b). The water elevations were surveyed after the event. Most photographs were taken with digital SLR cameras. Figure F-1 presents a map of Brisbane with the locations of the surveys, and the survey data are listed in Table F-1.

The water elevations were compared with the closest permanent marker and reported in m AHD relative to the Australian Height Datum (AHD) (Table F-1, column 8).

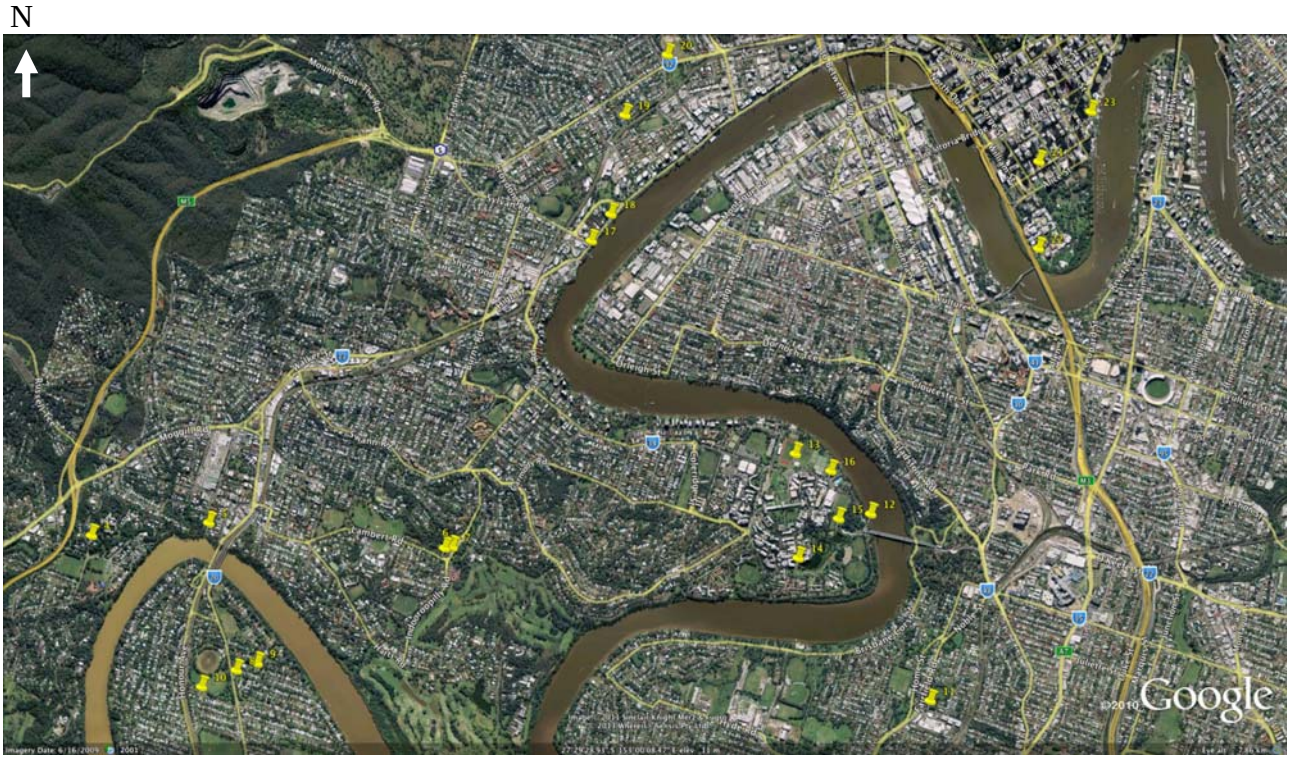

Fig. F-1 - Map of Brisbane area showing the locations of the surveys (Courtesy of Google Earth, accessed in May 2011 & Angus MacDIARMID)

Table F-1 - Surveyed water elevations during the January 2011 flood of the Brisbane River in Brisbane

Ref. (1)	Source (2)	Suburb (3)	Location (4)	Longitude & latitude (5)	Date (6)	Time (7)	Water elev. m AHD (8)
1A	FR	Jindalee	Sinnamon Park South of Seventeen Mile Rocks Rd Bridge	(-27° 32' 14.85", +152° 56' 48.58")	12/01/2011	6:09 PM	11.487
2B	SM	Fig Tree Pocket	72 Cubberla Street	--	12/01/2011	10:26 AM	9.047 / 9.013
2C	SM	Fig Tree Pocket	Corner Fig Tree Pocket Rd and Ormsby St	(-27° 32' 18.14", +152° 58' 2.50")	12/01/2011	11:24 AM	9.134
3A	AW	Indooroopilly	35 Kate Street	(-27° 30' 22.16", +152° 57' 52.43")	12/01/2011	8:40 AM	8.53/8.51
3B	AM	Indooroopilly	35 Kate Street	(-27° 30' 22.16", +152° 57' 52.43")	12/01/2011	8:40 AM	8.53/8.51
3C	AM	Indooroopilly	35 Kate Street	(-27° 30' 22.16", +152° 57' 52.43")	12/01/2011	8:47 AM	8.53/8.51
3D	AM	Indooroopilly	35 Kate Street	(-27° 30' 22.14", +152° 57' 52.13")	13/01/2011	1:02 PM	9.794
3E	AM	Indooroopilly	35 Kate Street	(-27° 30' 22.15", +152° 57' 52.98")	13/01/2011	1:02 PM	8.701
4A	HC	Indooroopilly	Corner Foxton St and Radnor St	(-27° 30' 15.77", +152° 58' 22.68")	12/01/2011	2:15 PM	9.246
4B	HC	Indooroopilly	255 Lambert Rd	(-27° 30' 11.98", +152° 59' 21.09")	12/01/2011	2:30 PM	8.875
4D	HC	Indooroopilly	Intersection Indooroopilly Rd and Bicycle Path	(-27° 30' 9.52", +152° 59' 25.49")	12/01/2011	2:56 PM	8.912
5A	FR	Chelmer	Milpera, 72 Oxley Road	--	13/01/2011	12:11 PM	8.438
5C	FR	Chelmer	25 Glenwood Street	(-27° 30' 45.71", +152° 58' 40.28")	13/01/2011	12:18 PM	8.474
5D	FR	Chelmer	25 Glenwood Street	(-27° 30' 46.26", +152° 58' 39.98")	14/01/2011	8:44 AM	9.254
5E	FR	Chelmer	Appel Street	(-27° 31' 13.87", +152° 58' 43.80")	12/01/2011	5:40 PM	9.248
5E	FR	Chelmer	Appel Street	(-27° 31' 13.87", +152° 58' 43.80")	12/01/2011	5:40 PM	9.146
7B	JS	Fairfield	Broughham St near Bus Stop and Lot 5	(-27° 30' 30.35", +153° 1' 31.81")	11/01/2011	4:52 PM	3.809
8A	HC	St Lucia	Ferry Terminal, University of Queensland St Lucia Campus	(-27° 29' 50.02", +153° 1' 9.25")	12/01/2011	6:19 AM	6.066
8B	HC	St Lucia	Main Rugby Oval(Field 5), University of Queensland St Lucia Campus	(-27° 29' 40.00", +153° 0' 46.95")	12/01/2011	3:10 PM	6.143
8C	HC	St Lucia	Main Rugby Oval(Field 5), University of Queensland St Lucia Campus	(-27° 29' 40.00", +153° 0' 46.95")	12/01/2011	3:12 PM	6.092
8D	HC	St Lucia	Corner of College Rd and Staff House Rd, University of Queensland St Lucia Campus	(-27° 30' 2.72", +153° 0' 52.69")	13/01/2011	6:02 AM	7.32
8E	HC	St Lucia	UQ Lakes Walk, University of Queensland St Lucia Campus	(-27° 29' 55.04", +153° 0' 59.97")	13/01/2011	6:11 AM	7.332
8F	HC	St Lucia	UQ Pool, University of Queensland St Lucia Campus	(-27° 29' 41.69", +153° 0' 58.55")	13/01/2011	6:15 AM	6.555

8G	HC	St Lucia	UQ Tennis Centre, University of Queensland St Lucia Campus	(-27° 29' 40.78", +153° 0' 54.43")	13/01/2011	6:19 AM	6.478
8I	HC	St Lucia	Main Rugby Oval(Field 5), University of Queensland St Lucia Campus	(-27° 29' 40.00", +153° 0' 46.95")	13/01/2011	6:24 AM	6.459
9A	HC	Toowong	Corner of Coronation Dr and Patrick Lane	(-27° 28' 51.56", +152° 59' 51.55")	12/01/2011	5:45 AM	4.989
9B	HC	Toowong	Regatta Hotel, Coronation Drive	(-27° 28' 57.92", +152° 59' 46.99")	13/01/2011	5:24 AM	6.332
9D	HC	Toowong	Coronation Drive Bicycle path opposite Regatta Hotel	(-27° 28' 58.40", +152° 59' 47.27")	12/01/2011	5:38 AM	4.984
9E	HC	Toowong	Regatta Ferry Terminal	--	14/01/2011	5:06 AM	3.966
9F	HC	Toowong	Regatta Ferry Terminal	--	14/01/2011	5:07 AM	3.745
9G	HC	Toowong	Regatta Ferry Terminal	--	13/01/2011	5:21 AM	6.38
9H	HC	Toowong	Pedestrian stairs at Regatta Ferry Terminal	--	14/01/2011	5:05 AM	3.74
9I	HC	Toowong	Pedestrian stairs at Regatta Ferry Terminal	--	13/01/2011	5:19 AM	6.336
10B	HC	Auchenflower	Corner of Cue St and Eagle Tce	(-27° 28' 29.13", +152° 59' 50.59")	14/01/2011	5:22 AM	3.354
11B	HC	Milton	Instersection of Eagle Tce and Milton Rd	(-27° 28' 13.80", +152° 59' 59.44")	12/01/2011	4:01 PM	5.798
11D	HC	Milton	Instersection of Eagle Tce and Milton Rd	(-27° 28' 13.80", +152° 59' 59.44")	13/01/2011	5:38 PM	6.057
11E	HC	Milton	Instersection of Eagle Tce and Milton Rd	(-27° 28' 13.80", +152° 59' 59.44")	14/01/2011	5:26 AM	3.796
12B	HC	CBD	Intersection Margaret Street and Albert Street	(-27° 28' 21.27", +153° 1' 41.69")	12/01/2011	4:29 PM	3.455
12C	HC	CBD	Carpark, QUT Gardens Point	(-27° 28' 43.14", +153° 1' 40.46")	13/01/2011	11:40 AM	4.086
12D	HC	CBD	1 Eagle Street	--	High Water Mark	--	8.946 (?)
12D	HC	CBD	2 Eagle Street	--	High Water Mark	--	5.701
12D	HC	CBD	3 Eagle Street	--	High Water Mark	--	5.504

F.2 DISCUSSION

The photographs provided some information on the instantaneous water elevations at a point in time. These cannot be compared with high water level marks which might be biased by waves and local disturbances (e.g. from vehicles). The accuracy of the survey data were about 10 mm for the vertical elevations and 10 cm in the horizontal directions. The time of the photographs was accurate within 5-10 minutes.

From the surveyed water levels, the friction slope was estimated during the flood event. The friction slope S_f or total head line slope is defined as:

$$S_f = -\frac{\partial H}{\partial X} \qquad \text{(F-1)}$$

where H is the total head in m AHD and X is the longitudinal distance measured along the channel centreline (middle thread) and positive downstream. S_f was estimated at 5 different stages of the flood (Table F-1), the water levels being surveyed within 1 hour in each case. The friction slope

ranged from 1.4×10^{-4} to 3.0×10^{-4}. On average, $S_f = 2.3\times10^{-4}$. For comparison, the average friction slope between Jindalee and the Port Office in the City during the 1974 flood was 3×10^{-4} on 18 January 1974 (COSSINS 1974).

Table F-2 - Total head line slope during the January 2011 flood of the Brisbane River in Brisbane

Ref.	Date	Time	Location	Distance km	S_f
(1)	(2)	(3)	(4)	(5)	(6)
A	12 Jan. 2011	14:15-15:12	Indooroopilly-St Lucia	10.4	0.0003037
B	12 Jan. 2011	16:01-17:40	Chelmer-CBD	13.7	0.0002987
C	13 Jan. 2011	05:19-06:24	Toowong-St Lucia	5.25	0.0001583
D	13 Jan. 2011	11:40-13:02	Chelmer-CBD	17.6	0.0002669
E	14 Jan. 2011	05:06-05:26	Toowong-Milton	1.2	0.0001403

F.3 ACKNOWLEDGEMENTS

All the people who provided photographs of interest are acknowledged. The surveys were undertaken by Andrew WILSON and Angus MACDIARMID as part of their CIVL4560 Project under the academic supervision of Hubert CHANSON.

APPENDIX G - SURVEY OF EASTERN GARDENS POINT

(A) Map of Gardens Point area showing the locations of the survey (Courtesy of Google Earth, accessed in June 2011) - The red arrow points to the ADV location

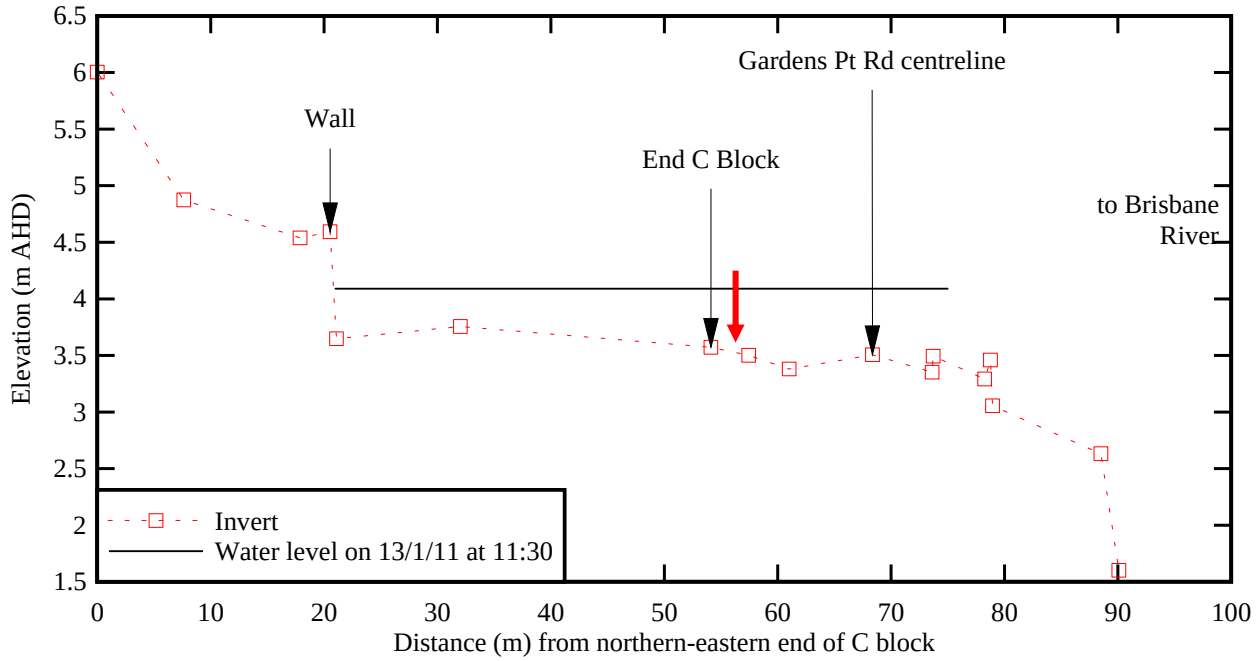

(B) Surveyed cross-section looking downstream (South-East) - The red arrow marks the ADV location

Fig. G-1 - Surveyed cross-section though C Block

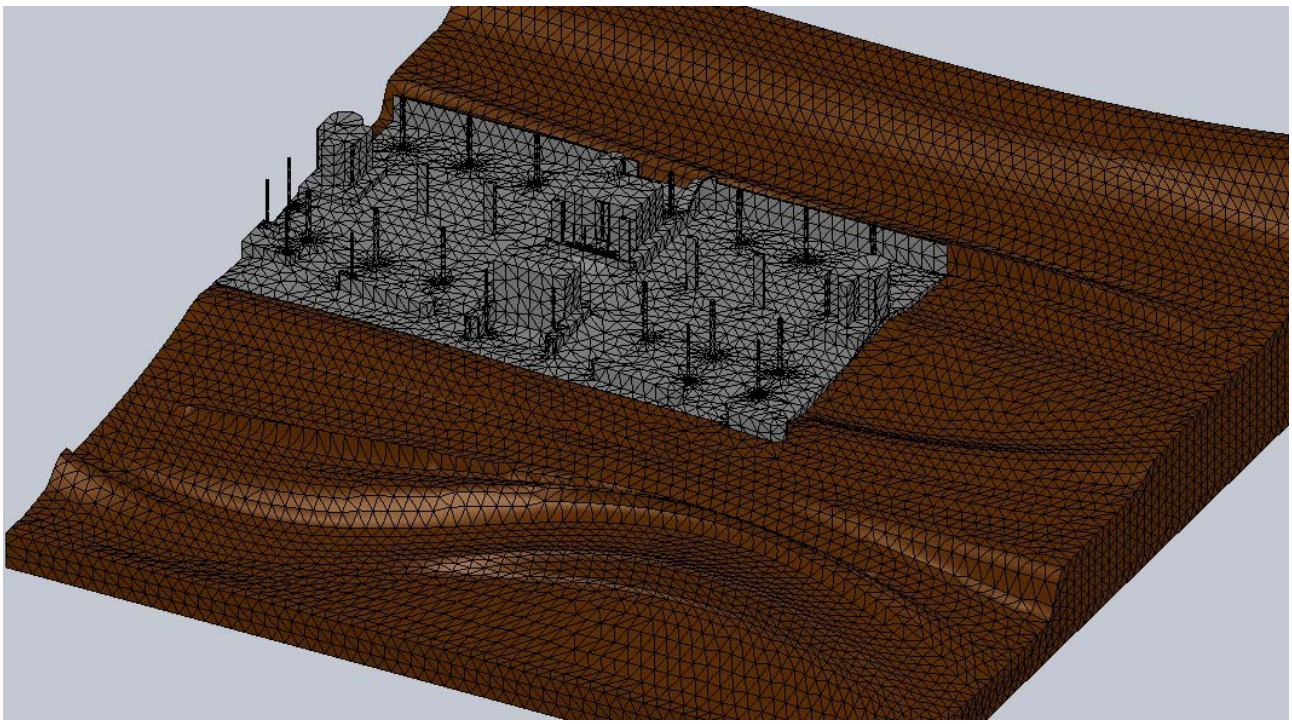

Fig. G-2 - Three-dimensional drawing of C Block car park and surroundings with the Brisbane River channel in foreground - The vertical scale was exaggerated by 250%.

ACKNOWLEDGEMENTS

The surveys were supervised by Dr Rob WEBB (QUT, Faculty of Built Environment and Engineering). All the people who assisted with the surveys are acknowledged. The three-dimensional drawing was prepared by Ken TAN.

REFERENCES

ASAI, Y., ISHIGAKI, T., BABA, Y., and TODA, K. (2010). "Safety Analysis of Evacuation Routes Considering Elderly Persons during Underground Flooding." *Jl of Hydroscience and Hydraulic Eng.*, JSCE, Vol. 28, No. 2, pp. 15-21.

BATES, P.D., HORRITT, M.S., ARONICA, G., and BEVE, K. (2004). "Bayesian Updating of Flood Inundation Likelihoods Conditioned on Flood Extent Data." *Hydrological Processes*, Vol. 18, No. 17, pp. 3347-3370.

BRIER-MILLS, M. (1982). "The Romance of the Bremer." *Historical Society of Ipswich*, Australia.

BOM (2010). "Monthly Weather Review. Queensland. December 2010." *Monthly Weather Review*, Bureau of Meteorology, Melbourne VIC, Australia, 28 pages.

BOM (2011). "Frequent heavy rain events in late 2010/early 2011 lead to widespread flooding across eastern Australia." *Special Climate Statement 24*, National Climate Centre, Bureau of Meteorology, Melbourne VIC, Australia, Revision b, 23 January 2011, 28 pages.

CHANSON, H. (2004). "The Hydraulics of Open Channel Flow: An Introduction." *Butterworth-Heinemann*, 2nd edition, Oxford, UK, 630 pages (ISBN 978 0 7506 5978 9).

CHANSON, H. (2011). "The 2010-2011 Floods in Queensland (Australia): Photographic Observations, Comments and Personal Experience." *Hydraulic Model Report No. CH82/11*, School of Civil Engineering, The University of Queensland, Brisbane, Australia, 127 pages (ISBN 9781742720234).

CHANSON, H. (2011b). "The 2010-2011 Floods in Queensland (Australia): Observations, First Comments and Personal Experience." *Journal La Houille Blanche*, No. 1, pp. 5-11.

CHANSON, H., JARNY, S., and COUSSOT, P. (2006). "Dam Break Wave of Thixotropic Fluid." *Journal of Hydraulic Engineering*, ASCE, Vol. 132, No. 3, pp. 280-293 (DOI: 10.1061/(ASCE)0733-9429(2006)132:3(280)).

CHANSON, H., TAKEUCHI, M., and TREVETHAN, M. (2008). "Using Turbidity and Acoustic Backscatter Intensity as Surrogate Measures of Suspended Sediment Concentration in a Small Sub-Tropical Estuary." *Journal of Environmental Management*, Vol. 88, No. 4, Sept., pp. 1406-1416 (DOI: 10.1016/j.jenvman.2007.07.009).

CHANSON, H., LUBIN, P., SIMON, B., and REUNGOAT, D. (2010). "Turbulence and Sediment Processes in the Tidal Bore of the Garonne River: First Observations." *Hydraulic Model Report No. CH79/10*, School of Civil Engineering, The University of Queensland, Brisbane, Australia, 97 pages (ISBN 9781742720104).

COSSINS, G. (1974). "Flood Forecasting in the Brisbane River." *Proceedings of Symposium January 1974 Floods Moreton Region*, The Institution of Engineers, Australia, Queensland Division, F. COSSINS and G. HEATHERWICK Eds., Aug., pp. 81-123. Discussion: pp. 124-133.

DIAZ, H.F., and MARKGRAF, V. (1992). "El Niño: Historical and Paleoclimatic Aspects of the Southern Oscillations." *Cambridge University Press*, UK.

FOX, J.F., PAPANICOLAOU, A.N., and KJOS, L. (2005). "Eddy Taxonomy Methodology around Submerged Barb Obstacle within a Fixed Rough Bed." *Jl of Eng. Mech.*, ASCE, Vol. 131, No. 10, pp. 1082-1101.

FUGATE, D.C., and FRIEDRICHS, C.T. (2002). "Determining Concentration and Fall Velocity of Estuarine Particle Populations using ADV, OBS and LISST." *Continental Shelf Research*, Vol. 22, pp. 1867-1886.

GORING, D.G., and NIKORA, V.I. (2002). "Despiking Acoustic Doppler Velocimeter Data." *Jl of Hyd. Engrg.*, ASCE, Vol. 128, No. 1, pp. 117-126. Discussion: Vol. 129, No. 6, pp. 484-489.

GRAF, W.H. (1971). "Hydraulics of Sediment Transport". *McGraw-Hill*, New York, USA.

HA, H.K., HSU, W.Y., MAA, J.P.Y., SHAO, Y.Y., and HOLLAND, C.W. (2009). "Using ADV Backscatter Strength for Measuring Suspended Cohesive Sediment Concentration." *Continental Shelf Research*, Vol. 29, pp. 1310-1316.

HENDERSON, F.M. (1966). "Open Channel Flow." *MacMillan Company*, New York, USA.

HORN, A., JOO, M., and POPLAWSKI, W. (1999). "Sediment Transport Rates in Highly Episodic River Systems: a Preliminary Comparison between Empirical Formulae and Direct Flood Measurements." *Proc. Water 99 Joint Congress*, 25th Hydrology & Water Res. Symp. and 2nd Intl Conf. Water Res. & Environ. Research, Brisbane, Australia, Vol. 1, pp. 238-243 (ISBN 185 825 7165).

HUANG, X., and GARCIA, M. (1998). "A Herschel-Bulkley Model for Mud Flow down a Slope." *Jl of Fluid Mech.*, Vol. 374, pp. 305-333.

HUSSAIN, A.K.M.F., and REYNOLDS, W.C. (1972). "The Mechanics of on Organized Wave in Turbulent Shear Flow. Part 2: Experimental Results." *Jl of Fluid Mech.*, Vol. 54, Part 2, pp. 241-261.

ISHIGAKI, T., KEIICHI, T., and KAZUYA, I. (2003). "Hydraulic Model Tests of Inundation in Urban Area with Underground Space." *Proc. 30th IAHR Biennial Congress*, Thessaloniki, Greece, Vol. B, p. 487-493.

JULIEN, P.Y. (1995). "Erosion and Sedimentation." *Cambridge University Press*, Cambridge, UK, 280 pages.

KAWANISI, K., and YOKOSI, S. (1997). "Characteristics of Suspended Sediment and Turbulence in a Tidal Boundary Layer." *Estuarine, Coastal and Shelf Science*, Vol. 38, pp. 447-469.

KOCH, C., and CHANSON, H. (2005). "An Experimental Study of Tidal Bores and Positive Surges: Hydrodynamics and Turbulence of the Bore Front." *Hydraulic Model Report No. CH56/05*, Dept. of Civil Engineering, The University of Queensland, Brisbane, Australia, July, 170 pages (ISBN 1864998245).

KOCH, C., and CHANSON, H. (2009). "Turbulence Measurements in Positive Surges and Bores." *Journal of Hydraulic Research*, IAHR, Vol. 47, No. 1, pp. 29-40 (DOI: 10.3826/jhr.2009.2954).

McLELLAND, S.J., and NICHOLAS, A.P. (2000). "A New Method for Evaluating Errors in High-Frequency ADV Measurements." *Hydrological Processes*, Vol. 14, pp. 351-366.

MONTES, J.S. (1998). "Hydraulics of Open Channel Flow." *ASCE Press*, New-York, USA, 697 pages.

MORRIS, P.H., and LOCKINGTON, D.A. (2002). "Geotechnical Compressibility and Consolidation Parameters and Correlations for Remoulded Fine-Grained Marine and Riverine Sediments." *Research Report*, CRC Sustainable Tourism, 51 pages.

NANIA, L., GOMEZ, M., and DOLZ, J. (2004). "Experimental Study of the Dividing Flow in Steep Street Crossings." *Jl of Hyd. Res.*, IAHR, Vol. 42, No. 4, pp. 406-412.

NEZU, I. (2005). "Open-Channel Flow Turbulence and its Research Prospect in the 21st Century." *Jl of Hyd. Engrg.*, ASCE, Vol. 131, No. 4, pp. 229-246.

NEZU, I., and NAKAGAWA, H. (1993). "Turbulence in Open-Channel Flows." *IAHR Monograph*, IAHR Fluid Mechanics Section, Balkema Publ., Rotterdam, The Netherlands, 281 pages.

O'CONNOR, T. (1996). "A Pictorial History of Queensland." *Robert Brown and Associates*, Brisbane, Channel 7 and Courier Mail, Brisbane, Australia.

ROUSSEL, N., LE ROY, R., and COUSSOT, P. (2004). "Thixotropy Modelling at Local and Macroscopic Scales." *Jl of Non-Newtonian Fluid Mech.*, Vol. 117, No. 2-3, pp. 85-95.

SALEHI, M., and STROM, K. (2011). "Using Velocimeter Signal to Noise Ratio as a Surrogate Measure of Suspended Mud Concentration." *Continental Shelf Research*, Vol. 31, pp. 1020-1032 (DOI: 10.1016/j.csr.2011.03.2008).

SHERRY, M.J., JACONO, D.L., SHERIDAN, J., MATHIS, R., and MARUSIC, I. (2009). "Flo Separation Characterisation of a Forward Facing Step Immersed in a Turbulent Boundary Layer." *Proc. 6th Intl Symp. on Turbulence and Shear Flow Phenomena*, Seoul, Korea, 22-24 June, pp. 1325-1330.

SHI, F. (2011). "Rheological and Sizing Analysis of Brisbane Flood Sediment Samples Collected by QUT." *Technical Report*, JKMRC, Brisbane, Australia, 6 pages.

SHI, F., and NAPIER-MUNN, T.J. (1996). "Measuring the Rheology of Slurries Using an On-line Viscometer." *Intl. Jl Miner.Process*, Vol. 47, pp. 153-176.

SOARES-FRAZAO, S., and ZECH, Y. (2008). "Dam-break Flow through an Idealised City." *Jl of Hyd. Res.*, IAHR, Vol. 46, No. 5, pp. 648-658.

SOLO-GABRIELE, H.M., and PERKINS, F.E. (1997). "Streamflow and Suspended Sediment Transport in an Urban Environment." *Jl of Hyd. Engrg.*, ASCE, Vol. 123, No. 9, pp. 807-811

Sontek (2008). "16-MHz microADV Expanded Description." *Sontek/YSI*, San Diego, USA, 4 pages.

TACHIE, M.F. (2001). "Open Channel Turbulent Boundary Layers and wall Jets on Rough Surfaces." *Ph.D. thesis*, Dept. of Mech. Eng., Univers. of Saskatchewan, Canada, 238 pages.

TACHIE, M.F., BALACHANDAR, R., and BERGSTROM, D.J. (2004). "Open Channel Boundary Layer Relaxation behind a Forward Facing Step at Low Reynolds Numbers." *Jl of Fluids Eng.*, ASME, Vol. 123, pp. 539-544.

THIEKEN, A.H., MULLER, M., KREIBICH, H., and MERZ, B. (2005). "Flood Damage and Influencing Factors: New Insights from the August 2002 Flood in Germany." Water Rees. Res., AGU, Vol. 41, No. 12, Paper W12430 (DOI: 10.1029/2005WR004177).

VELICKOVIC, M. SOARES, FRAZÃO, S., and ZECH, Y. (2011). "Porosity Model of Flow through an Idealised Urban District. Influence of City Alignment and of Transient Flow Character." *Proc. 34th IAHR World Congress*, Brisbane, Australia, 26 June-1 July, Engineers

Australia Publication, Eric VALENTINE, Colin APELT, James BALL, Hubert CHANSON, Ron COX, Rob ETTEMA, George KUCZERA, Martin LAMBERT, Bruce MELVILLE and Jane SARGISON Editors, pp. 3823-3830.

WAHL, T.L. (2003). "Despiking Acoustic Doppler Velocimeter Data. Discussion." *Jl of Hyd. Engrg.*, ASCE, Vol. 129, No. 6, pp. 484-487.

WALES, M. (1976). "The Early Floods of the Brisbane-Bremer River System, 1823-1867." *Brisbane City Council*, Australia.

WERNER, M.G.F., HUNTER, N.M., and BATES, P.D. (2005). "Identifiability of Distributed Floodplain Roughness Values in Flood Extent Estimation." *Jl of Hydrology*, Vol. 314, No. 1-4, pp. 139-157.

WILSON, S.D.R., and BURGESS, S.L. (1998). "The Steady, Spreading Flow of a Rivulet of Mud." *Jl Non-Newtonian Fluid Mech.*, Vol. 79, pp. 77-85.

XIE, Q. (1998). "Turbulent Flows in Non-Uniform Open Channels: Experimental Measurements and Numerical Modelling." *Ph.D. thesis*, Dept. of Civil Eng., University Of Queensland, Australia, 339 pages.

Bibliography

APELT, C.J. (2011). "Joint Flood Taskforce Report March 2011." Brisbane City Council, Australia, 52 pages.

Australian Geographic (2011). "World's first live flood test yields vital data." *Australian Geographic News*, 1 Feb. 2011. {http://www.australiangeographic.com.au/journal/world-first-live-flood-experiment-conducted.htm} accessed on 10 Feb. 2011.

BOM (1974). "Brisbane Floods January 1974." *Australian Government Publishing Service*, Canberra, Australia.

BOM (2011). "Frequent heavy rain events in late 2010/early 2011 lead to widespread flooding across eastern Australia." *Special Climate Statement 24*, National Climate Centre, Bureau of Meteorology, Melbourne VIC, Australia, Revision c, 24 February 2011, 28 pages.

COX, M.E. (1998). "Chemical and Turbidity Character of the Tidal Brisbane River." in "Moreton Bay and Catchment", I.R. TIBBETTS N.J. HALL and W.C. DENNISON Eds., School of Marine Science, The University of Queensland, Brisbane, Australia, pp. 175-184.

Institution of Engineers, Australia (1974). "Proceedings of Symposium January 1974 Floods Moreton Region." *The Institution of Engineers, Australia*, Queensland Division, F. COSSINS and G. HEATHERWICK Eds., Aug., 275 pages.

SEQ Water (2011). "January 2011 Flood Event - Report on the Operation of Somerset Dam and Wivenhoe Dam." *SEQ Water*, 2 March, 1180 pages.

SMEC (1975). "Brisbane River Flood Investigations. Final Report." *Cities Commission*, Snowy Mountains Engineering Corporation, Nov., 201 pages.

Sontek (2001). "Sontek/YSI ADVField/Hydra Acoustic Doppler Velocimeter (Field) Technical Documentation." *Sontek/YSI*, San Diego, USA, Sept., 110 pages.

Internet bibliography

Bureau of Meteorology	{http://www.bom.gov.au}
Known Floods in the Brisbane and Bremer River Basin, Including the Cities of Brisbane and Ipswich	{http://www.bom.gov.au/hydro/flood/qld/fld_history/brisbane_history.shtml}
World's first live flood test yields vital data	{http://www.australiangeographic.com.au/journal/world-first-live-flood-experiment-conducted.htm}
Premier's Flood Relief Appeal	{http://www.qld.gov.au/floods/donate.html}
Q&A - Dam expert analyses Wivenhoe	{http://www.abc.net.au/news/stories/2011/01/21/3118379.htm}
The 2010-2011 Floods in Queensland (Australia): Photographic Observations, Comments and Personal Experience	{http://espace.library.uq.edu.au/view/UQ:241445}

Bibliographic reference of the Report CH83/11

The Hydraulic Model research report series CH is a refereed publication published by the School of Civil Engineering at the University of Queensland, Brisbane, Australia.

The bibliographic reference of the present report is:

BROWN, R., CHANSON, H., McINTOSH, D., and MADHANI, J. (2011). "Turbulent Velocity and Suspended Sediment Concentration Measurements in an Urban Environment of the Brisbane River Flood Plain at Gardens Point on 12-13 January 2011." *Hydraulic Model Report No. CH83/11*, School of Civil Engineering, The University of Queensland, Brisbane, Australia, 120 pages (ISBN 9781742720272).

The Report CH83/11 is available, in the present form, as a PDF file on the Internet at UQeSpace:

http://espace.library.uq.edu.au/

It is listed at:

http://espace.library.uq.edu.au/list/author_id/193/

HYDRAULIC MODEL RESEARCH REPORT CH

The Hydraulic Model Report CH series is published by the School of Civil Engineering at the University of Queensland. Orders of any reprint(s) of the Hydraulic Model Reports should be addressed to the School Secretary.

School Secretary, School of Civil Engineering, The University of Queensland
Brisbane 4072, Australia - Tel.: (61 7) 3365 3619 - Fax : (61 7) 3365 4599
Url: http://www.eng.uq.edu.au/civil/ Email: hodciveng@uq.edu.au

Report CH	**Unit price**	Quantity	**Total price**
BROWN, R., CHANSON, H., McINTOSH, D., and MADHANI, J. (2011). "Turbulent Velocity and Suspended Sediment Concentration Measurements in an Urban Environment of the Brisbane River Flood Plain at Gardens Point on 12-13 January 2011." *Hydraulic Model Report No. CH83/11*, School of Civil Engineering, The University of Queensland, Brisbane, Australia, 120 pages (ISBN 9781742720272).	AUD$60.00		
CHANSON, H. "The 2010-2011 Floods in Queensland (Australia): Photographic Observations, Comments and Personal Experience." *Hydraulic Model Report No. CH82/11*, School of Civil Engineering, The University of Queensland, Brisbane, Australia, 127 pages (ISBN 9781742720234).	AUD$60.00		
MOUAZE, D., CHANSON, H., and SIMON, B. (2010). "Field Measurements in the Tidal Bore of the Sélune River in the Bay of Mont Saint Michel (September 2010)." *Hydraulic Model Report No. CH81/10*, School of Civil Engineering, The University of Queensland, Brisbane, Australia, 72 pages (ISBN 9781742720210).	AUD$60.00		
JANSSEN, R., and CHANSON, H. (2010). "Hydraulic Structures: Useful Water Harvesting Systems or Relics." *Proceedings of the Third International Junior Researcher and Engineer Workshop on Hydraulic Structures (IJREWHS'10)*, 2-3 May 2010, Edinburgh, Scotland, R. JANSSEN and H. CHANSON (Eds), Hydraulic Model Report CH80/10, School of Civil Engineering, The University of Queensland, Brisbane, Australia, 211 pages (ISBN 9781742720159).	AUD$60.00		
CHANSON, H., LUBIN, P., SIMON, B., and REUNGOAT, D. (2010). "Turbulence and Sediment Processes in the Tidal Bore of the Garonne River: First Observations." *Hydraulic Model Report No. CH79/10*, School of Civil Engineering, The University of Queensland, Brisbane, Australia, 97 pages (ISBN 9781742720104).	AUD$60.00		
CHACHEREAU, Y., and CHANSON, H., (2010). "Free-Surface Turbulent Fluctuations and Air-Water Flow Measurements in Hydraulics Jumps with Small Inflow Froude Numbers." *Hydraulic Model Report No. CH78/10*, School of Civil Engineering, The University of Queensland, Brisbane, Australia, 133 pages (ISBN 9781742720036).	AUD$60.00		
CHANSON, H., BROWN, R., and TREVETHAN, M. (2010). " Turbulence Measurements in a Small Subtropical Estuary under King Tide Conditions." *Hydraulic Model Report No. CH77/10*, School of Civil Engineering, The University of Queensland, Brisbane, Australia, 82 pages (ISBN 9781864999969).	AUD$60.00		

DOCHERTY, N.J., and CHANSON, H. (2010). "Characterisation of Unsteady Turbulence in Breaking Tidal Bores including the Effects of Bed Roughness." *Hydraulic Model Report No. CH76/10*, School of Civil Engineering, The University of Queensland, Brisbane, Australia, 112 pages (ISBN 9781864999884).	AUD$60.00		
CHANSON, H. (2009). "Advective Diffusion of Air Bubbles in Hydraulic Jumps with Large Froude Numbers: an Experimental Study." *Hydraulic Model Report No. CH75/09*, School of Civil Engineering, The University of Queensland, Brisbane, Australia, 89 pages & 3 videos (ISBN 9781864999730).	AUD$60.00		
CHANSON, H. (2009). "An Experimental Study of Tidal Bore Propagation: the Impact of Bridge Piers and Channel Constriction." *Hydraulic Model Report No. CH74/09*, School of Civil Engineering, The University of Queensland, Brisbane, Australia, 110 pages and 5 movies (ISBN 9781864999600).	AUD$60.00		
CHANSON, H. (2008). "Jean-Baptiste Charles Joseph BÉLANGER (1790-1874), the Backwater Equation and the Bélanger Equation." *Hydraulic Model Report No. CH69/08*, Div. of Civil Engineering, The University of Queensland, Brisbane, Australia, 40 pages (ISBN 9781864999211).	AUD$60.00		
GOURLAY, M.R., and HACKER, J. (2008). "Reef-Top Currents in Vicinity of Heron Island Boat Harbour, Great Barrier Reef, Australia: 2. Specific Influences of Tides Meteorological Events and Waves." *Hydraulic Model Report No. CH73/08*, Div. of Civil Engineering, The University of Queensland, Brisbane, Australia, 331 pages (ISBN 9781864999365).	AUD$60.00		
GOURLAY, M.R., and HACKER, J. (2008). "Reef Top Currents in Vicinity of Heron Island Boat Harbour Great Barrier Reef, Australia: 1. Overall influence of Tides, Winds, and Waves." *Hydraulic Model Report CH72/08*, Div. of Civil Engineering, The University of Queensland, Brisbane, Australia, 201 pages (ISBN 9781864999358).	AUD$60.00		
LARRARTE, F., and CHANSON, H. (2008). "Experiences and Challenges in Sewers: Measurements and Hydrodynamics." *Proceedings of the International Meeting on Measurements and Hydraulics of Sewers*, Summer School GEMCEA/LCPC, 19-21 Aug. 2008, Bouguenais, Hydraulic Model Report No. CH70/08, Div. of Civil Engineering, The University of Queensland, Brisbane, Australia (ISBN 9781864999280).	AUD$60.00		
CHANSON, H. (2008). "Photographic Observations of Tidal Bores (Mascarets) in France." *Hydraulic Model Report No. CH71/08*, Div. of Civil Engineering, The University of Queensland, Brisbane, Australia, 104 pages, 1 movie and 2 audio files (ISBN 9781864999303).	AUD$60.00		
CHANSON, H. (2008). "Turbulence in Positive Surges and Tidal Bores. Effects of Bed Roughness and Adverse Bed Slopes." *Hydraulic Model Report No. CH68/08*, Div. of Civil Engineering, The University of Queensland, Brisbane, Australia, 121 pages & 5 movie files (ISBN 9781864999198)	AUD$70.00		
FURUYAMA, S., and CHANSON, H. (2008). "A Numerical Study of Open Channel Flow Hydrodynamics and Turbulence of the Tidal Bore and Dam-Break Flows." *Report No. CH66/08*, Div. of Civil Engineering, The University of Queensland, Brisbane, Australia, May, 88 pages (ISBN 9781864999068).	AUD$60.00		
GUARD, P., MACPHERSON, K., and MOHOUPT, J. (2008). "A Field Investigation into the Groundwater Dynamics of Raine Island." *Report No. CH67/08*, Div. of Civil Engineering, The University of Queensland, Brisbane, Australia, February, 21 pages (ISBN 9781864999075).	AUD$40.00		
FELDER, S., and CHANSON, H. (2008). "Turbulence and Turbulent Length and Time Scales in Skimming Flows on a Stepped Spillway. Dynamic Similarity, Physical Modelling and Scale Effects." *Report No. CH64/07*, Div. of Civil Engineering, The University of Queensland, Brisbane, Australia, March, 217 pages (ISBN 9781864998870).	AUD$60.00		

TREVETHAN, M., CHANSON, H., and BROWN, R.J. (2007). "Turbulence and Turbulent Flux Events in a Small Subtropical Estuary." Report No. CH65/07, Div. of Civil Engineering, The University of Queensland, Brisbane, Australia, November, 67 pages (ISBN 9781864998993)	AUD$60.00		
MURZYN, F., and CHANSON, H. (2007). "Free Surface, Bubbly flow and Turbulence Measurements in Hydraulic Jumps." *Report CH63/07*, Div. of Civil Engineering, The University of Queensland, Brisbane, Australia, August, 116 pages (ISBN 9781864998917).	AUD$60.00		
KUCUKALI, S., and CHANSON, H. (2007). "Turbulence in Hydraulic Jumps: Experimental Measurements." *Report No. CH62/07*, Div. of Civil Engineering, The University of Queensland, Brisbane, Australia, July, 96 pages (ISBN 9781864998825).	AUD$60.00		
CHANSON, H., TAKEUCHI, M, and TREVETHAN, M. (2006). "Using Turbidity and Acoustic Backscatter Intensity as Surrogate Measures of Suspended Sediment Concentration. Application to a Sub-Tropical Estuary (Eprapah Creek)." *Report No. CH60/06*, Div. of Civil Engineering, The University of Queensland, Brisbane, Australia, July, 142 pages (ISBN 1864998628).	AUD$60.00		
CAROSI, G., and CHANSON, H. (2006). "Air-Water Time and Length Scales in Skimming Flows on a Stepped Spillway. Application to the Spray Characterisation." *Report No. CH59/06*, Div. of Civil Engineering, The University of Queensland, Brisbane, Australia, July (ISBN 1864998601).	AUD$60.00		
TREVETHAN, M., CHANSON, H., and BROWN, R. (2006). "Two Series of Detailed Turbulence Measurements in a Small Sub-Tropical Estuarine System." *Report No. CH58/06*, Div. of Civil Engineering, The University of Queensland, Brisbane, Australia, Mar. (ISBN 1864998520).	AUD$60.00		
KOCH, C., and CHANSON, H. (2005). "An Experimental Study of Tidal Bores and Positive Surges: Hydrodynamics and Turbulence of the Bore Front." *Report No. CH56/05*, Dept. of Civil Engineering, The University of Queensland, Brisbane, Australia, July (ISBN 1864998245).	AUD$60.00		
CHANSON, H. (2005). "Applications of the Saint-Venant Equations and Method of Characteristics to the Dam Break Wave Problem." *Report No. CH55/05*, Dept. of Civil Engineering, The University of Queensland, Brisbane, Australia, May (ISBN 1864997966).	AUD$60.00		
CHANSON, H., COUSSOT, P., JARNY, S., and TOQUER, L. (2004). "A Study of Dam Break Wave of Thixotropic Fluid: Bentonite Surges down an Inclined plane." *Report No. CH54/04*, Dept. of Civil Engineering, The University of Queensland, Brisbane, Australia, June, 90 pages (ISBN 1864997710).	AUD$60.00		
CHANSON, H. (2003). "A Hydraulic, Environmental and Ecological Assessment of a Sub-tropical Stream in Eastern Australia: Eprapah Creek, Victoria Point QLD on 4 April 2003." *Report No. CH52/03*, Dept. of Civil Engineering, The University of Queensland, Brisbane, Australia, June, 189 pages (ISBN 1864997044).	AUD$90.00		
CHANSON, H. (2003). "Sudden Flood Release down a Stepped Cascade. Unsteady Air-Water Flow Measurements. Applications to Wave Run-up, Flash Flood and Dam Break Wave." *Report CH51/03*, Dept of Civil Eng., Univ. of Queensland, Brisbane, Australia, 142 pages (ISBN 1864996552).	AUD$60.00		
CHANSON, H,. (2002). "An Experimental Study of Roman Dropshaft Operation : Hydraulics, Two-Phase Flow, Acoustics." *Report CH50/02*, Dept of Civil Eng., Univ. of Queensland, Brisbane, Australia, 99 pages (ISBN 1864996544).	AUD$60.00		
CHANSON, H., and BRATTBERG, T. (1997). "Experimental Investigations of Air Bubble Entrainment in Developing Shear Layers." *Report CH48/97*, Dept. of Civil Engineering, University of Queensland, Australia, Oct., 309 pages (ISBN 0 86776 748 0).	AUD$90.00		

CHANSON, H. (1996). "Some Hydraulic Aspects during Overflow above Inflatable Flexible Membrane Dam." *Report CH47/96*, Dept. of Civil Engineering, University of Queensland, Australia, May, 60 pages (ISBN 0 86776 644 1).	AUD$60.00		
CHANSON, H. (1995). "Flow Characteristics of Undular Hydraulic Jumps. Comparison with Near-Critical Flows." *Report CH45/95*, Dept. of Civil Engineering, University of Queensland, Australia, June, 202 pages (ISBN 0 86776 612 3).	AUD$60.00		
CHANSON, H. (1995). "Air Bubble Entrainment in Free-surface Turbulent Flows. Experimental Investigations." *Report CH46/95*, Dept. of Civil Engineering, University of Queensland, Australia, June, 368 pages (ISBN 0 86776 611 5).	AUD$80.00		
CHANSON, H. (1994). "Hydraulic Design of Stepped Channels and Spillways." *Report CH43/94*, Dept. of Civil Engineering, University of Queensland, Australia, Feb., 169 pages (ISBN 0 86776 560 7).	AUD$60.00		
POSTAGE & HANDLING (per report)	AUD$10.00		
GRAND TOTAL			

OTHER HYDRAULIC RESEARCH REPORTS

Reports/Theses	Unit price	Quantity	Total price
TREVETHAN, M. (2008). "A Fundamental Study of Turbulence and Turbulent Mixing in a Small Subtropical Estuary." Ph.D. thesis, Div. of Civil Engineering, The University of Queensland, 342 pages.	AUD$100.00		
GONZALEZ, C.A. (2005). "An Experimental Study of Free-Surface Aeration on Embankment Stepped Chutes." *Ph.D. thesis*, Dept of Civil Engineering, The University of Queensland, Brisbane, Australia, 240 pages.	AUD$80.00		
TOOMBES, L. (2002). "Experimental Study of Air-Water Flow Properties on Low-Gradient Stepped Cascades." *Ph.D. thesis*, Dept of Civil Engineering, The University of Queensland, Brisbane, Australia.	AUD$100.00		
CHANSON, H. (1988). "A Study of Air Entrainment and Aeration Devices on a Spillway Model." *Ph.D. thesis*, University of Canterbury, New Zealand.	AUD$60.00		
POSTAGE & HANDLING (per report)	AUD$10.00		
GRAND TOTAL			

CIVIL ENGINEERING RESEARCH REPORT CE

The Civil Engineering Research Report CE series is published by the School of Civil Engineering at the University of Queensland. Orders of any of the Civil Engineering Research Report CE should be addressed to the School Secretary.

School Secretary, School of Civil Engineering, The University of Queensland

Brisbane 4072, Australia

Tel.: (61 7) 3365 3619 Fax : (61 7) 3365 4599

Url: http://www.eng.uq.edu.au/civil/ Email: hodciveng@uq.edu.au

Recent Research Report CE	Unit price	Quantity	Total price
CALLAGHAN, D.P., NIELSEN, P., and CARTWRIGHT, N. (2006). "Data and Analysis Report: Manihiki and Rakahanga, Northern Cook Islands - For February and October/November 2004 Research Trips." *Research Report CE161*, Division of Civil Engineering, The University of Queensland (ISBN No. 1864998318).	AUD$10.00		
GONZALEZ, C.A., TAKAHASHI, M., and CHANSON, H. (2005). "Effects of Step Roughness in Skimming Flows: an Experimental Study." *Research Report No. CE160*, Dept. of Civil Engineering, The University of Queensland, Brisbane, Australia, July (ISBN 1864998105).	AUD$10.00		
CHANSON, H., and TOOMBES, L. (2001). "Experimental Investigations of Air Entrainment in Transition and Skimming Flows down a Stepped Chute. Application to Embankment Overflow Stepped Spillways." *Research Report No. CE158*, Dept. of Civil Engineering, The University of Queensland, Brisbane, Australia, July, 74 pages (ISBN 1 864995297).	AUD$10.00		
HANDLING (per order)	AUD$10.00		
GRAND TOTAL			

Note: Prices include postages and processing.

PAYMENT INFORMATION

1- VISA Card

Name on the card :	
Visa card number :	
Expiry date :	
Amount :	AUD$ .....

2- Cheque/remittance payable to: THE UNIVERSITY OF QUEENSLAND and crossed "Not Negotiable".

N.B. For overseas buyers, cheque payable in Australian Dollars drawn on an office in Australia of a bank operating in Australia, payable to: THE UNIVERSITY OF QUEENSLAND and crossed "Not Negotiable".

Orders of any Research Report should be addressed to the School Secretary.

School Secretary, School of Civil Engineering, The University of Queensland
Brisbane 4072, Australia - Tel.: (61 7) 3365 3619 - Fax : (61 7) 3365 4599
Url: http://www.eng.uq.edu.au/civil/ Email: hodciveng@uq.edu.au